Manipulator Grasping and Pushing Operations

Matthew Thomas Mason

REPORT DOCUMENTATION PAGE	READ INSTRUCTIONS BEFORE COMPLETING FORM

1. REPORT NUMBER TR-690	2. GOVT ACCESSION NO.	3. RECIPIENT'S CATALOG NUMBER

4. TITLE (and Subtitle) Manipulator Grasping and Pushing Operations	5. TYPE OF REPORT & PERIOD COVERED technical report
	6. PERFORMING ORG. REPORT NUMBER

7. AUTHOR(s) Matthew Thomas Mason	8. CONTRACT OR GRANT NUMBER(s) N00014-81-K-0491 N00014-77-C-0389 and N00014-80-C-0505

9. PERFORMING ORGANIZATION NAME AND ADDRESS Artificial Intelligence Laboratory 545 Technology Square Cambridge, Massachusetts 02139	10. PROGRAM ELEMENT, PROJECT, TASK AREA & WORK UNIT NUMBERS

11. CONTROLLING OFFICE NAME AND ADDRESS Advanced Research Projects Agency 1400 Wilson Blvd Arlington, Virginia 22209	12. REPORT DATE May 21, 1982
	13. NUMBER OF PAGES 137

14. MONITORING AGENCY NAME & ADDRESS(If different from Controlling Office) Office of Naval Research Information Systems Arlington, Virginia 22217	15. SECURITY CLASS. (of this report) UNCLASSIFIED
	15a. DECLASSIFICATION/DOWNGRADING SCHEDULE

16. DISTRIBUTION STATEMENT (of this Report)

Distribution of this document is unlimited.

17. DISTRIBUTION STATEMENT (of the abstract entered in Block 20, if different from Report)

18. SUPPLEMENTARY NOTES

None

19. KEY WORDS (Continue on reverse side if necessary and identify by block number)

Robot   Manipulator
Grippers   Friction
Automatic Assembly

20. ABSTRACT (Continue on reverse side if necessary and identify by block number)

The Primary goal of this research is to develop theoretical tools for analysis, synthesis, and application of primitive manipulator operations. The primary method is to extend and apply traditional tools of classical mechanics. The results are of such a general nature that they address many different aspects of industrial robotics, including effector and sensor design, planning and programming tools, and design of auxiliary equipment. Some of the manipulator operations studied are: OVER

1. Grasping an object. The object will usually slide and rotate during the period between first contact and prehension.

2. Placing an object. The object may slip slightly in the fingers upon contact with the table as the base aligns with the table.

3. Pushing. Often the final stage of mating two parts involves pushing one object into the other.

In each of these operations the motion of the object is determined partly by the manipulator and partly by frictional forces. Hence the theoretical analysis focuses on the problem of partially constrained motion with friction. When inertial forces are dominated by frictional forces, we find that the fundamental motion of the object - whether it will rotate, and if so in what direction- may be determined by inspection. In many cases the motion may be predicted in detail, and in any case it is possible to find bounds on the motion. With these analytical tools it is sometimes possible to predict the outcome of a given manipulator operation, or, on the other hand, to plan an operation producing a given desired outcome.

MANIPULATOR GRASPING

AND PUSHING OPERATIONS

by

Matthew Thomas Mason

B.S., M.I.T.
(1976)
M.S., M.I.T.
(1978)

Submitted in Partial Fulfillment
of the Requirements for the Degree of

Doctor of Philosophy
at the
Massachusetts Institute of Technology

June 1982

Signature of Author _____
Department of Electrical Engineering and Computer Science
· May 21, 1982

Certified by _____
Tomas Lozano-Perez
Thesis Supervisor

Certified by _____
Berthold K. P. Horn
Thesis Supervisor

Accepted by _____
Joel Moses
Chairman, Department of Electrical Engineering and Computer Science

MANIPULATOR GRASPING

AND PUSHING OPERATIONS

by

Matthew Thomas Mason

Submitted to the Department of
Electrical Engineering and Computer Science
in partial fulfillment of the requirements
for the degree of Doctor of Philosophy

ABSTRACT

The primary goal of this research is to develop theoretical tools for analysis, synthesis, and application of primitive manipulator operations. The primary method is to extend and apply traditional tools of classical mechanics. The results are of such a general nature that they address many different aspects of industrial robotics, including effector and sensor design, planning and programming tools, and design of auxiliary equipment.

Some of the manipulator operations studied are:

1. Grasping an object. The object will usually slide and rotate during the period between first contact and prehension.

2. Placing an object. The object may slip slightly in the fingers upon contact with the table as the base aligns with the table.

3. Pushing. Often the final stage of mating two parts involves pushing one object into the other.

In each of these operations the motion of the object is determined partly by the manipulator and partly by frictional forces. Hence the theoretical analysis focuses on the problem of partially constrained motion with friction. When inertial forces are dominated by frictional forces, we find that the fundamental motion of the object—whether it will rotate, and if so in what direction—may be determined by inspection. In many cases the motion may be predicted in detail, and in any case it is possible to find bounds on the motion. With these analytical tools it is sometimes possible to predict the outcome of a given manipulator operation, or, on the other hand, to plan an operation producing a given desired outcome.

Thesis Supervisors: Tomas Lozano-Perez and Berthold K. P. Horn

Titles: Assistant Professor and Associate Professor, respectively, of Computer Science and Electrical Engineering

Acknowledgements

Table of Contents

Chapter 1

Introduction

Grasping of an object by a computer-controlled manipulator is an important but poorly understood operation. It is important because it usually precedes any attempt by the manipulator to move an object, and because it is the point at which uncertainty in the position/orientation of an object is first encountered. It is poorly understood in that we are unable to predict reliably the consequences of an attempted grasping maneuver, and are also unable to plan reliably a successful grasping maneuver for a given situation. The purpose of this thesis is to develop a thorough understanding of grasping, especially including the ability to predict automatically the outcome of an attempted grasping motion and the ability to plan automatically a grasp of an object whose position/orientation is only approximately known. The approach taken is to formulate each stage of a grasping motion as a problem in mechanics. The problems are complicated due to the largely unpredictable frictional forces, but nonetheless yield simple, useful results.

Of the many aspects of grasping, we focus on uncertainty in the position and orientation of the object to be grasped. An important result of the thesis is the identification of a number of methods for eliminating uncertainty during the task without sensory feedback; indeed, without adaptive motion of the manipulator. Most grasping motions deal with uncertainty to a degree, but it is now possible to apply this idea confidently to situations involving much greater uncertainty, and to tasks other than grasping, such as placing objects on a table top.

There are a number of manipulator operations, including some stages of a grasp motion, which are kinematically identical. For example, figure 1 shows an early

stage of a typical grasp motion. Initial contact has occurred between one of the fingers and a vertex of the object, but no other contacts have yet occurred. Until at least one more contact occurs, the object's motion is only partly determined by the motion of the finger, the remaining degrees of freedom being determined primarily by frictional forces. The figure could just as well represent a box being pushed into a desired location on the floor. Other operations in this class include: *aligning* two or more objects much as one straightens a pack of cards; *placing* an object in the hand onto a table; and of course *pushing* and *grasping*. All of these operations involve planar motion of an object, and occur without having the object rigidly held in the hand.

The goal of this thesis is to improve our understanding of this class of operations, thereby supporting the development of better robotic manipulation systems—including application programs, general robot planning and programming tools, auxiliary machinery, and the manipulator itself. We will begin by working through an example which illustrates the utility of the theory to be developed in chapter two.

1.1. Analysis of an Example Grasping Motion

To demonstrate the nature and utility of the theory, we begin by proving a particular grasping operation will succeed if certain initial conditions are met. This grasping operation exhibits the property of eliminating all uncertainty in the position of the object as the operation proceeds. It was invented by R. P. Paul and appears on film [Pingle et. al. 1974]. The motion is illustrated in figure 2. The object is part of a hinge which is to be assembled. The hand will grasp the hinge-plate with the leading edge of each finger contacting an inside corner formed by the hinge-sleeves. The interesting thing about this maneuver is that it is essentially an open-loop motion. The hand moves at a fixed rate in a straight line while the fingers close at a fixed rate. The hand deliberately moves past the range of possible positions of the hinge-plate. At some point in its trajectory it strikes the hinge and pushes it forward as the fingers close. The motion is constructed so that the hinge will align itself with the fingers, eliminating uncertainty in orientation. The remaining uncertainty in position is eliminated by a self-centering action which
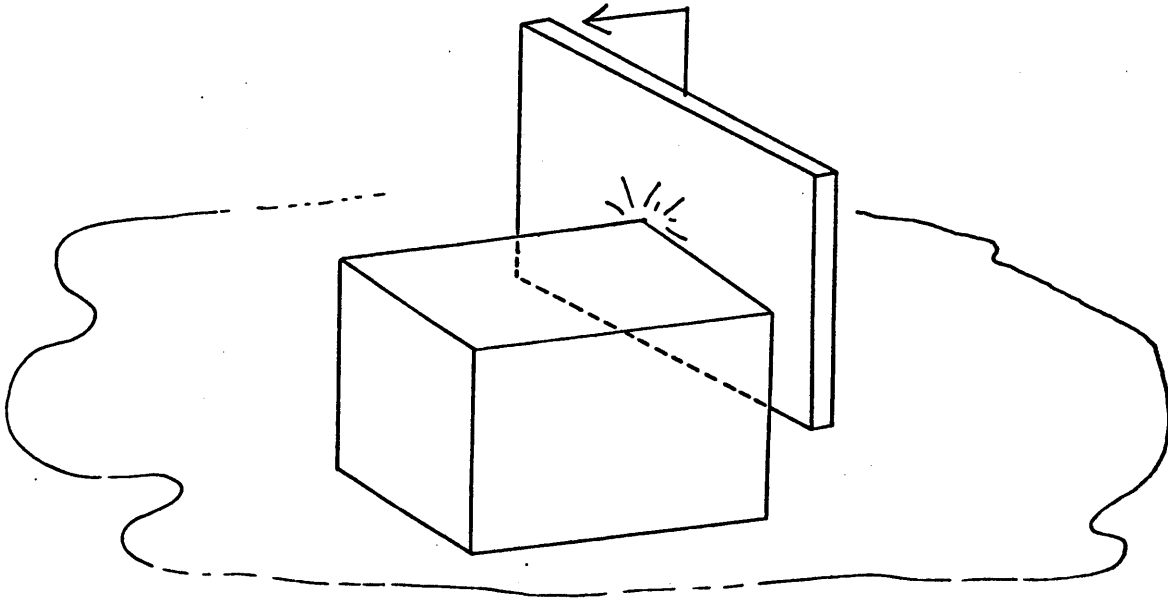
Figure 1. Typical Problem

occurs as the hinge-sleeves are squeezed between the closing fingers.

The progress of the grasping operation through stages is shown in figure 3, showing the fingers and hinge-plate in cross-section. Beginning with no contact (stage 0), the fingers proceed in the direction shown. When one of the fingers strikes the hinge-plate, the hinge-plate will begin to move on the table, rotating with respect to the fingers (stage 1). Eventually the hinge-plate rotates to contact the second finger, which initiates stage 2. In stage 2, the hinge-plate translates, while one or both of the fingers slides towards the sleeves. Stage 3 occurs with one sleeve in contact with a finger, and complete prehension occurs when the second finger contacts its sleeve.

That is what is *supposed* to happen. Our purpose is to find a set of initial conditions which guarantees that this sequence of events actually takes place. The first condition is a geometric one: the initial position/orientation of the hinge-plate
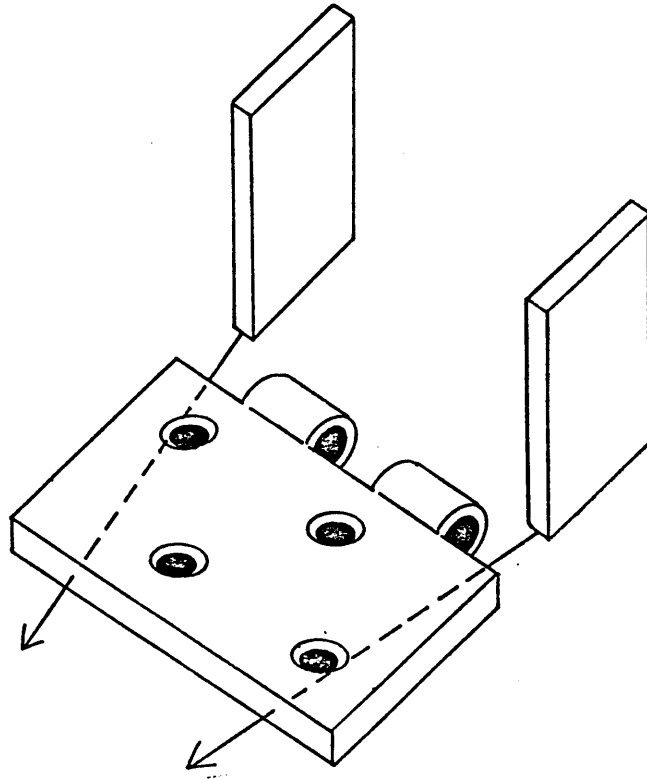
Figure 2. Hinge grasping

must ensure that initial contact is between the leading edge of one finger and the corresponding edge of the hinge-plate. The second condition is that the contact must occur early enough in the motion that the fingers have not closed too much. This condition is a complicated one, depending on the initial position of the hinge-plate, the orientation, the finger closing speed, and on the rate at which the hinge-plate will rotate as the grasping motion proceeds. Conditions on the initial finger separation and the finger closing speed are postponed to a more detailed discussion in section 3.3.

Thus we are assured that the grasping operation successfully reaches stage one, so that one finger is in contact with the appropriate edge of the hinge-plate.
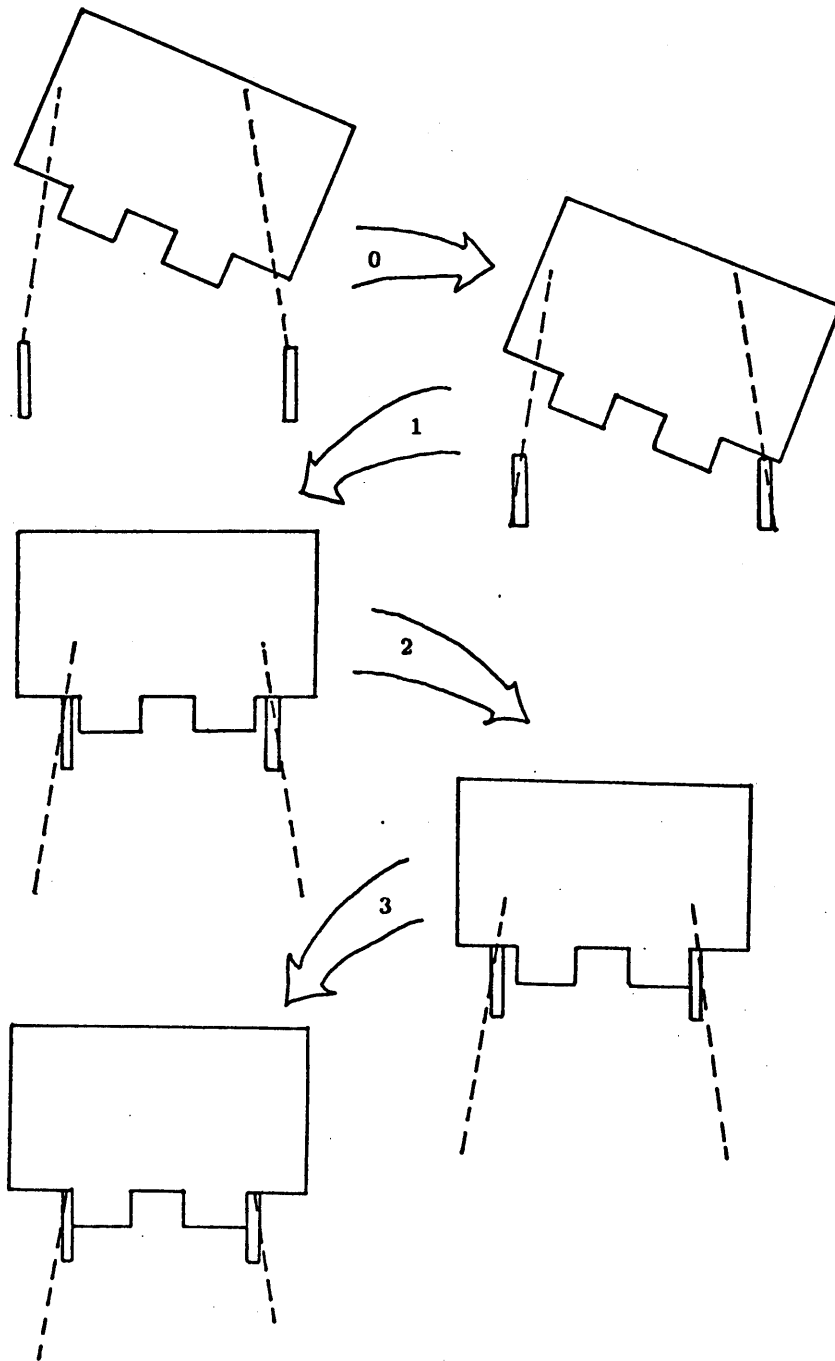
Figure 3. Stages in hinge grasping

We wish to ensure that the hinge-plate will rotate in the proper direction until contact with the second finger occurs. Without loss of generality, we assume the initial contact is between the hinge-plate and the finger on the right. For this step, a simple construction is sufficient (figure 4). From the contact we construct the normal to the hinge-plate edge, and also lines at an angle from the normal equal to the arc-tangent of the coefficient of friction. The area between these two lines is the *cone of friction*. We also indicate the center of gravity of the hinge. It will be proven in the next chapter (theorem 11) that the hinge must rotate counter-clockwise if the friction cone passes entirely to the right of the center of gravity. With the center of gravity as shown, the friction cone will pass to the right of the center of gravity no matter where on the edge the finger is. Hence the hinge-plate must rotate to contact with the second finger.

Theorem 11, and most of the other results of chapter two, make two assumptions which must be included in this verification. First, it is assumed that the frictional forces obey Coulomb's law. Second, it is assumed that frictional forces dominate the inertial forces arising from acceleration of the hinge-plate. In typical manipulator grasping motions these assumptions are valid, provided the velocity of the fingers is not excessive. In section 2.5 a simulation shows the theory is very accurate at a finger speed of 20 cm/sec or less.

Stage two commences when the second finger makes contact with the hinge-plate (figure 5). We can guarantee that stage three will be reached if we can show that the orientation of the hinge-plate is stable during stage two. Again using the cone of friction argument, it is clear that the hinge-plate cannot rotate. If a rotation about one of the finger commences, the deviation is immediately corrected by a rotation in the opposite direction. Since the fingers are coming together, eventually one of them will contact its hinge-sleeve. This signals the commencement of stage three.

It may appear that the analysis of stage two also applies to stage three, but the friction cone at the contact with the left finger is no longer applicable because the finger can no longer slide along the edge of the hinge-plate. Instead of using the friction cone, we must use the *line of pushing*, that is, the line parallel to the
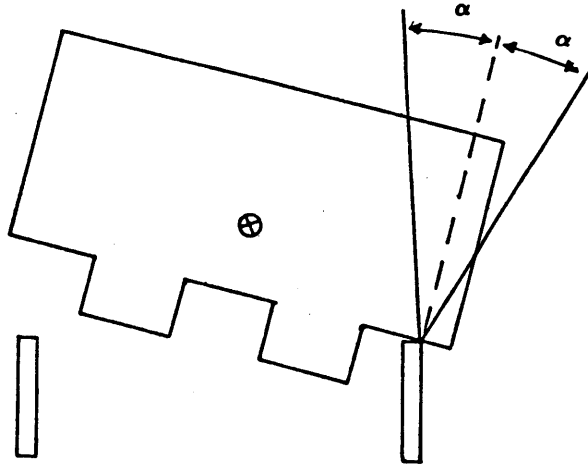
Figure 4. Analysis of stage one. α is the angle of friction: $\tan^{-1} \mu$.
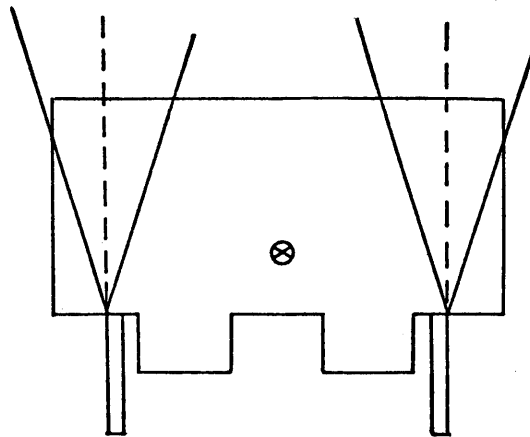
Figure 5. Analysis of stage 2.
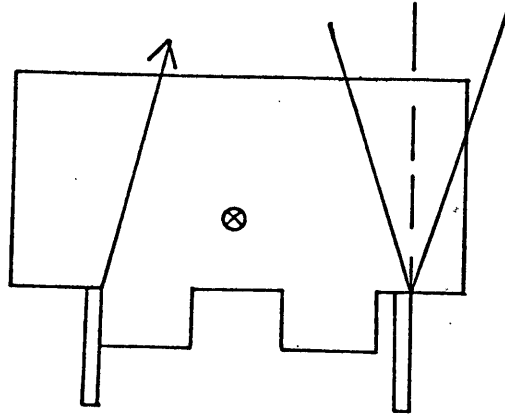
Figure 6. Analysis of stage 3.

motion of the finger, drawn through the contact point. In figure 6 we have shown the left finger in contact with the left sleeve. We wish to show that the hinge-plate orientation is stable, so that it will be preserved until the right finger contacts its sleeve. A small counter-clockwise perturbation will be corrected, as before, because the line of pushing passes to the left of the center of gravity, causing a clockwise rotation. Hence the other finger will contact its sleeve and prehension will be obtained, with the object in a completely determined position and orientation.

But what if the first finger slides into contact with its hinge-sleeve before the second finger contacts the hinge-plate? The situation is illustrated in figure 7. With the finger in the corner formed by the sleeve and the other edge, the condition for proper rotation is that the line of pushing pass to the right of the center of gravity. If this condition is satisfied stage three will be reached, and the rest of the analysis proceeds as before.

To summarize, the initial conditions for this operation are:

1. The initial position/orientation must ensure initial contact between one
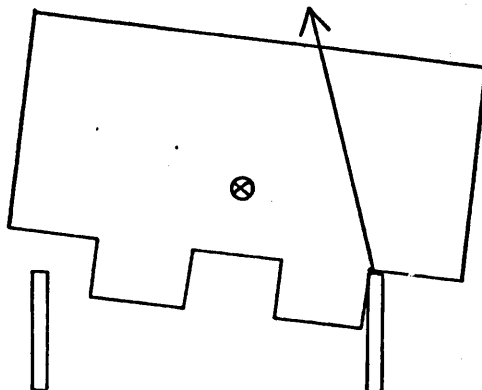
Figure 7. Analysis of stage 2a.

finger and the corresponding hinge-plate edge.

2. Conditions on the initial finger separation and the finger closing speed must be satisfied (postponed to section 3.3.)

3. The friction cone, drawn from any point on the hinge-plate edge, must not include the center of gravity of the hinge-plate. This condition is independent of the hinge-plate orientation.

4. The line of pushing, drawn from the junction of the hinge-sleeve and the hinge-plate edge, must pass outside the center of gravity of the hinge-plate. This constraint is dependent on the details of the hinge's motion, since the condition is only active when the finger hits the junction of the hinge-sleeve and the edge of the hinge-plate. However, it is sufficient that it hold in the initial orientation of the hinge-plate.

This verification demonstrates a deep understanding of the hinge grasp program. We know why it works, and can find conditions which guarantee success of the program. We can also construct similar grasping maneuvers for other objects. Figure 8 shows three different "grippers", and the associated grasp motions, which

will grasp a block and at the same time completely constrain its position and orientation. Figure 8a is analogous to the hinge grasp example analyzed above, except that initial contact is between an object vertex and a finger edge rather than between a finger vertex and an object edge. It is interesting that all of the orienting and positioning of the block may be accomplished with one finger, given the proper finger trajectory (figure 8b). The other finger is only necessary for prehension. Figure 8c is similar except that instead of a single specially-shaped finger we use three fingers from a general-purpose dexterous gripper, with one additional finger required for prehension.

1.2. Discussion

The long-range goal of our work is to develop a deep understanding of manipulation. The structure of such an understanding should comprise:

- *A comprehensive set of manipulation operations.* This set of operations should provide a language capable of describing any desired manipulator action. There should be at least a few levels of operations, each level composed of operations at lower levels.

- *The ability to predict the outcome of a given operation in a given situation.* The primary application of this ability is in verifying that a given manipulation will produce a desired outcome. This verification may take the form of a proof using logical assertions and rules of deduction, or it may be a simulation, which produces a model of the outcome of the operation, to be compared with the desired outcome. This ability is useful because (1) manipulator programs can be tested without the use of a manipulator, (2) design of a manipulator can be tested without the expense of constructing it, and (3) manufacturability aspects of a new product can be tested during the initial design of the product.

- *The ability to recognize an observed instance of an operation.* There are two applications of this ability: study and programming. Our ability to interpret human manipulation is limited by our lack of fundamental theoretical knowledge of manipulation. Our ability to learn from human manipulation is dependent to some degree on our understanding of the basic methods of

14
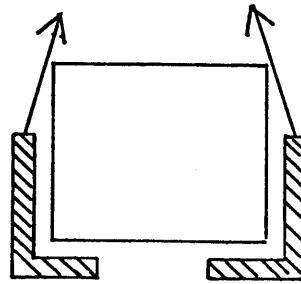
(a)
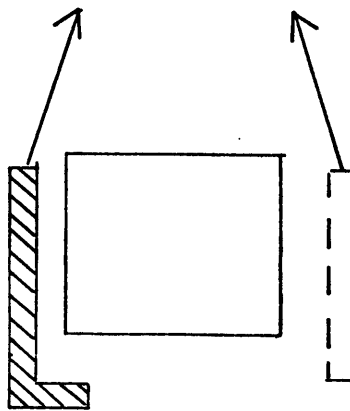
(b)
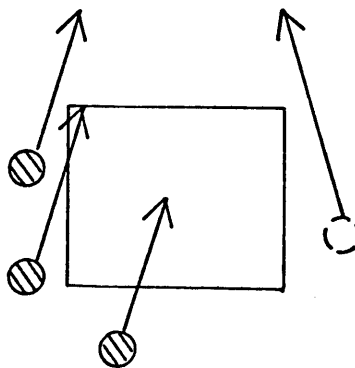
(c)

Figure 8. Grippers

producing motions. Recognition of operations is also relevant to the problem of programming manipulators. A number of circumstances arise in which it is much easier to "show" the robot what to do than it is to "tell" it what to do. [Lozano-Perez 1982]

- *The ability to plan an operation obtaining a given outcome in a given situation.* The primary advantage of a better understanding of manipulation is that robot planning and programming will be improved. Our present capacity to synthesize successful robot programs relies on a combination of intuition, trial and error, and individual experience. Developing a theoretical basis for manipulator planning provides valuable conceptual tools to human programmers, and allows some of the planning work to be performed automatically.

- *The ability to implement the operations on a robot.* A manipulator operation is useful in robotic manipulation only if it can be performed by robots.

It is instructive to try to fit the present state of manipulation into this structure. There are five low-level manipulator operations which have been extensively studied. The first three of these are:

MOVETO. This is clearly the best understood manipulation primitive. There are two versions of this operation, depending on whether an object is held in the gripper or not. The goal of the operation is to move the object or the robot from its present position/orientation to a specified position/orientation.

GRASP. This operation assumes that the gripper is perfectly positioned so that the object will not move as the fingers close. The goal of the operation is to totally constrain the position/orientation of the object relative to the hand by closing the fingers.

UNGRASP. This operation assumes that the object is held by the gripper, but that the object position is stable even without the gripper, hence opening the gripper doesn't move the object.

These operations form a language which is comprehensive and well-understood only in a very weak sense, because there is no provision for uncertainty. It is necessary

to assume that the world is composed of rigid objects, that all initial positions and orientations are precisely known, and that the robot is a perfect positioner. Given these assumptions all of the abilities listed above have been attained to some extent. Simulations have been demonstrated [Meyer 1981, Soroka 1980], and some aspects of the planning process have been successfully automated [Lozano-Perez 1980]. Programming a robot by leading it through a task constitutes recognition of the primitives, although recognition is essentially trivial in a universe containing only three objects. Many industrial manipulator systems and most research systems implement the three primitives. So the three primitives are fairly well understood. Unfortunately, the inability to deal with uncertainty is a severe limitation when real manipulation tasks are addressed.

The three-primitive language can be augmented by the addition of two other operations, which are useful in many situations involving uncertainty:

MOVE-UNTIL-TOUCH. The robot moves in a stated direction until a specified sensor or combination of sensors signals that contact has occurred.

COMPLIANT-MOVE. The robot executes a motion while accommodating to position constraints due to contact with an object.

For MOVE-UNTIL-TOUCH there has been some work in simulation [Meyer 1981], recognition [Summers and Grossman 1981], and automatic planning[Taylor 1976], although it lags the work on the first three primitives considerably. For COMPLIANT-MOVE, there has been some work on automatic planning [Mason 1981]. Both primitives have been implemented on research manipulators [Bolles and Paul 1973, Shimano 1978, Silver 1973, Finkel et. al. 1974, Goto et. al. 1974, Hanafusa and Asada 1977a, Inoue 1971], and MOVE-UNTIL-TOUCH has been implemented on a few commercial manipulators. These operations are useful for dealing with small errors in the placement of objects, by allowing the manipulator to adapt to perceived force or touch feedback. However, large uncertainty in object placement renders these strategies useless, because *if* they touch an object they are unable to interpret the information obtained.

In summary, our present understanding of manipulation is limited to situations

17

involving little or no uncertainty, either in the robot, in the shape of parts, or in the placement of parts. This observation is corroborated by industrial practice—most robot assembly requires accurate robots and accurately oriented and fed parts. The drawbacks of this limitation are considerable. Even though a robot is a general-purpose positioning device, easily programmed for new tasks, it must be surrounded by peripheral equipment—orienters, feeders, and the gripper—which must be designed and constructed anew for every application. This situation compromises the advantages of industrial robots over fixed automation: development cycles for new products are lengthened, and capital expenditures for new equipment are required for major changes.

There are two approaches to alleviating our inability to cope adequately with uncertainty. One is to study further the five primitives outlined above, with the hope that they will still form a "comprehensive" vocabulary when our model of the world is extended to include uncertainty. The other approach is to identify and study new primitives which are more suitable for dealing with uncertainty. This thesis identifies a class of manipulation primitives which are particularly appropriate for dealing with uncertainty, specifically *manipulation without prehension*, i.e. manipulation of objects which are *not* rigidly held by the gripper. The motion of the object is partially determined by the manipulator, and partially determined by other constraints and forces, such as support contact, gravity, and friction. The hinge grasp is a perfect example of manipulation without prehension. It also demonstrates the suitability of these primitives for coping with uncertainty. It is often taken as obvious that uncertainty in a task requires sensory feedback and adaptive motion by the robot. However, the hinge example provides a counter-example: *only the motion of the hinge-plate is adaptive, and no sensory feedback is required.*

The ultimate motive for the study of manipulation without prehension is the development of automatic planning. However, there are a number of other applications of the results of this thesis:

Immediate. The study of manipulation without prehension provides manipulator programmers with a number of useful conceptual tools. The

18

ability to deal reliably with uncertainly positioned objects is especially appealing. It is also useful to position an object by pushing it on a surface, or to align two objects by pushing. Certain problems in placing objects reliably are addressed. In addition, the results are useful in the design of auxiliary machinery, especially part-orienting machines and grippers.

Short-range. More realistic simulation systems can be implemented, allowing for grasping and pushing of objects whose positions are uncertain.

Long-range. With further study and experience it should be possible to embody the new primitives in manipulator programming languages. Likewise automatic planning, verification, and teaching-by-showing with uncertainty will become feasible.

These applications are described in greater detail in chapter three, with example implementations of some of them.

1.3. Overview of thesis

Chapters two and three focus on the mechanics and application of a class of manipulation operations which includes all of the stages of the hinge-plate grasp. It is assumed that the frictional forces obey Coulomb's law, and that the frictional forces dominate the inertial forces. It is shown in section 2.5 that the latter assumption is valid in many common manipulation situations. The subject of chapter two is the characterization of the motion of the object. We have already seen some of the results: that the direction of rotation of the object can be determined by inspection. In addition, means are developed for obtaining a complete characterization of the motion—not just the direction of rotation, but the instantaneous center of rotation and the angular velocity.

Chapter three addresses the issues of applying the theory to problems in practical manipulation. A number of potential applications are discussed in detail, and examples are presented in the design of automatic orientation machines and grippers, in the automatic planning of grasping motions, and in the verification of manipulation programs.

1.4. Previous Work

Manipulator operations

The first computer-controlled manipulator [Ernst 1961] had a hand with touch sensors, which it used to locate blocks scattered in its workspace. It grasped the blocks one at a time, moved them over a box, and dropped them in. This demonstrated four of the five common manipulator operations: MOVETO, GRASP, UNGRASP, and MOVE-UNTIL-TOUCH. The first COMPLIANT-MOVE was demonstrated by Inoue ten years later [Inoue 1971]. Implementation of these primitives has been an active research area since that time. Implementation of MOVETO has spawned research on manipulator kinematics [Uicker et. al. 1964, Pieper 1968, Paul et. al. 1981], path generation [Paul 1972, Taylor 1979, Paul 1979], and control [Bejczy 1974, Hollerbach 1980, Horn and Raibert 1978, Kahn and Roth 1971, Khatib 1980, Luh et. al. 1983, Luh et. al. 1980b, Raibert 1978, Whitney 1969, Whitney 1972, Young 1978].

Implementation of MOVE-UNTIL-TOUCH was investigated primarily at Stanford [Bolles and Paul 1973] and IBM [Will and Grossman 1975, Darringer and Blasgen 1975]. Implementation of COMPLIANT-MOVE has been approached using purely mechanical compliance [Drake 1977], using open-loop compliant actuation [Inoue 1971, Paul 1972], and using closed loop servos with force sensors [Silver 1973, Goto et.al. 1974].

There are a number of other operations which are less well known than the five cited above. The hinge-plate grasp studied in section 1.1 is such an operation. Another example is the object-alignment operation depicted in figure 9, programmed by R. H. Taylor [Albus and Evans 1976]. In order to precisely align the lid on the box, they are simultaneously squeezed in the vise. Alignment in the other horizontal direction may be obtained by squeezing with the robot gripper. This is a good application of manipulation without prehension.

Of course, GRASP and UNGRASP apply to a material handling or assembly robot. There are a number of operations, e.g. WELD, DRILL, SCREW, which occur in other applications.
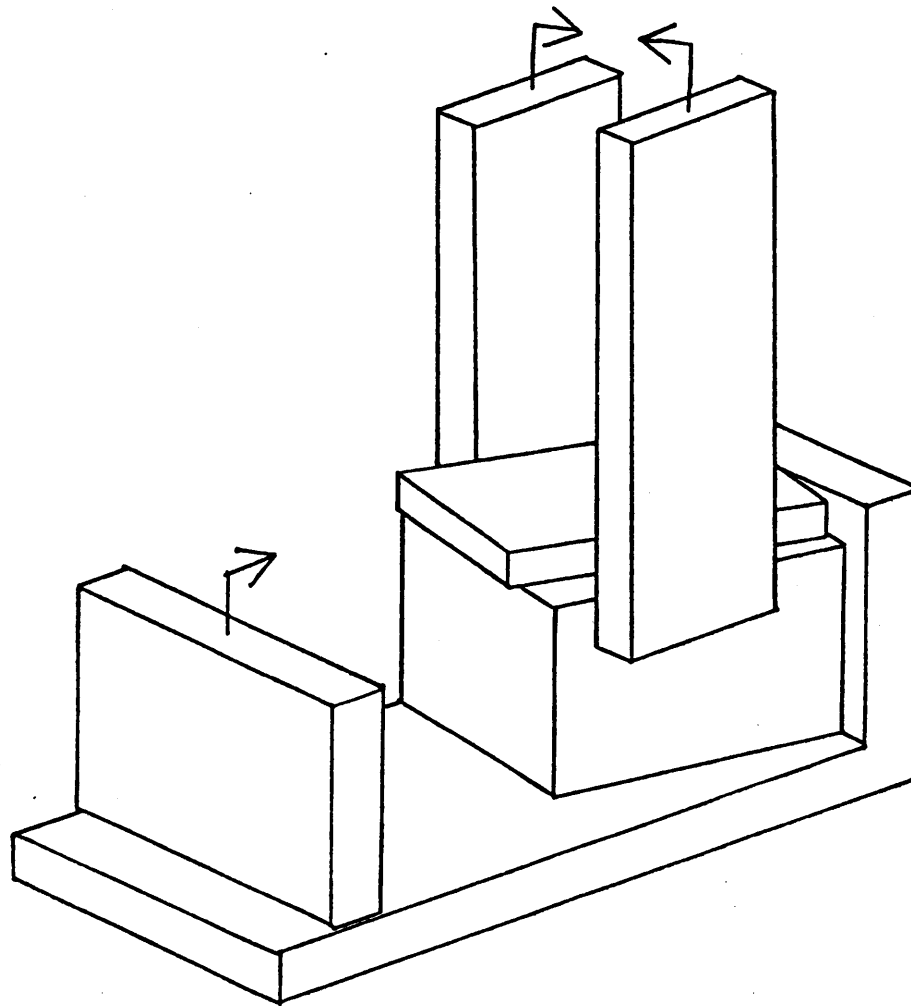
Figure 9. Aligning a lid on a box

Simulation and Verification

By verification, I mean that initial conditions, goals, and a manipulator program are expressed symbolically, and a procedure is applied which attempts to deduce that the goals will be fulfilled if the initial conditions are met. By simulation, I mean that an initial state and a manipulator program are provided, and that a procedure is applied which generates successive states. A verification is generally more powerful (and harder to invent) since the initial conditions need not completely specify the manipulator and task state. This is particularly relevant to the

problem of dealing with uncertainty, where the initial state may be unpredictable. Simulations generally require a complete specification of the initial state, although one could imagine a simulation which generates a set of possible states at each iteration, rather than one particular state.

There has been very little work on verifying manipulator programs. One approach to automatic planning [Taylor 1976] includes a verification step. The AL system [Finkel et.al. 1974] included a simulation so that trajectories could be generated before execution time. MOVE-UNTIL-TOUCH is included in a simulation developed at IBM [Meyer 1981].

Recognition

It was noted above that recognition is essentially trivial when the universe includes only the three operations MOVETO, GRASP, and UNGRASP. A number of manipulators are programmed by leading the robot through the desired sequence of operations. Programming by showing has also been demonstrated for the more difficult situation including the fourth primitive MOVE-UNTIL-TOUCH [Summers and Grossman 1981].

Planning

Planning manipulation programs, even using only three basic primitives, is an extremely complex process. For programs composed of just GRASP, UNGRASP, and MOVETO, it is necessary to plan a hand position to grasp an object [Lozano-Perez 1976] and to calculate collision-free trajectories [Udupa 1977, Lozano-Perez and Wesley 1979, Lozano-Perez 1981]. When MOVE-UNTIL-TOUCH is included, it is necessary to determine where its use is necessary [Taylor 1976]. It is also useful to accept just a statement of goals, which is transformed into a particular sequence of manipulator operations [Ambler et. al. 1975, Ambler and Popplestone 1975, Taylor 1976, Lozano-Perez 1976, Lieberman and Wesley 1975, Lozano-Perez 1980]. Total automation of manipulator programming is not imminent, but this line of research also leads to near-term benefits, such as programming aids and conceptual tools to ease the burden on human programmers and enable more sophisticated robot applications.

Chapter 2

Theory of Pushing

In this chapter we analyze a class of manipulator operations by formulating a few. closely related problems in mechanics. The solutions to these problems help us to predict the outcomes of particular manipulator operations and to plan manipulator operations that produce specified outcomes.

The manipulator operations studied will be referred to as quasi-static planar pushing operations, or simply pushing. We precede the definition of quasi-static planar pushing with some examples. All three stages of the hinge-plate grasp maneuver were examples of quasi-static planar pushing (figure 3). Figure 10 shows a block held in the gripper being placed on a tabletop. If the block's position in the hand is uncertain, it is impossible to place the block without a collision. When the collision occurs, several alternatives are possible: the hand may deform; the block might be crushed; the block may rotate in the fingers to a cocked position; or all of these might occur. One possibility is that the block slides in the fingers, maintaining planar contact with one of the fingers. This is an instance of quasi-static planar pushing. Figure 11 shows a block being packed in a box. Due to the presence of obstacles, it is impossible to position the block while it is in the gripper, so it is being slid into place. As long as the block does not tip up on its back edge, this is also an example of quasi-static planar pushing.

In each example, the object is in planar motion, being driven by a partial constraint on the position of the object. The planar motion is due to a constraint called the *support constraint*, and the other constraint is called the *pushing constraint*.
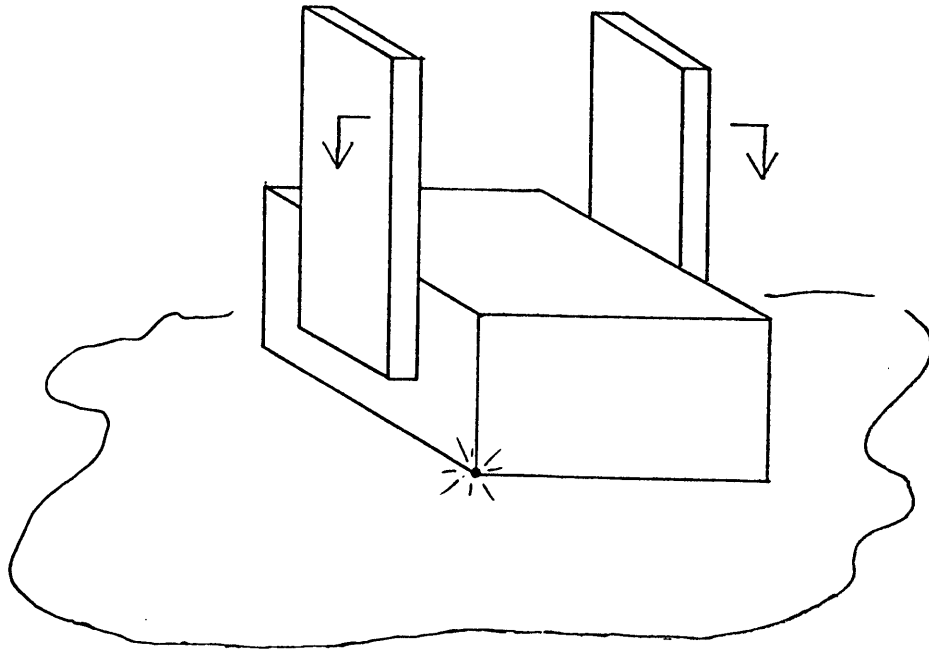
Figure 10. Placing an object

In the hinge example, the contact between the hinge-plate and the tabletop provides the support constraint, while pushing constraints arise during contact with each finger. For the placing example, it is the finger contact which formed the support constraint, while the tabletop provides the pushing constraint. In the block-packing example, the bottom of the box provides the support constraint, with pushing constraints arising whenever the block contacts the fingers, the side of the box, or any of the other blocks. "Planar Pushing" refers to the kinematics of the operation: an object in planar motion being pushed. "Quasi-Static" refers to the fact that inertial forces are assumed to be negligible in the analysis. Very fast motions and collisions fall outside the range of our analysis.
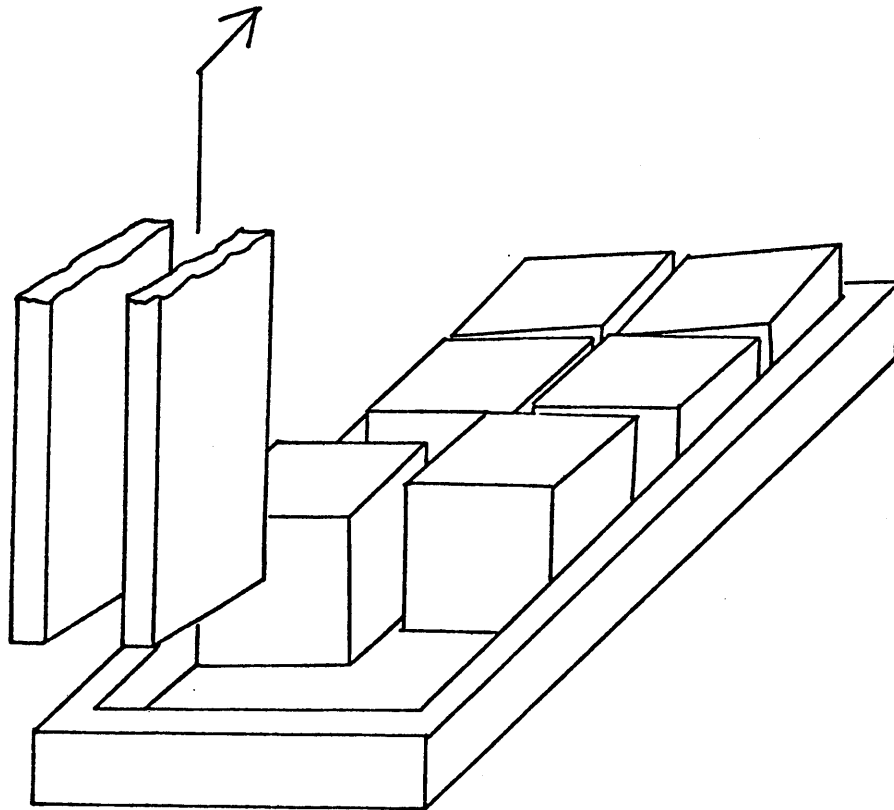
Figure 11. Palletizing a block

Frictional forces play a crucial role in determining the motion of an object during quasi-static planar pushing. The next section presents a brief summary of the relevant theory of sliding friction. The remainder of the chapter is concerned with formulation and solution of various problems involving pushing. The most important result is that we can predict, by inspection, whether the object will rotate, and if so, in what direction. The utility of this result has already been demonstrated in the verification of the hinge-plate grasp in chapter one, and further applications will be demonstrated in chapter three. However, this result by itself is not sufficient for our purposes. It is sometimes also necessary to characterize completely the object's motion. Besides the direction of rotation, we must know

the instantaneous center of rotation, and the rate of rotation. Numerical means are developed to solve this problem. The analysis is developed by cases, distinguished by whether the contact is *sliding* or *fixed* with respect to the pushing constraint. The analysis is then extended to the case when it is not known a priori whether sliding contact or fixed contact occurs. The final section addresses the quasi-static assumption (that inertial forces are negligible compared to frictional forces), with the goal of characterizing the conditions under which the assumption is valid.

The primary difficulty encountered in analyzing the problem of sliding objects is that the distribution of pressure at the contact between the object and the supporting surface is generally indeterminate. Consequently the system of frictional forces arising at the contact between the object and the support is also indeterminate. Surprisingly, the most important results are obtained without any assumption on the form of the pressure distribution, except that the pressure is bounded. Even this restriction is awkward—occasionally in the thesis the results will be applied to examples with a finite number of support points, corresponding to infinite pressures.

2.1. Friction of Planar Motion

2.1.1. Review of Sliding Friction

Coulomb's Law

Coulomb conducted the first thorough investigation of sliding friction [Coulomb 1781]. He searched for dependencies of the frictional force on every conceivable parameter, including the time of repose before sliding commences, elapsed time of sliding, speed of sliding, types of surfaces, cleanliness of surfaces, and, of course, the magnitude of the normal force. Although all of these factors affect the frictional force, Coulomb found that over an enormous range of materials and normal forces the frictional force is virtually independent of every factor except the materials and the magnitude of the normal force. The result is now commonly identified as *Coulomb's Law*: the tangential force of friction during sliding is directed opposite to the direction of motion, with magnitude proportional to the normal force. The constant of proportionality is known as the *coefficient of dynamic friction*, and

depends on the contacting materials, but not on the speed of motion. If there is no motion in progress, a different, usually slightly higher, constant is used–the *coefficient of static friction*. The tangential force of friction is constrained to be no greater than the product of the normal force with the coefficient of static friction. During sliding, Coulomb's law completely determines the frictional force. When there is no motion, the frictional force may not be completely determined. In some cases, the potential indeterminacy is resolved by the tendency of the frictional force to resist any impending motion at the point in question.

This law is not original with Coulomb; Amontons [Amontons 1699] had previously asserted the law, and had published engineering tables based on it. But the earliest known statement of the law appears in the notes of Leonardo da Vinci:

> Every body resists in its friction with a power equal to the fourth of its heaviness if the motion is plane [or slow?] and the surfaces dense and polished [or clean?].[1]

Leonardo thought that there was a universal coefficient of sliding friction–one fourth. This value is nearly correct for many combinations of common materials. In spite of the prior claims of Leonardo and Amontons, there is ample justification for naming the law after Coulomb. Before his investigations the law was nothing more than conjecture. It is doubtful that Leonardo engaged in any substantial experimental verification of the law[2], and it is clear from the tables published by Amontons that most of the data is extrapolation from a few experiments of limited scope.[3]

Friction Cone and Friction Angle

There is a geometric interpretation of Coulomb's law, apparently first constructed by Moseley [Moseley 1839]. Consider a point moving on a surface (figure 12). We construct the vector $\underline{f}$ representing total contact force acting on the point, comprising the normal force f_n due to the surface stiffness and the tangential force f_t due to friction. Coulomb's law states that these are related by $f_t = \mu f_n$. If we construct the normal to the surface, then Coulomb's law is equivalent to the

---

[1] [Leonardo da Vinci 14??], 72*v*.b.

[2] [Truesdell 1968] p. 9.

[3] [Gillmor 1971] p. 123.
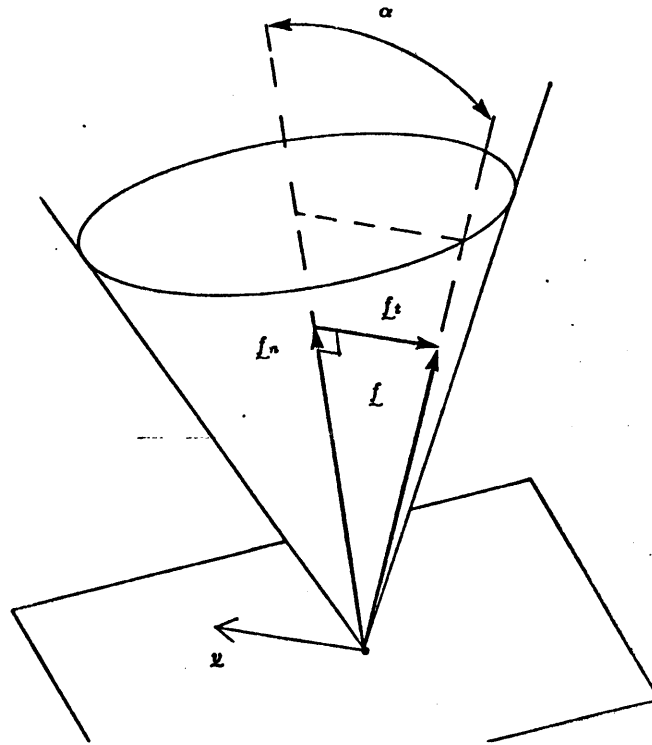
Figure 12. Friction Cone. A point is sliding on a surface with veb. .ty $\underline{v}$. α is the angle of friction: $\tan^{-1}\mu$.

statement that the total contact force $\underline{f}$ will make an angle $\alpha = \tan^{-1} f_t/f_n$ with the normal. The set of vectors making the proper angle with the surface normal form a cone, called the *friction cone*. The angle α is called the *friction angle*.

General Planar Motion with Friction

I have only located three previous works dealing with sliding friction during general planar motion [Jellett 1872, Prescott 1923, Macmillan 1936]. Jellett avoids most of the complications of general planar motion, but he does show that if all the applied forces (excluding the support contact forces) reduce to a single force, then the problem of planar motion of a body reduces to the problem of the motion of a point in the plane.

Prescott provides the first substantial discussion of friction in the context of general planar motion of a solid body. He developed expressions for the moment of frictional forces about the instantaneous rotation center, under the assumption that the weight of the object is uniformly distributed on its base. He also considers the problem of the motion of an object subject to a force applied at a single point. For

objects with a finite number of supporting points, with the support forces known, he develops the conditions under which the object will rotate about a given point. For a special case (two points of support equidistant from the point of application of the external force) he derives the set of all possible rotation centers. Similar plots of rotation centers will play an important role in sections 2.3.2 and 2.4.2 of this thesis.

MacMillan considered a more general problem. Rather than assuming uniform pressure or known pressure with a finite number of points of support, MacMillan assumes a linear pressure distribution:

$$p(x,y) = ax + by + c$$

where (x,y) represents a point in the contact region. The three parameters a, b, and c can be determined if the external applied forces are known. He then derives expressions for the force and moment, given a planar motion of the object. Unfortunately these expressions are complicated—evaluation of them requires evaluation of seven different line integrals taken around the boundary of the contact region. MacMillan's most important result is that during a pure translation, the system of frictional forces arising in the contact area may be reduced to a single force acting through a fixed point—the *center of friction*.

This chapter generalizes MacMillan's results to arbitrary pressure distributions. Expressions for force and moment are developed for general planar motion. Without additional assumptions on the form of the pressure distribution, the location of the center of friction can be calculated from knowledge of the external applied forces. The generality of this result is very important, since the pressure distribution at the contact region of two surfaces is usually complicated and unpredictable.

MacMillan used the center of friction to find the frictional force and moment during translation, but its utility goes well beyond this—its position determines whether an object will rotate when it is pushed, and, if so, whether clockwise rotation or counter-clockwise rotation occurs. This gives a partial characterization of the motion of an object being pushed.

It would also be useful to have a complete characterization of the motion of an object being pushed. We approach this problem by developing methods for computing the instantaneous rotation center given the applied forces, and assuming no more than three points of support. It is shown that the set of rotation centers that can be produced by unconstrained pressure distributions is bounded by the set of rotation centers that can be produced with three point support.

Modern Work

The problem of general planar motion in the presence of friction has not attracted much attention in recent times. Frictional force is, of course, non-conservative, rendering many of the techniques of classical mechanics inapplicable. Most of the discussion of the problem in the mechanics literature is limited to systems with a single degree of freedom. There has been some modern applied mechanics work on sliding friction in oscillatory systems [Den Hartog 1956], but it does not extend to general planar motion.

Modern texts on sliding friction treat single degree of freedom problems, or problems which clearly reduce to a single degree of freedom or to a point on a plane. It is interesting to note that textbooks never discuss the circumstances under which the crucial reductions may be applied, but still expect students to apply the reductions. It is also interesting that this omission is not noticed by students.

The field of tribology [Bowden and Tabor 1950] focuses on the description and mechanism of frictional forces, not on the motion of objects subject to friction. One result of this work is the development of descriptions more accurate than Coulomb's law. This is certainly relevant to the present work, since determination of the frictional forces is an important part of the theory. Nonetheless, we will assume Coulomb friction throughout most of the thesis, and will furthermore assume that the static and dynamic coefficients of friction are equal. To quote Prescott:[4]

> But all these small inaccuracies we shall disregard for two very good reasons: firstly, because the laws are sufficiently accurate for most practical purposes; and secondly, because exact laws are not known.

---

[4][Prescott 1923], p. 106.

To this I should add that the focus of this thesis is the characterization of the planar motion of objects being pushed. This thesis goes considerably farther than the previous works cited, in spite of the relaxation of assumptions on the form of the pressure distribution. Further generalization would certainly be desirable, but it is a matter of addressing one problem at a time.

2.1.2. Force and Moment of Sliding Friction During Planar Motion

This section will develop expressions for the force and moment due to friction with the support during general planar motion. Following sections will use these results to analyze quasi-static planar pushing.

Any planar motion is either a translation or a rotation about some instantaneously motionless point. Translation and rotation are handled separately. For translation, we will find that the system of frictional forces reduces to a single force through a point whose position is independent of the direction of translation. This point is the *center of friction*. No analogous reduction occurs for rotation.

We will consider an object in motion on a planar surface (figure 13). Let R be the region of contact with the surface, let dA be the differential element of area of R, let $\underline{x}$ be the position of dA, let $p(\underline{x})$ be the pressure at $\underline{x}$, and let $\underline{v}_x$ be the velocity of the object relative to the supporting surface at $\underline{x}$. We will assume Coulomb friction, with coefficient of friction μ. The normal force at $\underline{x}$ is given by

$$p(\underline{x})\, dA$$

so the application of Coulomb's law gives for the tangential force at $\underline{x}$

$$-\mu \frac{\underline{v}_x}{|\underline{v}_x|} p(\underline{x})\, dA.$$

The total frictional force $\underline{f}_f$ is obtained by integrating over the support contact region R:

$$\underline{f}_f = \int_R -\mu \frac{\underline{v}_x}{|\underline{v}_x|} p(\underline{x})\, dA. \tag{2.1}$$

The total frictional moment m_f is obtained by similar means.

31
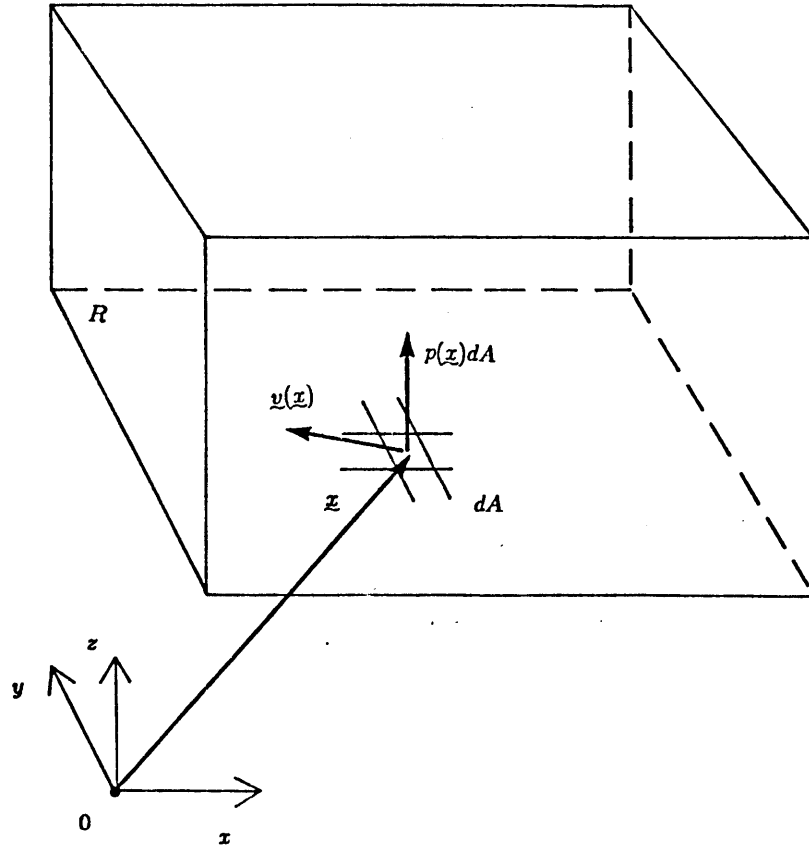
Figure 13. Force and Moment of Sliding Friction.

$$m_f = \int\limits_R \underline{x} \otimes -\mu \frac{\underline{v}_x}{|\underline{v}_x|} p(\underline{x}) \, dA \tag{2.2}$$

where by $(a, b)^T \otimes (c, d)^T$ we mean $ad - bc$, i.e. $\hat{k} \cdot (a, b, 0)^T \times (c, d, 0)^T$.

Translation

During a pure translation, all points in the object have the same relative velocity $\underline{v}_x/|\underline{v}_x|$. Hence this term may be factored out of the integral, along with the coefficient of friction:

$$\underline{f}_f = -\mu \frac{\underline{v}_x}{|\underline{v}_x|} \int\limits_R p(\underline{x}) \, dA \tag{2.3}$$

$$m_f = -\mu \int\limits_R \underline{x} p(\underline{x}) \, dA \otimes \frac{\underline{v}_x}{|\underline{v}_x|}. \tag{2.4}$$

32

Let f_0 be the total normal contact force, and let x_0 be the centroid of the pressure distribution $p(x)$:

$$f_0 = \int_R p(x)\, dA$$

$$x_0 = \frac{\int_R x p(x)\, dA}{f_0}.$$

Substituting into equations 2.3 and 2.4 we obtain

$$f_f = -\mu \frac{v_x}{|v_x|} f_0$$

$$m_f = x_0 \otimes f_f.$$

Inspection of these equations shows that the system of frictional forces reduces to a single force applied at x_0. This result is the basis for all of the remaining results.

Theorem 1. *The system of frictional forces of a translating object reduces to a single force, applied at the centroid of the pressure distribution, whose direction is opposite the direction of translation. Proof:* given above.

When the system of frictional forces reduces to a single force applied at a particular point, whose location is independent of the direction and velocity of motion, and whose direction is opposite the direction of motion, we say that that point is the *center of friction*. Theorem 1 says that during translation a center of friction exists, and it is the centroid of the pressure distribution. We also know that the magnitude of the frictional force is the product of the applied normal force with the coefficient of friction, and hence that the problem reduces to the problem of a point in a plane with the same coefficient of friction, but that is less important for our purposes.

This result may appear to be of limited value, because the pressure distribution is usually indeterminate. Fortunately we can show (section 2.1.3) that the centroid of the pressure distribution may be predicted even when the pressure distribution itself is indeterminate. We will also show that the assumption that the frictional forces obey Coulomb's law may be relaxed somewhat, but first we complete the present discussion by developing expressions for the force and moment of friction during rotation.

33

Rotation

Let $\underline{x}_r$ be the instantaneous center of rotation, and let $\dot{\theta}$ be the angular velocity. The velocity at $\underline{x}$ is given by

$$\underline{v}_x = \dot{\theta}\left(\hat{k} \times (\underline{x} - \underline{x}_r)\right)$$

so

$$\frac{\underline{v}_x}{|\underline{v}_x|} = \text{sgn}(\dot{\theta})\hat{k} \times \frac{\underline{x} - \underline{x}_r}{|\underline{x} - \underline{x}_r|}$$

where $\hat{k}$ is the unit vector normal to the x–y plane. Hence $\hat{k} \times \underline{x}$ indicates a rotation of $\underline{x}$ by $\pi/2$. Substituting into equations 2.1 and 2.2, we obtain after simplification

$$\underline{f}_f = -\mu \, \text{sgn}(\dot{\theta})\hat{k} \times \int_R \frac{\underline{x} - \underline{x}_r}{|\underline{x} - \underline{x}_r|} p(\underline{x}) \, dA \tag{2.5}$$

$$m_f = -\mu \, \text{sgn}(\dot{\theta}) \int_R \underline{x} \cdot \frac{\underline{x} - \underline{x}_r}{|\underline{x} - \underline{x}_r|} p(\underline{x}) \, dA. \tag{2.6}$$

Comparing with equations 2.3 and 2.4, we see that the simplification obtained for the case of translation does not apply to rotation. The center of friction plays no apparent role during rotation of an object.

It is sometimes useful to consider a translation to be a rotation about an infinitely distant rotation center. By allowing the range of $\underline{x}_r$ to include points at infinity, equations 2.5 and 2.6 may be used for both rotation and translation, provided we adopt some special conventions. Specifically, we will arrange that the expression

$$\text{sgn}(\dot{\theta}) \frac{\underline{x} - \underline{x}_r}{|\underline{x} - \underline{x}_r|}$$

continues to give the direction of motion of $\underline{x}$, even when $\underline{x}_r$ is infinitely distant. The convention is best illustrated by example. Suppose a point $\underline{x}$ is translating along a line l (figure 14). This could be considered to be the result of a clockwise rotation about (infinitely distant) rotation center $\underline{x}_{r1}$ or a counter-clockwise rotation about $\underline{x}_{r2}$. By convention, we will choose the rotation center so that a translation corresponds to a clockwise rotation. Hence, we will adopt the definition
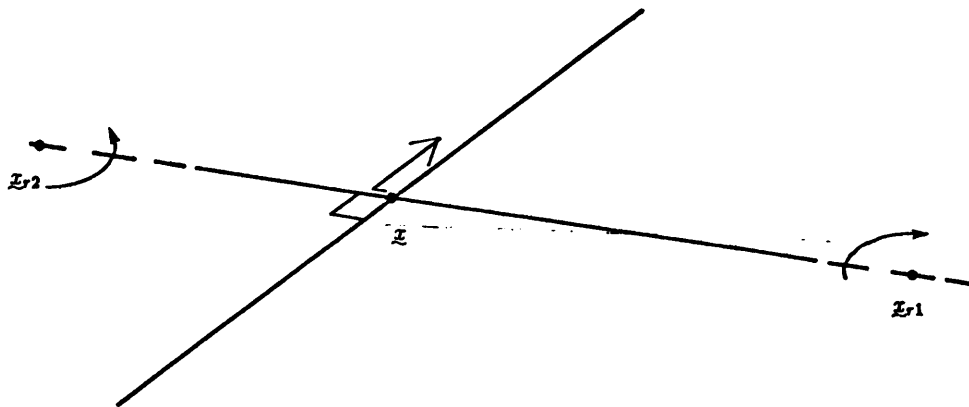
Figure 14. Convention for Rotation Center at Infinity

$$\text{sgn}(\dot{\theta}) = \begin{cases} 1, & \text{if } \dot{\theta} > 0; \\ -1, & \text{if } \dot{\theta} \leq 0. \end{cases}$$

This departure from the usual definition of the signum function (whose value at zero is zero instead of -1) allows us to use equations 2.5 and 2.6 for both translation and rotation.

2.1.3. The Center of Friction

In the previous section, we found that during translation a center of friction occurs at the centroid of the pressure distribution. In many practical situations, the pressure distribution is not known. Microscopic variations in the contact surfaces may drastically alter the pressure distribution. Fortunately, the contact pressure and moment must balance certain components of the applied forces, fixing the position of the centroid in the process. This gives us a practical method for finding the center of friction without concern for indeterminate details of the pressure distribution.

First consider the simple case of an object on a horizontal plane, with no applied force except the force of gravity. The only vertical forces acting on the object are

gravity, which reduces to a single force through the center of mass x_g, and the contact pressure. Due to the planar constraint there is no vertical acceleration, so the magnitude of the total force due to the contact pressure must equal the weight of the object:

$$f_0 = Mg$$

where M is the mass of the object, and g is the magnitude of the gravitational acceleration. The centroid of the pressure distribution x_0 can be found by similar means. Construct two lines through x_0 parallel to the x and y axes. The planar constraint prevents angular acceleration about these lines, so the moments of force are zero. The tangential frictional forces exhibit no moment about either of these lines, so for the total moments we obtain

$$\begin{bmatrix} \int_R (y - y_0) p(x)\, dA \\ \int_R (x - x_0) p(x)\, dA \end{bmatrix} + \begin{bmatrix} (y_g - y_0) \\ (x_g - x_0) \end{bmatrix} f_0 = \begin{bmatrix} 0 \\ 0 \end{bmatrix}$$

from which we easily obtain

$$\begin{bmatrix} x_0 \\ y_0 \end{bmatrix} = \begin{bmatrix} x_g \\ y_g \end{bmatrix}$$

So in the absence of applied forces other than gravity, the center of friction lies directly beneath the center of mass.

This result easily generalizes to the case of arbitrary systems of applied forces. Let $f_{a,z}$ be the normal component of the total applied force, and let $m_{a,x}$ and $m_{a,y}$ be the total moments of applied force about the x-axis and y-axis, respectively. Then the magnitude of the total force due to the contact pressure is

$$f_0 = f_{a,z}$$

and the center of friction is

$$x_0 = -\frac{1}{f_{a,z}} \begin{bmatrix} m_{a,y} \\ m_{a,x} \end{bmatrix}.$$

This result allows the determination of the center of friction given only the applied forces.

The proof of Theorem 1 assumes Coulomb friction. This assumption is unnecessary. The existence of the center of friction requires only two assumptions on the nature of friction: (1) that the direction of the frictional force is opposite to the direction of motion; and (2) that the magnitude of the frictional force is independent of the direction of motion. For ease of reference, we will refer to any friction law satisfying these two assumptions as *resistive friction*. That theorem 1 holds for resistive friction is easily demonstrated by expressing the differential frictional force at a point as the product of a magnitude dF and a direction $\hat{u}$. The total force and moment are obtained by integration:

$$E = \int \hat{u} \, dF$$
$$M = \int x \otimes \hat{u} \, dF.$$

By our first assumption, $\hat{u}$ is anti-parallel to the direction of motion. During translation, $\hat{u}$ is the same for all x.

$$E = \hat{u} \int dF$$
$$M = \int x \, dF \otimes \hat{u}$$
$$= \frac{\int x \, dF}{\int dF} \otimes \hat{u} \int dF.$$

Hence during translation, the system of frictional forces reduces to a single force E applied at a point $\int x \, dF / \int dF$. The location of this point is independent of the direction of translation, by assumption (2).

2.2. Pushing with Fixed or Rolling Contact

In this section we investigate the first of the modes of pushing: pushing with a fixed contact or a rolling contact, meaning that there is no relative motion at the contact between the object and the pushing constraint. In some texts, this is referred to as *perfectly rough* contact. Figure 15 shows a typical fixed contact situation. An object is sliding along the support plane, with point x_c touching a *constraint surface* which is in motion along the support plane. The contact point x_c is fixed with respect to the object and with respect to the constraint.

37
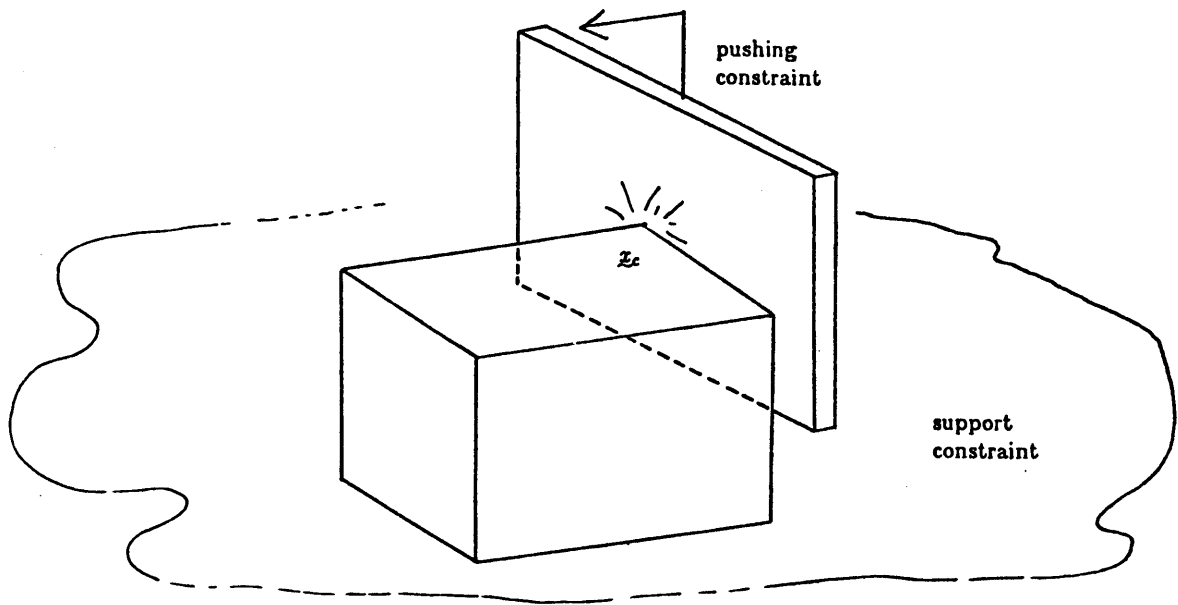
Figure 15. Typical fixed contact problem

Normal relative motion of the contact point is prevented by the pushing surface, and tangential relative motion is prevented by friction, so the instantaneous velocity of the contact point is completely determined, leaving only one degree of freedom in the motion of the object.

Most of our analysis is instantaneous, i.e. we investigate the instantaneous velocity and instantaneous angular velocity of the object. This analysis applies equally well to the case of rolling contact, in which the object rolls *without sliding* along the pushing constraint. The instantaneous velocity of a contact point is completely constrained as it is for fixed contact, so the instantaneous analysis is the same.

The goal of this section is to find the relation between the object's motion and the constraint surface's motion. The results depend on the object geometry for fixed contact. Given a straight line motion by the constraint plane, then if the object has a single point of support, the object's entire motion may be characterized in closed form. If the object has three points of support, or if the pressure distribution

is known by some other means, then the velocity can be obtained by numerical means (*not*, however, by integrating the acceleration). However, even if the pressure distribution is indeterminate, we may obtain one important piece of information by inspection–whether the object will rotate and if so in which direction.

These results will be demonstrated under the assumption that the inertial forces are dominated by the frictional forces. Analysis depending on this assumption will be referred to as *quasi-static* analysis. In section 2.5 the use of this assumption will be discussed in detail. The important point is that quasi-static analysis is appropriate at low speeds or for objects with low inertia. A quasi-static trajectory represents the limit of the object's motion as the time-scale of the constraint plane's motion is expanded. The results agree well with our intuition of the behavior of objects being pushed about on a table top.

2.2.1. Rotation Mode

First we will show how the position of the center of friction determines whether rotation occurs, and if so in which direction. For the sake of simplicity, we will demonstrate the result first for planar objects, and then generalize to three dimensions. The terms used are shown in figure 16. We will define the *line of pushing* to be the line passing through the contact point in the direction that the constraint is moving. The coordinate system is chosen so that the contact point x_c is at the origin, with the line of pushing coincident with the y-axis. x_0 is the center of friction. R is the support region, the area of contact between the object and the support plane. The pressure distribution is $p(x)$, defined on R. The contact force exerted on the object at x_c is f_c. The instantaneous center of rotation is x_r. An elementary result of kinematics is that the line from the center of rotation to any point must be perpendicular to the velocity of that point. Since the velocity of x_c lies on the y-axis, the center of rotation x_r must lie on the x-axis. The magnitude of the velocity of the constraint, and of the contact point, is v, and the angular velocity of the object is $\dot{\theta}$.

We wish to characterize the object's motion. The velocity of the contact point x_c is known, but the angular velocity $\dot{\theta}$ is unknown. The contact force is applied at x_c, and hence exhibits no moment about x_c. Neglecting the inertial forces, the
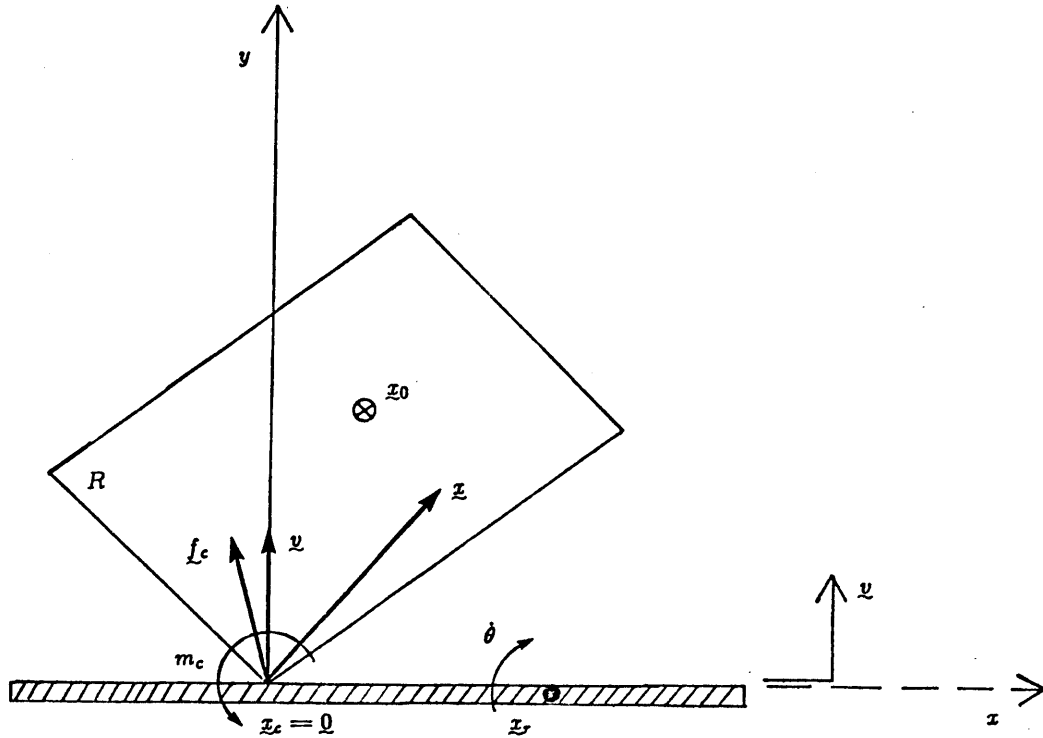
Figure 16. Planar Fixed Contact Pushing. ℓ_P is line of pushing.

moment of the frictional force about $\underline{x}_c$ must therefore be zero, which gives the necessary equation for determining $\dot{\theta}$:

$$m_f(x_r) = 0 \qquad (2.7)$$

where $\underline{x}_r = (x_r, 0)^T$. Equation 2.7 is the *quasi-static equation*. Exploitation of this equation yields the desired results.

Theorem 2. *If pushing at a single fixed point yields translation, then the center of friction must lie on the line of pushing.*

Proof: By our choice of coordinate system, the object is translating in the y direction. Theorem 1 says that the frictional forces reduce to a single force applied downward through the center of friction. For this force to exhibit no moment about the contact point, the center of friction must lie on the y-axis. ∎

Corollary. *When pushing at a single fixed point, if the center of friction does not lie on the line of pushing, then the object must rotate.*

Theorem 3. *During single fixed point pushing, if the center of friction lies on the line of pushing, and not all the normal support force is applied on the x-axis; then the object must translate.*

Proof: Translation corresponds to a rotation center at infinity, hence we must show that ∞ is the unique root of the quasi-static equation $m_f(x_r) = 0$. It is simple to show that ∞ is at least one of the roots; when the center of friction is on the line of pushing, the total frictional force will act along the line of pushing (theorem 1), exhibiting no moment about the contact point.

It is slightly more difficult to show that this root is unique. This will be proven by showing that the function $m_f(x_r)$ is an injection, that is, that no two values of x_r give the same moment. It follows that ∞ is the unique root of $m_f(x_r) = 0$.

The x-coordinate of the rotation center, x_r, may take on any value on the real line except zero, and may also take the value ∞, which corresponds to translation. We will consider this domain to be connected at ∞, so that x_r is considered to be increasing from the low end of the $+x$-axis through ∞ and on up to the high end of the $-x$-axis. For the moment due to friction we have equation 2.6:

$$m_f = -\mu \operatorname{sgn}(\dot{\theta}) \int_R x \cdot \frac{x - x_r}{|x - x_r|} p(x) \, dA$$

It is easily verified that the direction vector

$$\operatorname{sgn}(\dot{\theta}) \frac{x - x_r}{|x - x_r|}$$

does not change sense as x_r passes from the positive x-axis through infinity to the negative x-axis. The choice of conventions for $x_r = \infty$ guarantees that the moment as a function of x_r is continuous. By taking the derivative with respect to x_r, we find that the moment is a monotonic decreasing function of x_r:

$$\frac{dm_f}{dx_r} = -\mu\,\mathrm{sgn}(\dot{\theta}) \int_R \underline{x} \cdot \frac{d}{dx_r} \frac{\underline{x} - \underline{x}_r}{|\underline{x} - \underline{x}_r|} p(\underline{x})\, dA$$

$$= -\mu\,\mathrm{sgn}(\dot{\theta}) \int_R \underline{x} \cdot -\frac{|\underline{x} - \underline{x}_r|^2 \hat{i} - (\underline{x} - \underline{x}_r)(x - x_r)}{|\underline{x} - \underline{x}_r|^3} p(\underline{x})\, dA$$

$$= \mu\,\mathrm{sgn}(\dot{\theta}) \int_R \frac{(\underline{x}x_r - x_r\underline{x}) \cdot (\underline{x} - \underline{x}_r)}{|\underline{x} - \underline{x}_r|^3} p(\underline{x})\, dA$$

$$= \mu\,\mathrm{sgn}(\dot{\theta}) \int_R \frac{y^2 x_r}{|\underline{x} - \underline{x}_r|^3} p(\underline{x})\, dA$$

$\mathrm{sgn}\,\dot{\theta} = -\mathrm{sgn}\,x_r$, so finally we have

$$\frac{dm_f}{dx_r} = -\mu|x_r| \int_R \frac{y^2}{|\underline{x} - \underline{x}_r|^3} p(\underline{x})\, dA$$

The integrand is non-negative for all $\underline{x}$ in R, and is positive for at least some $\underline{x}$ in R. The derivative is continuous at ∞, taking on a value of zero. Hence the moment is a monotonic decreasing, continuous function of x_r, and is therefore an injection.

∎

Theorem 4. *Assume that not all of the support force lies on the x-axis. The rotation mode is respectively clockwise, fixed, counter-clockwise if and only if the center of friction lies respectively to the left, on, to the right of the line of pushing.*

Proof: The case of the center of friction on the line of pushing is given by theorems 2 and 3. We need to prove the result for the center of friction to the left or right of the line of pushing. For this proof we show that $m_f(x_r)$ has essentially the form shown in figure 17; that is, that it starts out positive on the low end of the $+x$-axis, and passes continuously and monotonically to negative values at the high end of the $-x$-axis. Again we use equation 2.6:

$$m_f = -\mu\,\mathrm{sgn}(\dot{\theta}) \int_R \underline{x} \cdot \frac{\underline{x} - \underline{x}_r}{|\underline{x} - \underline{x}_r|} p(\underline{x})\, dA$$

As x_r approaches 0 from the $+x$ direction, m_f approaches the limiting value $\mu \int_R |\underline{x}| p(\underline{x})\, dA$, which is positive. Let $0+$ be a number on the $+x$-axis close enough to 0 that $m_f(0+)$ is positive. In similar fashion we can define $0-$ to be close enough

42
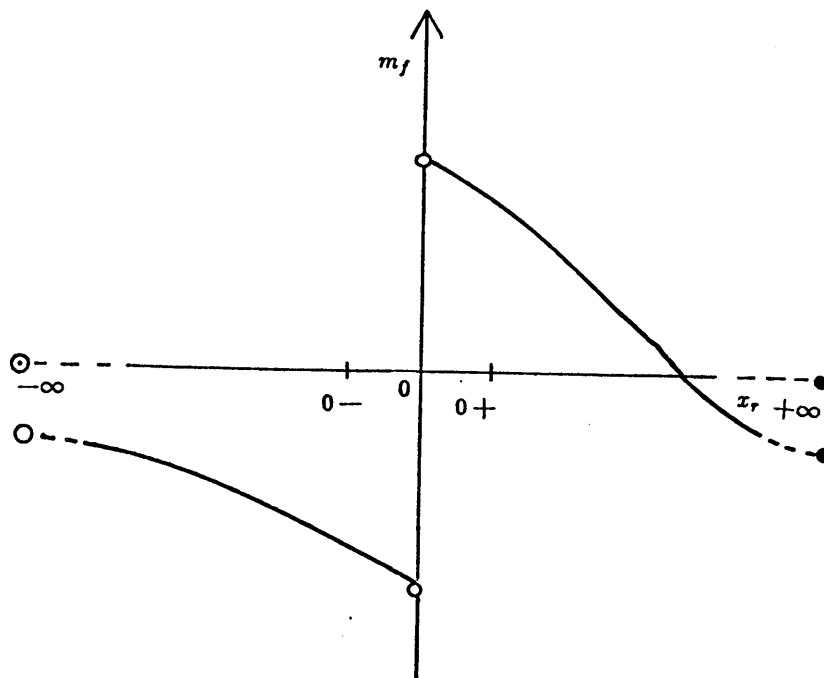
Figure 17. Typical plot of $m_f(x_r)$

to 0 from the minus side that $m_f(0-)$ is negative. Now, assume that the center of friction lies to the right of the line of pushing. Then by theorem(1) we know that $m_f(\infty)$ is negative. Since m_f is continuous, it must take on the value 0 for some x_r between $0+$ and ∞ by the mean-value theorem. Since m_f is an injection, this is the only root. Hence x_r must lie on the $+x$-axis, corresponding to clockwise rotation.

If the center of friction lies to the left of the line of pushing, then $m_f(\infty)$ is positive, and the root of $m_f(x_r)$ must lie on the $-x$-axis, corresponding to counter-clockwise rotation. ∎

Theorem 4 gives us a powerful method for reasoning about the motion of an object being pushed. It is possible to determine by inspection the gross characteristics of the object's motion. For example, figure 18 shows a block being pushed by a vertical plane. If the object is slightly tilted either to the left or to the right, contact will occur at the corresponding vertex, and corrective rotations will bring the lower edge of the block back into contact with the constraint. The orientation
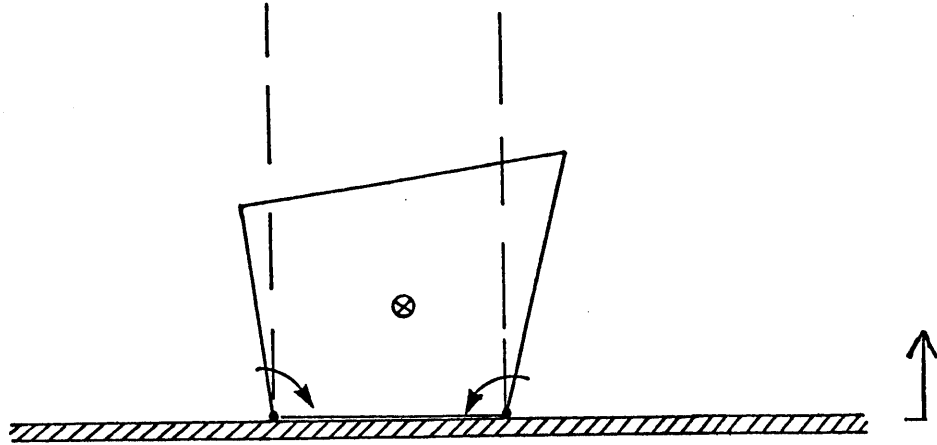
Figure 18. Stable Pushing of Block by Inspection

of the block on the constraint is therefore stable.

Theorem 4 only applies if some of the support force is off of the x-axis. What happens if the pressure distribution is zero except on the x-axis? Then $m_f(x_r)$ is not strictly decreasing, but will be constant for x_r in intervals of the x-axis where $p(\underline{x})$ vanishes. If a root of $m_f(x_r) = 0$ lies in one of these intervals, then any point in the interval is a root. This may seem strange, since it suggests that the location of the instantaneous rotation center is non-deterministic. The root of the problem is the quasi-static assumption, which neglects inertial forces. When this problem occurs, the angular momentum of the object must be taken into account to predict the location of the instantaneous rotation center.

2.2.2. Rotation Rate

Inspection tells us whether the object will rotate and in which direction. It does not tell us how fast the rotation will be. The answer to this question is given by the solution of the equation $m_f = 0$, where m_f is given by equation 2.6:

$$m_f = -\mu \operatorname{sgn}(\dot{\theta}) \int_R \underline{x} \cdot \frac{\underline{x} - \underline{x}_r}{|\underline{x} - \underline{x}_r|} p(\underline{x}) \, dA$$

44

The solution of this equation is investigated in particular circumstances in each of the next four sections. In some special cases the solution can be found, but in the most general case the indeterminacy of the pressure distribution prevents unique solution of the equation.

Known pressure distribution

Occasionally we have the luxury of knowing the actual pressure distribution, either by tactile feedback, by the use of especially well-behaved materials, or if the contact surface has a special shape. When this occurs, the moment as a function of the rotation center is easily computed from equation 2.6. In the proof of theorem 4, we found that this function is very nicely behaved, being continuous and monotonic, suggesting the use of numerical methods. A false-position type root-finder [Acton 1970] was implemented which converges quickly and reliably.

Single point of support

If there is a single point of support, the orientation of the object as a function of time may be obtained in closed form. A characterization of the motion can also be obtained using *centrodes*, a method of describing planar motion commonly used in kinematics [Reuleaux 1876, Hilbert and Cohn-Vossen 1952]. Any planar motion can be described as the motion obtained by letting one plane curve, the *moving centrode*, roll without slipping along a second plane curve, the *fixed centrode*. The point of contact between the two centrodes is the instantaneous rotation center.

If there is a single point of support, the entire normal force is applied at that point, which is therefore the center of friction. Equation 2.6 degenerates to:

$$m_f = -\mu \operatorname{sgn}(\dot{\theta}) \underline{x}_1 \cdot (\underline{x}_1 - \underline{x}_r) f_1$$

where $\underline{x}_1$ is the single point of support and f_1 is the force applied at $\underline{x}_1$. The root of $m_f = 0$ is most easily found geometrically. Clearly m_f vanishes only when $\underline{x}_1$ is orthogonal to $\underline{x}_1 - \underline{x}_r$, as in figure 19. We obtain from the figure

$$|\underline{x}_1| = x_r \cos\theta$$
$$x_r = \frac{|\underline{x}_1|}{\cos\theta}$$

45
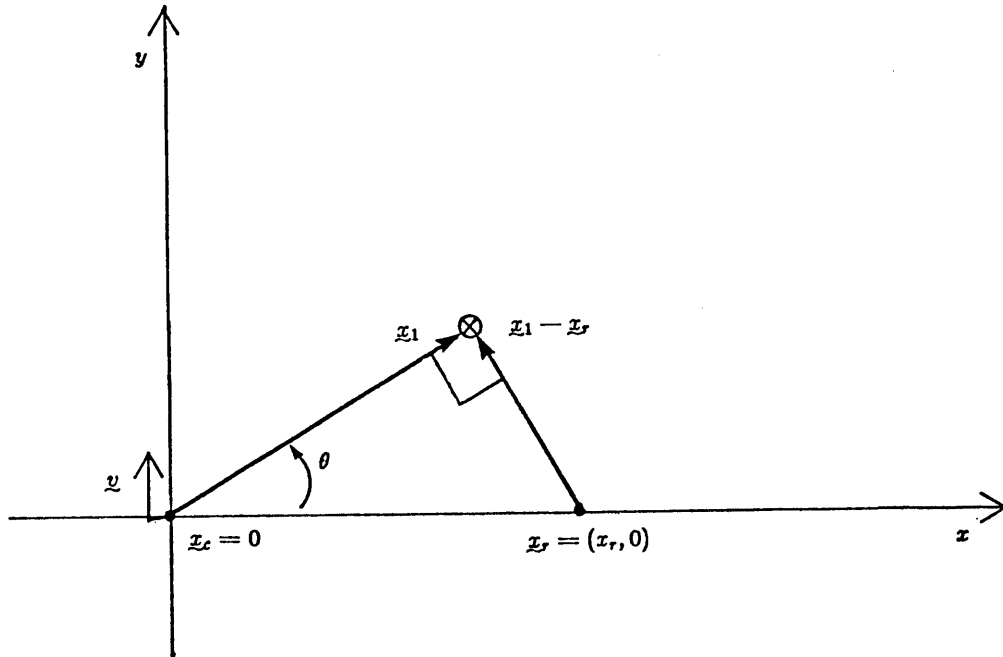
Figure 19. Pushing with single point of support

But $x_r = -v/\dot\theta$ so we have

$$\dot\theta = -\frac{v\cos\theta}{|x_1|}$$

This differential equation is separable; we solve by separating variables and integrating both sides:

$$-\frac{|x_1|}{v}\int\frac{d\theta}{\cos\theta} = \int dt$$

$$-\frac{|x_1|}{v}\ln|\sec\theta + \tan\theta| = t - t_0$$

obtaining a closed-form relation between the orientation θ and the time t.

To characterize the motion in terms of centrodes, we observe that the line through x_1 and x_r is fixed with respect to the object. Since the instantaneous rotation center is on this line, this is the *moving centrode*. To find the fixed

46
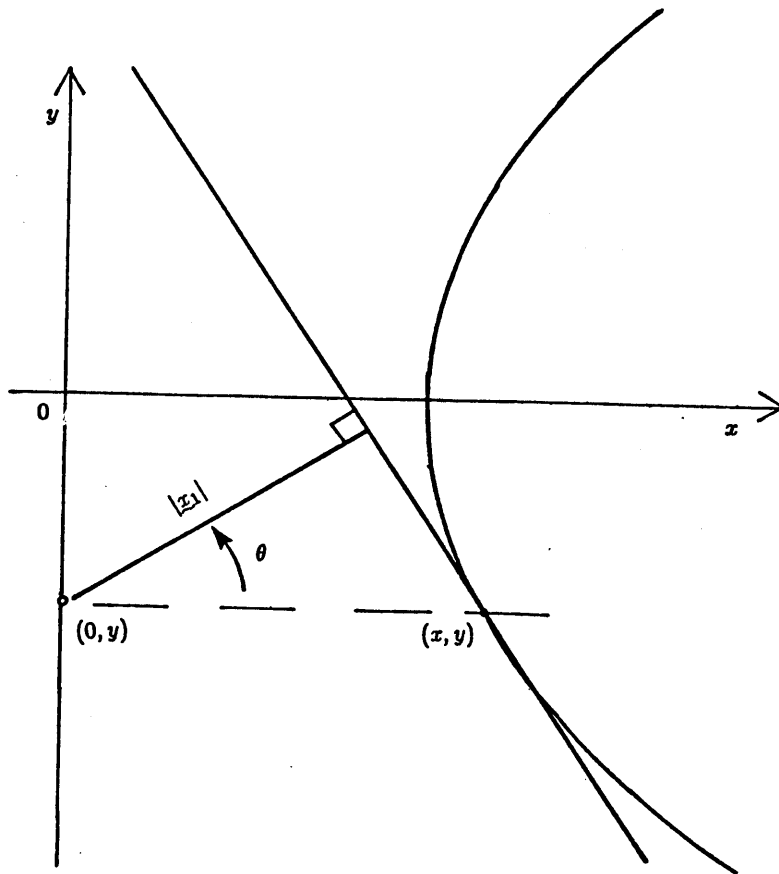
Figure 20. Finding the Fixed Centrode.

centrode, we must use a fixed coordinate system (figure 20). The y–axis coincides with the line of pushing, as before, but the contact point is not necessarily at the origin. If (x, y) is the position of the center of rotation, then $(0, y)$ is the position of the contact point. The differential change in y is related to the differential change in θ kinematically:

$$dy = x d\theta$$
$$= |x_1| \frac{d\theta}{\cos \theta}.$$

Integrating both sides,

$$y = |x_1| \ln |\sec \theta + \tan \theta|.$$
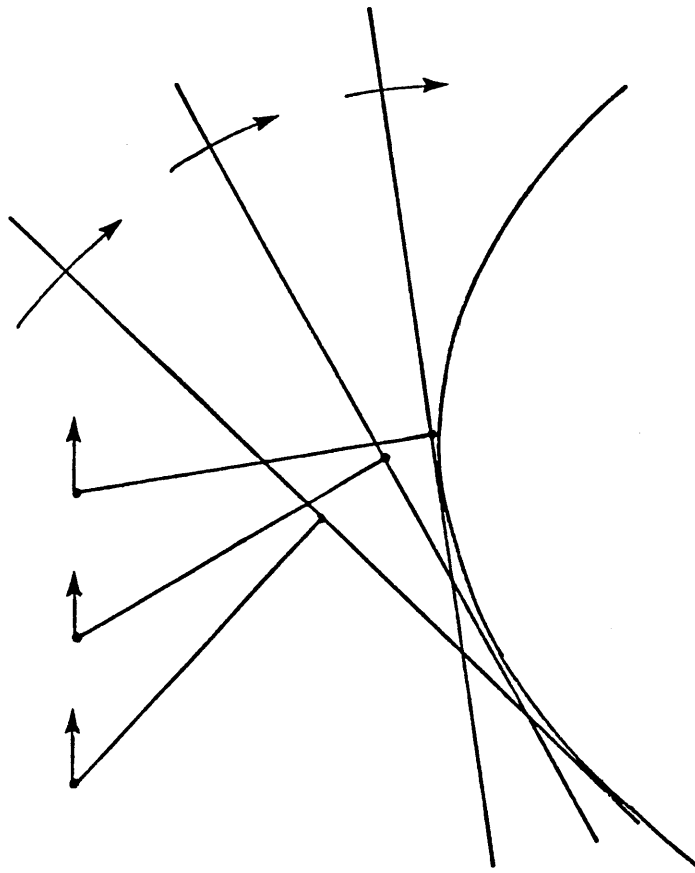
Figure 21. Centrodes resulting from single point of support

Finally, we substitute $x/|x_1|$ for $\sec\theta$ and substitute $\sqrt{x^2 + |x_1|^2}/|x_1|$ for $\tan\theta$ to obtain:

$$\frac{y}{|x_1|} = \ln\left(\frac{x}{|x_1|} + \sqrt{\frac{x^2}{|x_1|^2} - 1}\right)$$

which gives half of the fixed centrode curve. The other half is obtained by reflection in the x-axis. The two centrodes and the resulting motion are illustrated in figure 21.

Three point support

No closed form expression for x_r is available in the case of three points of

support. However, if the center of mass of the object and the object's weight are known, the pressure distribution may be determined as follows. Let x_1, x_2, x_3 be the three support points, and let f_1, f_2, and f_3 be the normal components of the corresponding support forces. Let x_0 be the center of mass and let f_0 be the total weight of the object. Then balancing force and moments gives:

$$x_1 f_1 + x_2 f_2 + x_3 f_3 = x_0 f_0$$
$$y_1 f_1 + y_2 f_2 + y_3 f_3 = y_0 f_0$$
$$f_1 + f_2 + f_3 = f_0$$

which can be rewritten as

$$X \underline{f} = f_0 \begin{bmatrix} x_0 \\ y_0 \\ 1 \end{bmatrix}$$

where

$$X = \begin{bmatrix} x_1 & x_2 & x_3 \\ y_1 & y_2 & y_3 \\ 1 & 1 & 1 \end{bmatrix}$$

$$\underline{f} = \begin{bmatrix} f_1 \\ f_2 \\ f_3 \end{bmatrix}.$$

X is singular if and only if x_1, x_2, and x_3 are collinear. Otherwise we may invert the matrix to obtain the complete pressure distribution:

$$\underline{f} = f_0 X^{-1} \begin{bmatrix} x_0 \\ y_0 \\ 1 \end{bmatrix}. \tag{2.8}$$

The solution yields positive forces if and only if x_0 is inside the triangle whose vertices are the points of support. If this condition is met, equation 2.8 allows computation of the pressure distribution given the weight and center of mass of the object. Hence the problem of three-point support is reduced to the problem of known support treated above, and the false-position root-finder previously described may now be applied.

In general, the pressure will be distributed over more than three points, even over finite area. When the pressure distribution is indeterminate, the angular velocity is also indeterminate. If we cannot predict the exact angular velocity, the next best thing is to determine the range of possible angular velocities, which is the subject of this section. The important result is that to search for the fastest or slowest angular velocity, we only have to consider three-point support–the range of angular velocities possible with three-point support is identical to the range of angular velocities possible with arbitrary support. While numerical search through all possible three-point pressure distributions is not an appealing prospect, it is certainly more appealing than search through all possible supports.

Theorem 5. x_r^* is an extremum of the set of all possible rotation centers if and only if it is an extremum of the set of all possible rotation centers obtainable with three-point support.

Proof: Recall that the rotation center may lie anywhere on the x–axis except at the origin, and may also be at ∞. This domain is considered to be ordered starting at the low end of the $+x$–axis and increasing through ∞ to the high end of the $-x$–axis. There are two extreme values of the set of possible rotation centers to consider: the greatest lower bound and the least upper bound. We will prove that x_r^* is the glb of the set of all possible rotation centers if and only if it is the glb of the set of all rotation centers obtainable with three-point support. The case of the lub is similar.

It will suffice to assume that x_r^* is the glb of the set of all possible rotation centers, and show that it may be obtained with three-point support. From this the "only if" part of the theorem follows immediately, since if x_r^* is attained with three-point support it must represent the glb of the three-point supports because three-point supports are a subset of the set of all possible supports. The "if" part is proven as follows: Suppose x_r^* represents the glb of three-point supports, but not of the set of general supports. The glb of general supports is known to be attainable with three-point support, contradictory to hypothesis.

All that remains is to show that if x_r^* is the glb of the rotation centers attainable with general support, then it may be attained with three-point support. This involves two steps: (1) show that if x_r^* is the glb of rotation centers giving zero moment (i.e. the glb of all roots of the quasi-static equation $m_f(x_r) = 0$), then zero is the glb of moments for x_r^*; and (2) show that for a given rotation center x_r, if zero is the glb of the moments, it can be attained with three-point support.

Some additional notation will be helpful at this point. Let $m_f(x_r, p)$ give the frictional moment as a function of the rotation center x_r and the pressure distribution p. Let P be the set of all feasible pressure distributions, i.e. those giving the proper force f_0 and centroid x_0. Let $P_3 \subset P$ be the set of feasible three-point supports. Let x_r^* be the glb of the set of possible rotation centers. We have:

$$x_r^* = \text{glb}\{x_r | \exists \text{ feasible } p \text{ in } P \text{ such that } m_f(x_r, p) = 0\}$$

First we wish to show that zero is the greatest lower bound of the possible frictional moments with rotation center x_r^*:

$$0 = \text{glb}\{m_f(x_r^*, p) | p \text{ is feasible}\}$$

For any given pressure distribution we know from the proof of theorem 4 that m_f is continuous in x_r, and that for x_r "low" enough, $m_f(x_r, p)$ is positive. Hence by the mean value theorem if $m_f(x_r^*, p)$ is less than zero, there will be some rotation center x_r less than x_r^* with $m_f(x_r, p)$ equal to zero, contrary to the definition of x_r^*.

Finally we need to show that if zero is the greatest lower bound of moments attained with a given rotation center x_r, then there is a three-point support p such that $m_f(x_r, p)$ is zero. For this part we will leave x_r fixed and write the moment as

$$m_f(p) = \int_R g(\underline{x}) \rho(\underline{x}) \, dA \tag{2.9}$$

where

$$g(\underline{x}) = -\mu \, \text{sgn}(\dot{\theta}) f_0 \underline{x} \cdot \frac{\underline{x} - \underline{x}_r}{|\underline{x} - \underline{x}_r|}$$

$$\rho(\underline{x}) = \frac{p(\underline{x})}{f_0}$$

51

ρ is the normalized pressure distribution. A given ρ is feasible if and only if

$$\int_R \rho \, dA = 1$$

$$\int_R x\rho \, dA = x_0$$

·Equation 2.9 gives the frictional moment as the weighted average of $g(x)$, and $g(x)$ represents the maximum potential contribution of a point x to the moment. Let G map the contact region R into $\Re^3$ by associating with each point x in R its potential moment $g(x)$:

$$G\left(\begin{bmatrix} x \\ y \end{bmatrix}\right) = \begin{bmatrix} x \\ y \\ g(x) \end{bmatrix}$$

This gives a nice geometrical interpretation of the calculation of the moment. G maps R into a surface in $\Re^3$, and the set $\{\int_R G(x)\rho(x) \, dA \mid \int_R \rho(x) \, dA = 1\}$ is the set of all convex linear combinations of the points in that surface in $\Re^3$, i.e. it is the convex hull of the surface. There is another constraint on ρ—the centroid must be x_0. Any feasible point in the convex hull of $G(R)$ must satisfy

$$\int_R G(x)\rho(x) \, dA = \int_R \begin{bmatrix} x \\ y \\ g(x) \end{bmatrix} \rho(x) \, dA$$
$$= \begin{bmatrix} x_0 \\ y_0 \\ \int_R g(x)\rho(x) \, dA \end{bmatrix}$$

Hence the feasible points give a line segment obtained by intersecting the convex hull of $G(R)$ with a vertical line through x_0. By hypothesis, zero is the greatest lower bound of all possible frictional moments, so the bottom of this line segment has third coordinate zero. The problem is to show that this point, which is the convex linear combination of a possibly infinite number of points of $G(R)$, is also a convex linear combination of just three points in $G(R)$. Intuition (and Caratheodory's theorem on convex sets [Grunbaum 1967]) tells us that every point in the convex hull of $G(R)$ may be expressed as a linear combination of just four points in $G(R)$. Hence the extremal point lies in the convex hull of just four points, which is a

52

polyhedral subset of the convex hull of $G(R)$. Being extremal, it must lie on a face of this polyhedron, and hence may be expressed using just three (or less) of the four vertices. ∎

2.2.3. Extension to three dimensions

We now wish to extend the planar analysis to the case of a rigid three-dimensional body, in planar contact with the support. Difficulties arise because the contact point is not necessarily in the horizontal plane. This gives rise to moments which can affect the position of the center of friction, and if large enough, can cause the object to tip over. These moments obviously depend on the magnitude and direction of the force at the contact point, which is determined by the object's motion. Since the planar analysis uses the position of the center of friction to determine the object's motion, there is a potential for circularity in the analysis which must be avoided. In this section, we review previous results and extend those affected by the indeterminacy of the center of friction. The final three-dimensional analysis is analogous to the planar analysis although algebraically more complex.

First we obtain an expression for the position of the center of friction. Let $\{\underline{f}_a\}$ be the set of all applied forces, including the contact force $\underline{f}_c$. The set of applied forces excluding the contact force will be called the *external* forces $\{\underline{f}_e\}$. As before, we define the center of friction $\underline{x}_0$ to be the point in the $x-y$ plane such that the system of applied forces reduces to a single force $\underline{F}_a$ through $\underline{x}_0$ and a single moment M_a about a vertical line through $\underline{x}_0$. In similar fashion let $\underline{x}_e$ be a point in the $x-y$ plane such that the system of external forces reduces to a single force $\underline{F}_e$ through $\underline{x}_e$ and a single moment M_e about a vertical line through $\underline{x}_e$. $\underline{x}_e$ would be the center of friction, but for the contact force. As a simple consequence of these definitions, we find:

$$M_a\hat{k} = (\underline{x}_e - \underline{x}_0) \times \underline{F}_e + (\underline{x}_c - \underline{x}_0) \times \underline{f}_c + M_e\hat{k}$$

The first and second component equations of this vector equation may easily be used to obtain the following expression for the center of friction:

$$x_0 = \frac{x_e F_{e,z} + \begin{bmatrix} x_c \\ y_c \end{bmatrix} f_{c,z}}{F_{e,z} + f_{c,z}} - \frac{z_c}{F_{e,z} + f_{c,z}} \begin{bmatrix} f_{c,x} \\ f_{c,y} \end{bmatrix}$$

where we use the components of $\underline{F}_e = (F_{e,x}, F_{e,y}, F_{e,z})^T$, $\underline{x}_c = (x_c, y_c, z_c)^T$, and $\underline{f}_c = (f_{c,x}, f_{c,y}, f_{c,z})^T$. In many cases, the external applied forces and the vertical contact force are known, with the x and y components of the contact force determined by the motion of the object. Hence we define the *nominal center of friction* $\underline{x}_n$:

$$\underline{x}_n = \frac{x_e F_{e,z} + \begin{bmatrix} x_c \\ y_c \end{bmatrix} f_{c,z}}{F_{e,z} + f_{c,z}} \tag{2.10}$$

giving a simple expression for the true center of friction:

$$\underline{x}_0 = \underline{x}_n - \frac{z_c}{F_{ez} + f_{cz}} \begin{bmatrix} f_{cx} \\ f_{cy} \end{bmatrix}. \tag{2.11}$$

The most important result of the planar analysis was the inspection method for finding the direction of rotation of the object. The formula giving the frictional moment at the point of contact remains unchanged, so theorem (4) is unchanged. Unfortunately, the center of friction is no longer easily determined. Fortunately, the theorems hold not just for the center of friction, but for the nominal center of friction as well. This is a simple consequence of theorem (6).

Theorem 6. *The center of friction and the nominal center of friction lie on the same side of the line of pushing (or are both on the line of pushing.)*

Proof: By equation 2.10 the nominal center of friction must lie on the line segment $\overline{\underline{x}_c \underline{x}_e}$. We will assume that $\underline{x}_0$ and $\underline{x}_n$ are on opposite sides of the line of pushing and obtain a contradiction. The assumed relation is illustrated in figure 22. By equation 2.11 the line determined by $\underline{x}_n$ and $\underline{x}_0$ is parallel to the contact force. It is easily verified by inspection of the figure that the relation shown can only occur if the center of friction falls between the line of pushing and the line of action of the contact force. It will later be shown (corollary to theorem 10) that the line of action of the contact force and the line of pushing lie on the same side of the center of friction, a contradiction. ∎

54

Figure 22. Construction for theorem 6. ℓ_P is line of pushing, ℓ_F is line of force.

Corollary. *Theorem (4) holds with "nominal center of friction" substituted for "center of friction".*

As with planar systems, the direction of rotation may be determined by inspection, if the applied forces, excluding the horizontal components of the pushing force, are known. The next problem is to determine the actual rate of rotation. If the pressure distribution is somehow determined, then again numerical means will yield the rate of rotation. As with the planar analysis, we begin by writing the quasi-static equation:

$$(\underline{x}_e - \underline{x}_c) \times \underline{F}_e \cdot \hat{k} + M_e + \mu \operatorname{sgn}(\dot{\theta}) \int_R (\underline{x} - \underline{x}_c) \cdot \frac{\underline{x} - \underline{x}_r}{|\underline{x} - \underline{x}_r|} p(\underline{x}) \, dA = 0. \qquad (2.12)$$

If the pressure distribution is not known, the position of the instantaneous rotation center cannot be predicted. In analogy with our treatment of the plane, we will focus on three-point support. Theorem 5 still holds, so bounds on the angular velocity can be obtained by investigating the space of all three-point supports, as before.

For three-point support, it is possible to find a single equation in x_r, as with the planar analysis, but the expression is much more complex. Ultimately a numerical approach will be required to find roots of equation 2.12, but first we must eliminate $p(\underline{x})$. As in section 2.2.2 we let f_1, f_2, and f_3 represent the forces at $\underline{x}_1$, $\underline{x}_2$, and $\underline{x}_3$ respectively, and let $\underline{f}$ be the vector $(f_1, f_2, f_3)^T$. As before, we obtain

$$\underline{f} = f_0 X^{-1} \begin{bmatrix} x_0 \\ y_0 \\ 1 \end{bmatrix} \tag{2.13}$$

where

$$X = \begin{bmatrix} x_1 & x_2 & x_3 \\ y_1 & y_2 & y_3 \\ 1 & 1 & 1 \end{bmatrix}.$$

This gives an expression for $\underline{f}$ which depends on $(x_0, y_0, 1)^T$ which must now be eliminated. We can modify equation 2.11 to give

$$\begin{bmatrix} x_0 \\ y_0 \\ 1 \end{bmatrix} = \begin{bmatrix} x_n \\ y_n \\ 1 \end{bmatrix} - \frac{z_c}{F_{ez} + f_{cz}} \begin{bmatrix} f_{cx} \\ f_{cy} \\ 0 \end{bmatrix}. \tag{2.14}$$

Substituting into equation 2.13 we obtain

$$\underline{f} = f_0 X^{-1} \left(\begin{bmatrix} x_n \\ y_n \\ 1 \end{bmatrix} - \frac{z_c}{F_{ez} + f_{cz}} \begin{bmatrix} f_{cx} \\ f_{cy} \\ 0 \end{bmatrix} \right). \tag{2.15}$$

Now we need another set of equations for f_{cx} and f_{cy}. Using equation 2.5 for the frictional force, balance of forces gives:

56

$$0 = \begin{bmatrix} F_{ex} \\ F_{ey} \\ 0 \end{bmatrix} + \begin{bmatrix} f_{cx} \\ f_{cy} \\ 0 \end{bmatrix} - \mu \operatorname{sgn}(\dot{\theta}) \hat{k} \times \sum_{i=1}^{3} \frac{x_i - x_r}{|x_i - x_r|} f_i.$$

This can be rewritten as

$$0 = \begin{bmatrix} F_{ex} \\ F_{ey} \\ 0 \end{bmatrix} + \begin{bmatrix} f_{cx} \\ f_{cy} \\ 0 \end{bmatrix} - \mu \operatorname{sgn}(\dot{\theta}) T \underline{f} \tag{2.16}$$

where

$$T = \begin{bmatrix} \hat{k} \times \frac{x_1 - x_r}{|x_1 - x_r|} & \hat{k} \times \frac{x_2 - x_r}{|x_2 - x_r|} & \hat{k} \times \frac{x_3 - x_r}{|x_3 - x_r|} \\ 0 & 0 & 0 \end{bmatrix}.$$

Substituting equation 2.15 into equation 2.16 we obtain

$$0 = \begin{bmatrix} F_{e,x} \\ F_{e,y} \\ 0 \end{bmatrix} + \begin{bmatrix} f_{c,x} \\ f_{c,y} \\ 0 \end{bmatrix} - \mu \operatorname{sgn}(\dot{\theta}) T \left(f_0 X^{-1} \left(\begin{bmatrix} x_n \\ y_n \\ 1 \end{bmatrix} - \frac{z_c}{F_{e,z} + f_{c,z}} \begin{bmatrix} f_{c,x} \\ f_{c,y} \\ 0 \end{bmatrix} \right) \right).$$

Expanding, we have

$$0 = \begin{bmatrix} F_{e,x} \\ F_{e,y} \\ 0 \end{bmatrix} + \begin{bmatrix} f_{c,x} \\ f_{c,y} \\ 0 \end{bmatrix} - \mu \operatorname{sgn}(\dot{\theta}) T f_0 X^{-1} \begin{bmatrix} x_n \\ y_n \\ 1 \end{bmatrix} + \varsigma T X^{-1} \begin{bmatrix} f_{c,x} \\ f_{c,y} \\ 0 \end{bmatrix}$$

where

$$\varsigma = \mu \operatorname{sgn}(\dot{\theta}) f_0 \frac{z_c}{F_{e,z} + f_{c,z}}.$$

Collecting terms, we obtain

$$- \begin{bmatrix} F_{e,x} \\ F_{e,y} \\ 0 \end{bmatrix} + \mu \operatorname{sgn}(\dot{\theta}) T f_0 X^{-1} \begin{bmatrix} x_n \\ y_n \\ 1 \end{bmatrix} = \left(I + \varsigma T X^{-1} \right) \begin{bmatrix} f_{c,x} \\ f_{c,y} \\ 0 \end{bmatrix}.$$

In order to solve for $(f_{c,x}, f_{c,y})$ it is necessary to invert $I + \varsigma T X^{-1}$. First we must verify that this matrix is non-singular. The matrix can be rewritten

$$I + \varsigma T X^{-1} = (X + \varsigma T) X^{-1}.$$

The matrix X is non-singular if and only if the points $\underset{\sim}{x}_1$, $\underset{\sim}{x}_2$, and $\underset{\sim}{x}_3$ are not collinear. This same condition also guarantees that $X + \varsigma T$ is non-singular. This is best demonstrated geometrically. The matrix may be rewritten

$$X + \varsigma T = \begin{bmatrix} \underset{\sim}{x}_1 + \varsigma \hat{k} \times \frac{\underset{\sim}{x}_1 - \underset{\sim}{x}_r}{|\underset{\sim}{x}_1 - \underset{\sim}{x}_r|} & \underset{\sim}{x}_2 + \varsigma \hat{k} \times \frac{\underset{\sim}{x}_2 - \underset{\sim}{x}_r}{|\underset{\sim}{x}_2 - \underset{\sim}{x}_r|} & \underset{\sim}{x}_3 + \varsigma \hat{k} \times \frac{\underset{\sim}{x}_3 - \underset{\sim}{x}_r}{|\underset{\sim}{x}_3 - \underset{\sim}{x}_r|} \\ 1 & 1 & 1 \end{bmatrix}.$$

This matrix is non-singular if and only if the vectors

$$\underset{\sim}{x}_i + \varsigma \hat{k} \times \frac{\underset{\sim}{x}_i - \underset{\sim}{x}_r}{|\underset{\sim}{x}_i - \underset{\sim}{x}_r|}, i = 1, 2, 3$$

are not collinear. Figure 23 shows an example construction of these vectors. It is easily verified that the vectors form a non-degenerate triangle similar to the triangle formed by the vectors $\underset{\sim}{x}_1$, $\underset{\sim}{x}_2$, $\underset{\sim}{x}_3$. Hence the matrix in question is singular if and only if the matrix X is singular.

Inverting the matrix gives the desired expression for $(f_{c,x}, f_{c,y}, 0)$:

$$\begin{bmatrix} f_{c,x} \\ f_{c,y} \\ 0 \end{bmatrix} = X(X + \varsigma T)^{-1} \left(\mu \operatorname{sgn}(\dot{\theta}) f_0 T X^{-1} \begin{bmatrix} x_n \\ y_n \\ 1 \end{bmatrix} - \begin{bmatrix} F_{e,x} \\ F_{e,y} \\ 0 \end{bmatrix} \right). \tag{2.17}$$

Equation 2.17 can be substituted back into equation 2.15 to get an expression for $\underset{\sim}{f}$. The expression for $\underset{\sim}{f}$ can be substituted into equation 2.12 which gives a single equation in a single unknown – x_r. The next step, not yet attempted, is to apply numerical methods to find the root of this equation.

2.3. Pushing with Sliding Contact

The problem of pushing an object restricted to planar motion was divided into two cases. The first case, studied above, assumes that the contact of the pushing constraint with the object is fixed or rolling. In this section, we assume that the contact is sliding. The results for sliding contact are similar to those for fixed contact, except that the role of the line of pushing is now assumed by a *line of force*, which is simply the line along which the contact force acts. As before, we first show that the rotation mode may be determined by inspection, and then turn our attention to the problem of finding the location of the instantaneous rotation
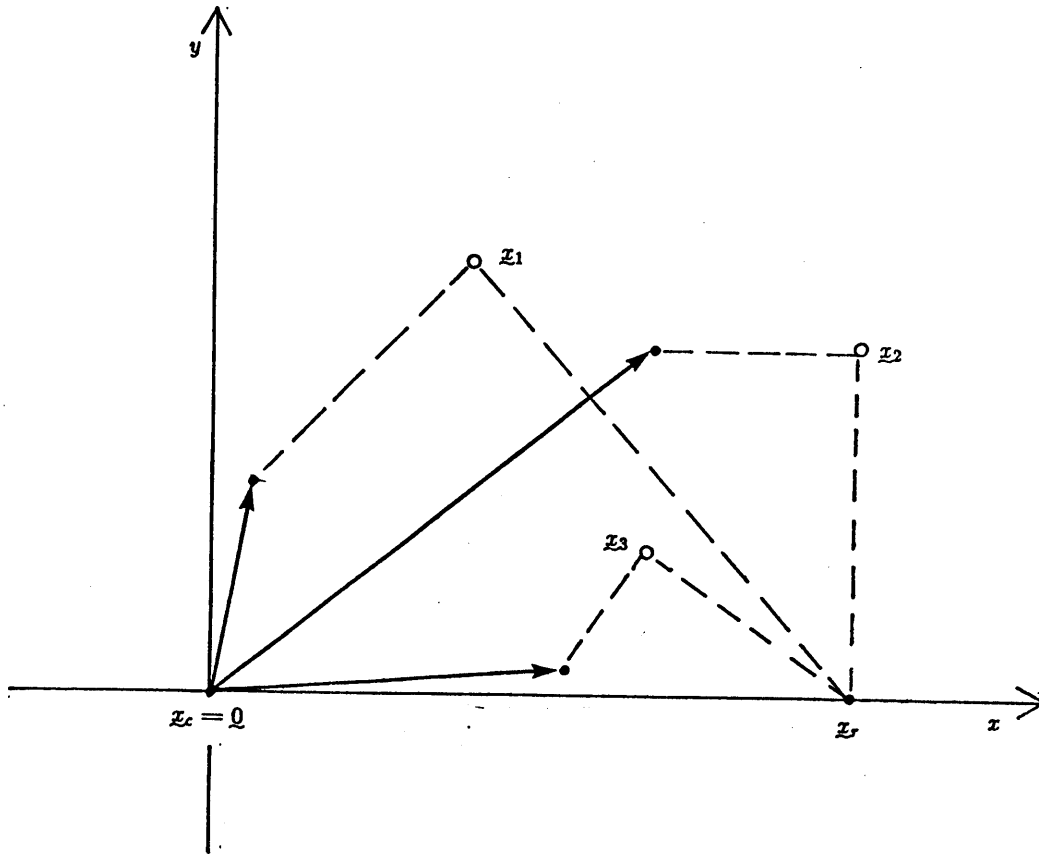
Figure 23. Columns of $X + \varsigma T$

center. The main difficulty arises because there are now *two* degrees of freedom, rather than one. The instantaneous rotation center may be almost anywhere in the extended plane. We therefore require two quasi-static equations, rather than one, whose simultaneous root is the rotation center.

Figure 24 illustrates some of the differences between the fixed contact case and the sliding contact case. In the case of fixed contact, the instantaneous velocity of the contact point is completely determined; that is, the pushing surface imposes two constraints on the contact point. In the case of sliding contact, there is only one constraint on the instantaneous velocity of the contact point. On the other hand, the contact force must now lie on the edge of the friction cone, as a consequence of Coulomb's law. We have lost a constraint on the instantaneous velocity of the contact point, but we have gained a constraint on the contact force.
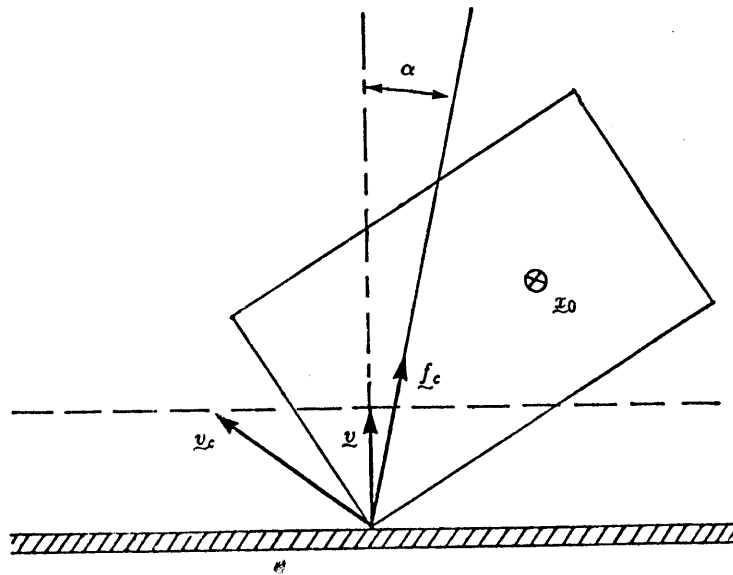
Figure 24. Sliding contact at pushing constraint. α is the friction angle $\tan^{-1}\mu$.

2.3.1. Rotation Mode

First we will show how to determine the rotation mode by inspection. In order to proceed with the development, we will distinguish two different sliding contact modes: *left-sliding* and *right-sliding*. By left-sliding we mean that the object is sliding to the left, from the point of view of the pushing constraint. Right-sliding is defined similarly.

If we apply Coulomb's law to the contact force between the object and the pushing constraint, we know that the force must lie on the edge of the friction cone. If left-sliding contact occurs, then the force must lie on the right edge of the friction cone. If right-sliding contact occurs, then the force must lie on the left edge of the friction cone. In either case we can predict the line along which the force must act, which we will term the *line of force*. The line of force plays the same role for sliding contact that the line of pushing plays for fixed contact.

Figure 25 shows the terminology for the analysis. It is most convenient to work in a coordinate frame whose origin coincides with the center of mass of the object

60
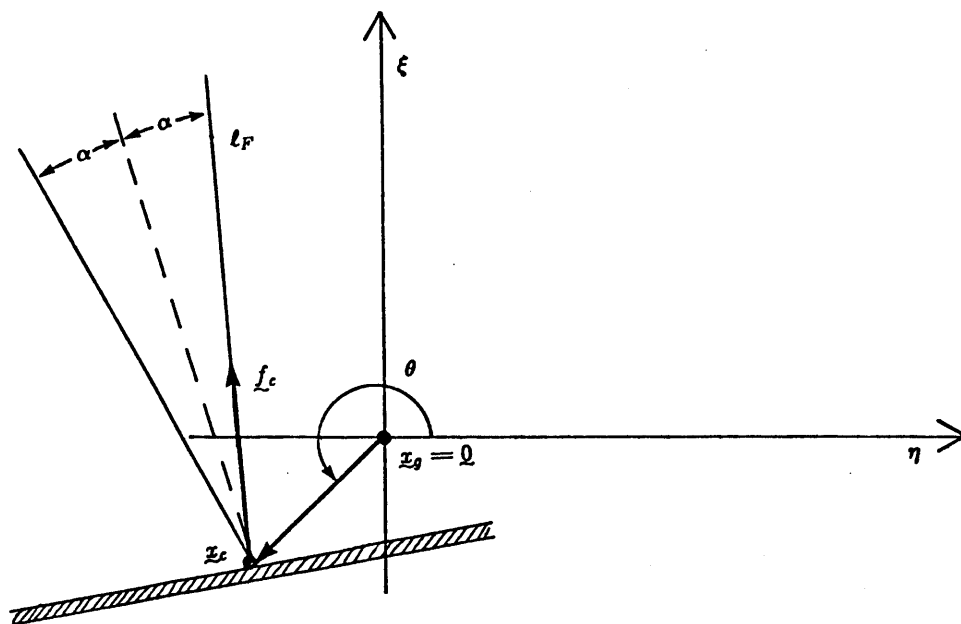
Figure 25. Terminology for sliding contact analysis. ℓ_F is the line of force.

(projected into the plane), and with one axis aligned with the line of force. Hence we define the η–ξ coordinate frame, with the ξ-axis parallel to the line of force. Let (η_c, ξ_c) be the coordinate representation of the contact point $\underline{x}_c$, and let (r_c, θ) be the the polar representation of (η_c, ξ_c).

The figure shows one possible circumstance giving rise to the particular line of force shown. The object is sliding to the left along the pushing constraint, which makes an angle of $\tan^{-1} \mu$ with the η-axis. The same line of force would occur if the object were sliding to the right with the pushing constraint making an angle of $-\tan^{-1} \mu$ with the η-axis.

We will assume that the applied forces are simply a gravitational component perpendicular to the plane of motion and the contact force applied along the line of force. If we write the equations of motion we obtain

$$\underline{F} = m\underline{\ddot{x}}_g$$
$$M = I\ddot{\theta}$$

where $\underline{F}$ is the total force tangent to the plane, M is the total moment of force about the vertical through $\underline{x}_g$, m is the total mass, and I is the rotational inertia about the vertical through $\underline{x}_g$. As in the case of fixed contact, we will work with the quasi-static equations, obtained by assuming that the inertial forces are negligible:

$$\underline{F} = \underline{0}$$
$$M = 0$$

If we expand $\underline{F}$ and M, we obtain

$$\underline{f}_f + \underline{f}_c = \underline{0}$$
$$m_f + (\underline{x}_c - \underline{x}_g) \otimes \underline{f}_c = 0$$

Now $\underline{f}_c$ is constrained to be parallel to the ξ-axis, so we have

$$\underline{f}_c = \begin{bmatrix} 0 \\ f_c \end{bmatrix}$$

Applying this constraint, and using the choice of origin as the center of mass $\underline{x}_g$, we obtain

$$f_{f,\eta} = 0$$
$$f_{f,\xi} + f_c = 0$$
$$m_f + \eta_c f_c = 0$$

The contact force magnitude f_c can be eliminated from these to obtain

$$f_{f,\eta} = 0 \tag{2.18}$$
$$m_f - \eta_c f_{f,\xi} = 0. \tag{2.19}$$

Sometimes the quasi-static equations will be rewritten as:

$$Q_1(\underline{x}_r, \theta) = 0$$
$$Q_2(\underline{x}_r, \theta) = 0$$

where $Q_1 = f_{f,\eta}$ and $Q_2 = m_f - \eta_c f_{f,\xi}$.

The quasi-static assumption gives two very simple equations in the force and moment due to friction. Equations 2.5 and 2.6 give the force and moment as

functions of the rotation center and the object's orientation. Hence equations 2.18 and 2.19 give the rotation center x_r as an implicit function of the object's orientation. Although we cannot solve the resulting equations for the rotation center x_r, we can use the equations to show that the rotation mode depends on the position of the center of friction with respect to the line of force.

First, a simple observation is required on theorem 4 (which says that the center of friction and the center of rotation are on the same side of the line of pushing). Define the *line of motion* to be the line tangent to the path of the contact point. If we substitute "line of motion" for "line of pushing", then theorem 4 applies to sliding-contact as well as to fixed-contact. The best way to look at this is to assume fixed contact is occurring, and consider the contact forces arising. If the same forces are applied by means other than fixed contact with a pushing constraint, the object's behavior must be the same. The only reason a change of terminology is required is that "line of pushing" is undefined for sliding contact.

Theorem 7. *Assume that not all of the support force lies on the x-axis. The rotation mode is respectively clockwise, fixed, counter-clockwise if and only if the center of friction lies respectively to the left, on, to the right of the line of motion. Proof:* above.

One other result is required before theorem 9 is taken up. By combining some kinematic considerations with the quasi-static assumption, we can show that the center of rotation can not be within the interior of the friction cone during pushing with sliding contact. Figure 26 shows the reasoning. In this figure are shown the pushing constraint, the constraint normal, the friction cone, and the line of pushing. We will apply two kinematic considerations. First of all, the velocity of the contact point on the object must have a positive component along the constraint normal. In terms of the location of the instantaneous rotation center, this means that if the rotation center is to the right of the constraint normal, clockwise rotation must occur, and if it is on the opposite side counter-clockwise rotation must occur. The second kinematic consideration has to do with the direction of sliding. For clockwise rotation, left-sliding occurs when the rotation center is above the normal to the line of pushing and right-sliding occurs when the rotation center is below the normal to

63

the line of pushing. For counter-clockwise rotation, these are reversed.

Now suppose the quasi-static equations give a center of rotation in the friction cone, as shown in the figure. Since the total force and the total moment at the center of mass are zero, the total moment of force about the rotation center, or any other point, must also be zero. There are two contributors to the total moment of force at the rotation center: the contact force, and the frictional forces. We can immediately observe that left-sliding occurs, hence the contact force acts on a line passing to the right of the rotation center. This contributes a positive moment to the total moment at the rotation center. We can also observe that clockwise rotation occurs, so the frictional force at every contact point contributes a positive moment to the total moment at the rotation center. The total moment at the rotation center must be positive, contrary to our assumption.

Theorem 8. *During pushing with sliding contact, the instantaneous center of rotation cannot be in the interior of the friction cone. Proof: above.*

Theorem 9. *Assume an object is being pushed with sliding contact, and that the pressure distribution is non-pathological (to be defined.) Then if the instantaneous rotation center lies to the right of the line of force, clockwise rotation occurs, if the instantaneous rotation center lies to the left of the line of force, counter-clockwise rotation occurs, and if the rotation center lies on the line of force, translation occurs.*

Proof: There are three main steps in this proof: (1) show that the quasi-static equations define the rotation center $x_r(\theta)$ as a continuous function of the orientation; (2) use the previous step to show that if the result is obtained for just one orientation then it applies for all orientations; and (3) construct a single orientation for which the result holds.

First we will show that the quasi-static equations 18 and 19 implicitly define a continuous function $x_r(\theta)$ giving the instantaneous rotation center as a function of the object orientation. The domain of this function is the interval $[0, 2\pi)$, and the range is the extended plane (i.e. the plane plus a line at infinity) with the line orthogonal to the pushing constraint through the contact point deleted. The two
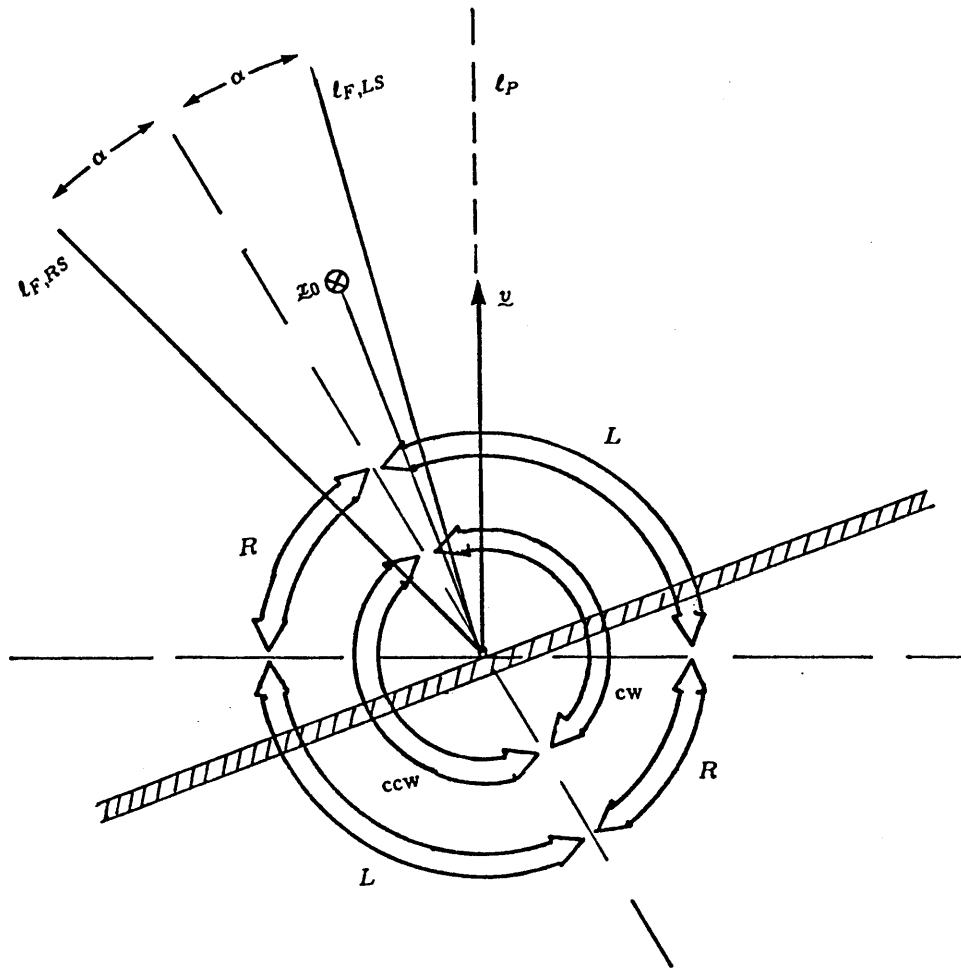
Figure 26. The COF cannot be in the friction cone. $\ell_{F,RS}$ is the line of force for right-sliding contact. $\ell_{F,LS}$ is the line of force for left-sliding contact. If the rotation center is in the L quadrants, left-sliding must occur; if it is in the R quadrants, right-sliding must occur.

half-planes are connected at the line at ∞, so the topology of the range is that obtained by cutting along the line orthogonal to the pushing constraint through the contact point, and gluing along the line at ∞ (figure 27).

To show that the function exists, and is continuous, we will apply the implicit function theorem [Rektorys 1969] to the quasi-static equations
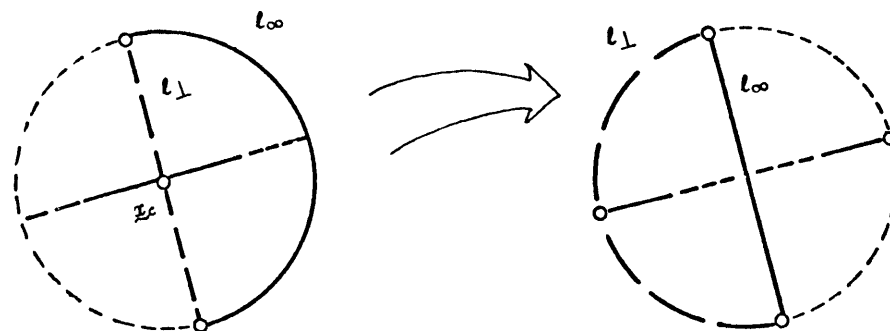
$$Q_1(x_r, \theta) = 0$$
$$Q_2(x_r, \theta) = 0.$$

Figure 27. Range of $x_r(\theta)$. $\ell_\perp$ is perpendicular to the pushing constraint. ℓ_∞ is the line at infinity.

For this we need to show two things:

1. that the partial derivatives $\partial Q_\alpha/\partial x_r$, $\partial Q_\alpha/\partial y_r$, and $\partial Q_\alpha/\partial \theta$, for $\alpha = 1, 2$, exist and are continuous; and

2. that the determinant

$$
\begin{vmatrix}
\dfrac{\partial Q_1}{\partial x_r} & \dfrac{\partial Q_1}{\partial y_r} \\[2mm]
\dfrac{\partial Q_2}{\partial x_r} & \dfrac{\partial Q_2}{\partial y_r}
\end{vmatrix}
$$

is non-zero.

The first condition may be shown to hold for arbitrary bounded pressure distributions, but there are some pressure distributions for which the second condition fails. When the second condition holds, we say the pressure distribution is *non-pathological*. Following the proof some examples of pathological pressure distributions will be presented.

Returning to the first condition, we require the existence of continuous partial derivatives of Q_1 and Q_2 with respect to x_r, y_r, and θ. Now Q_1 and Q_2 are simple linear combinations of components of the total frictional force and the frictional moment (equations 2.18 and 2.19.) These in turn are integrals over terms of the form

$$\text{sgn}(\dot{\theta})\frac{x - x_r}{|x - x_r|}$$

which is a unit vector parallel to the line $\overline{xx_r}$. We have already observed that this term is continuous at ∞, by virtue of the multiplication by the term $\text{sgn}(\dot{\theta})$. This term is clearly continuous in the rest of the plane, except where $x = x_r$. However, this happens only at a single point in the region of integration. For bounded pressure distributions, the value of the integrand at a single point cannot affect the value of the integral [Kolmogorov and Fomin 1970]. We conclude that the integrals are continuous in x and $\dot{x_r}$, and therefore Q_1 and Q_2 are also continuous in x and x_r. Finally, we must observe that x is actually a function of θ: $x(\theta)$, a detail that we have suppressed up to now for the sake of simplicity. The location of any point x fixed in the object varies smoothly with the object orientation θ. We conclude that Q_1 and Q_2 have continuous partial derivatives with respect to x_r, y_r, and θ. It follows that the quasi-static equations implicitly define a continuous function $x_r(\theta)$.

The second step reduces the proof to the problem of finding a single orientation giving the desired result. For this we depend on the fact that continuous functions map connected subsets of the domain to connected subsets of the range.

Let Θ_L be the set of all θ such that the center of friction is to the left of the line of force, and let Θ_R be the set of all θ such that the center of friction is to the right of the line of force. This divides the domain $[0, 2\pi)$ of $x_r(\theta)$ into four intervals: Θ_L, Θ_R, $\{\theta_+\}$, and $\{\theta_-\}$ (figure 28.) A simple application of theorem 1 shows that an orientation in Θ_L or Θ_R cannot give translation. Hence each of the images $x_r(\Theta_L)$ and $x_r(\Theta_R)$ do not intersect the line at infinity. Since a continuous map of a connected region must be connected, each image must lie either entirely to the left of the line at ∞, giving clockwise rotation, or entirely to the right of the line at infinity, giving counter-clockwise rotation. Examination of a single case will tell which of these two alternatives actually occurs. If just one orientation in each of the intervals Θ_L and Θ_R is constructed whose image is on the predicted side of the line at infinity, then the entire interval must also lie on the predicted side of the line at infinity, giving the desired result.

For the third step, we must demonstrate an orientation in each of the intervals
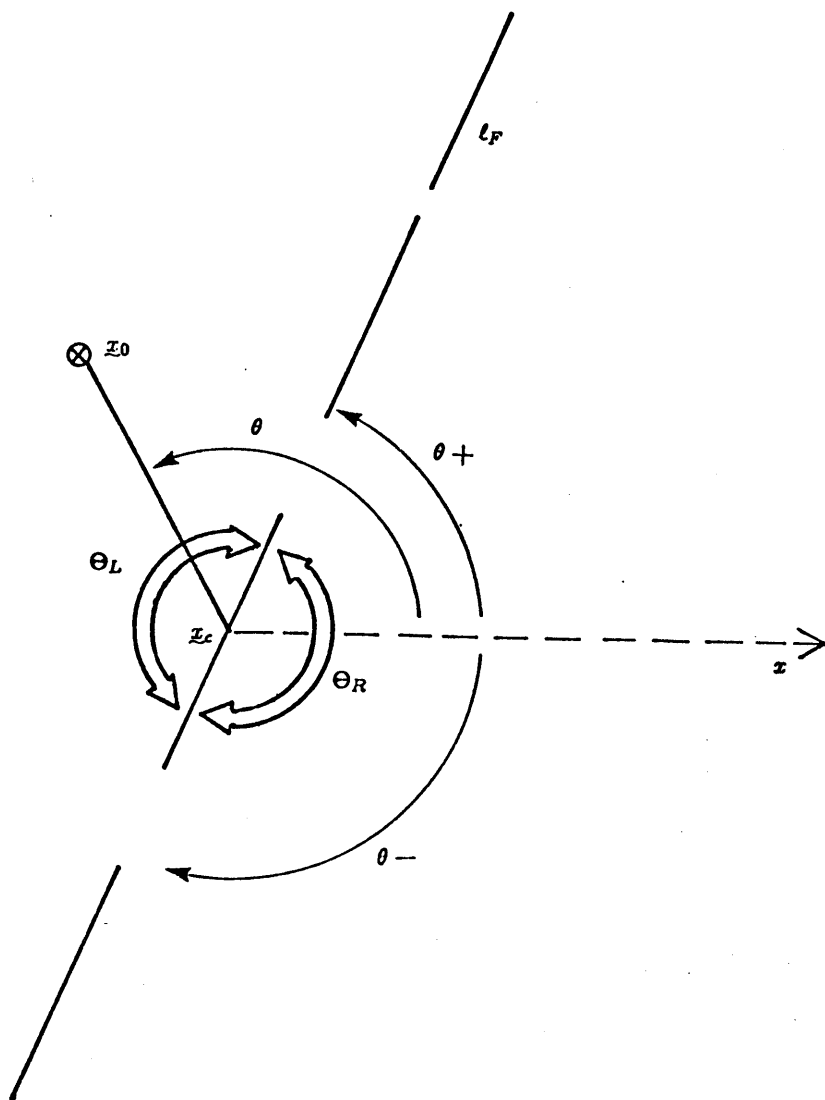
Figure 28. Domain of $x_r(\theta)$. ℓ_F is the line of force.

Θ_L and Θ_R for which the result holds. Figure 29 shows an orientation in Θ_R for which the result is easily demonstrated, namely the orientation at which the line $\overline{x_c x_0}$ coincides with the pushing constraint, with the line of pushing passing to the left of the center of friction. Since the line of force must lie in the friction cone, the center of friction must lie to the right of the line of force, so this orientation is in the interval Θ_R. The velocity of the contact point in the object must have a positive component along the normal to the pushing constraint due to kinematic constraint. Hence it is impossible for the line of motion to pass to the right of the
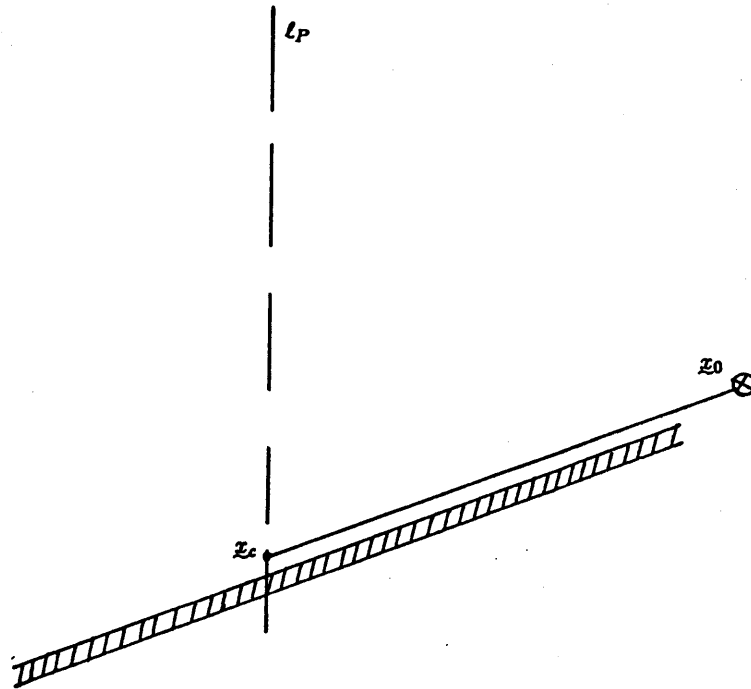
Figure 29. A single case giving the result of theorem 9. ℓ_P is the line of pushing.

center of friction. In this case the object must rotate clockwise, which is the desired result. An orientation in the interval Θ_L giving the desired result is obtained by rotating the object an additional 180 degrees. ∎

Again we have a very simple rule whereby the rotation mode of an object being pushed may be determined by inspection. The result is very similar to the result for fixed contact.

Theorem 9 is restricted to "non-pathological" pressure distributions, meaning that the determinant D is non-zero, where D is given by:

$$\begin{vmatrix} \frac{\partial Q_1}{\partial x_r} & \frac{\partial Q_1}{\partial y_r} \\ \frac{\partial Q_2}{\partial x_r} & \frac{\partial Q_2}{\partial y_r} \end{vmatrix}.$$

Equivalently, the gradients $(\frac{\partial Q_1}{\partial x_r}, \frac{\partial Q_1}{\partial y_r})^T$ and $(\frac{\partial Q_2}{\partial x_r}, \frac{\partial Q_2}{\partial y_r})$ must not be parallel at any solution of the quasi-static equations. Let us consider the contribution from

Figure 30. Gradients of Q_1, Q_2 for single point.

one point in the contact region to these gradients. Figure 30 shows an example illustrating this contribution. The contou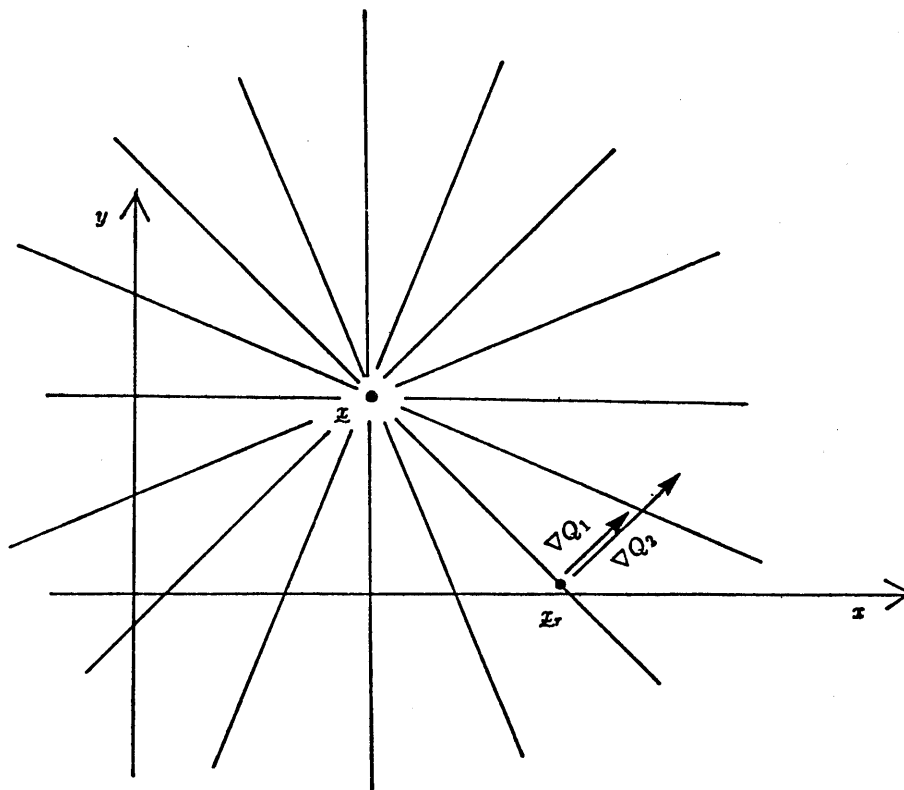rs of both Q_1 and Q_2 are radii extending from the point of integration $\underline{x}$. Both gradients must be perpendicular to the contour passing through the rotation center $\underline{x}_r$, and will therefor be parallel.

Now consider the situation with two points (figure 31.) We have drawn the contours for both points. At $\underline{x}_{r1}$, the contours are not parallel, and we would not expect the total gradients to be parallel. At $\underline{x}_{r2}$, on the other hand, the contours are parallel, and so the gradients are parallel. In fact, anywhere on the line $\overline{\underline{x}_1\underline{x}_2}$ the gradients will be parallel. Now, that only matters if a root of the quasi-static equations lies on that line. To construct an example, we need only place the contact point on the perpendicular bisector of $\overline{\underline{x}_1\underline{x}_2}$, and let the normal forces at $\underline{x}_1$ and $\underline{x}_2$ be equal. In that case, pushing in the direction of the bisector will give a root at infinity on the line $\overline{\underline{x}_1\underline{x}_2}$, by theorem 1. This happens to be the only pressure distribution for which the set of possible rotation centers was known previous to this thesis. Prescott [Prescott 1923] showed that the rotation center may lie on
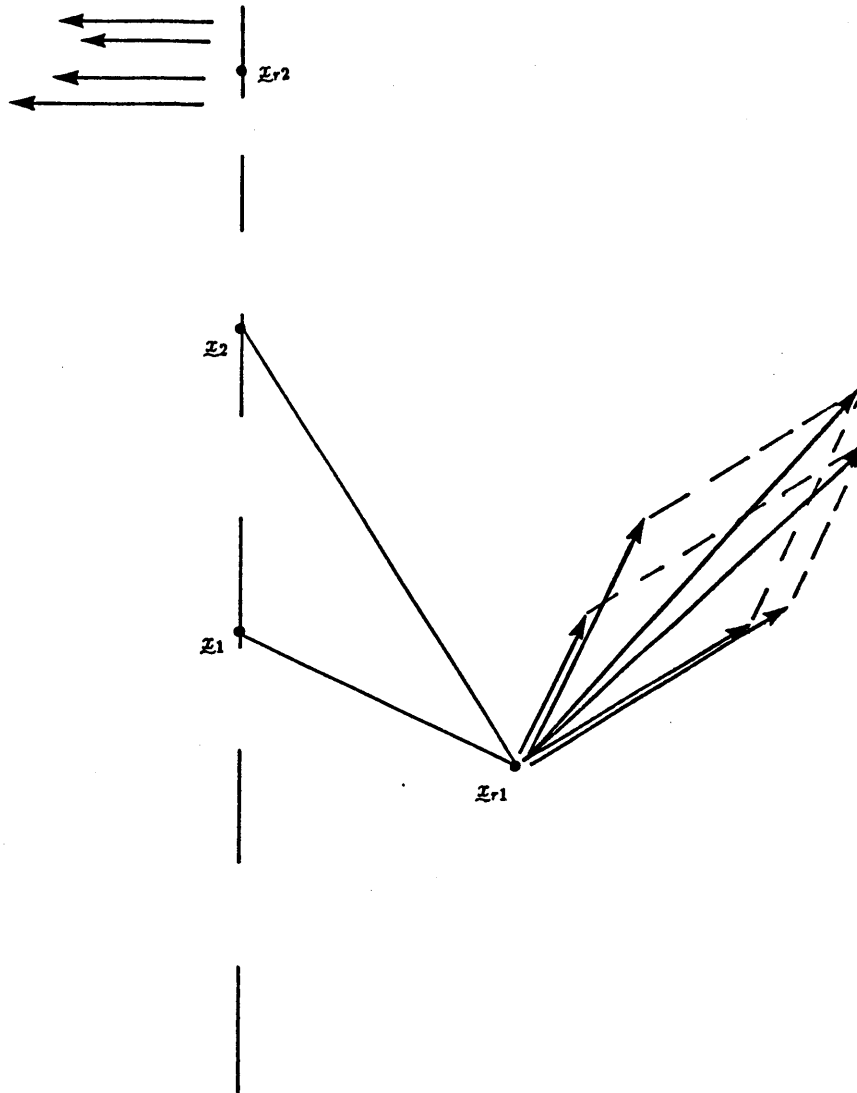
Figure 31. Gradients of Q_1, Q_2 for two points.

the circle through x_1, x_2, and the contact point, or it may lie on the part of the line through x_1 and x_2 exterior to the circle. Figure 32 shows this set of possible rotation centers. For each possible rotation center, we have noted the corresponding angle of the line of force. For all points on the line this angle is constant, due to the pathological nature of the pressure distribution and contact point.

Again there is a similarity to the case of fixed contact. In order to prove theorem 4, it was necessary to exclude pressure distributions concentrated on the x–axis. When this restriction was violated, the location of the rotation center was
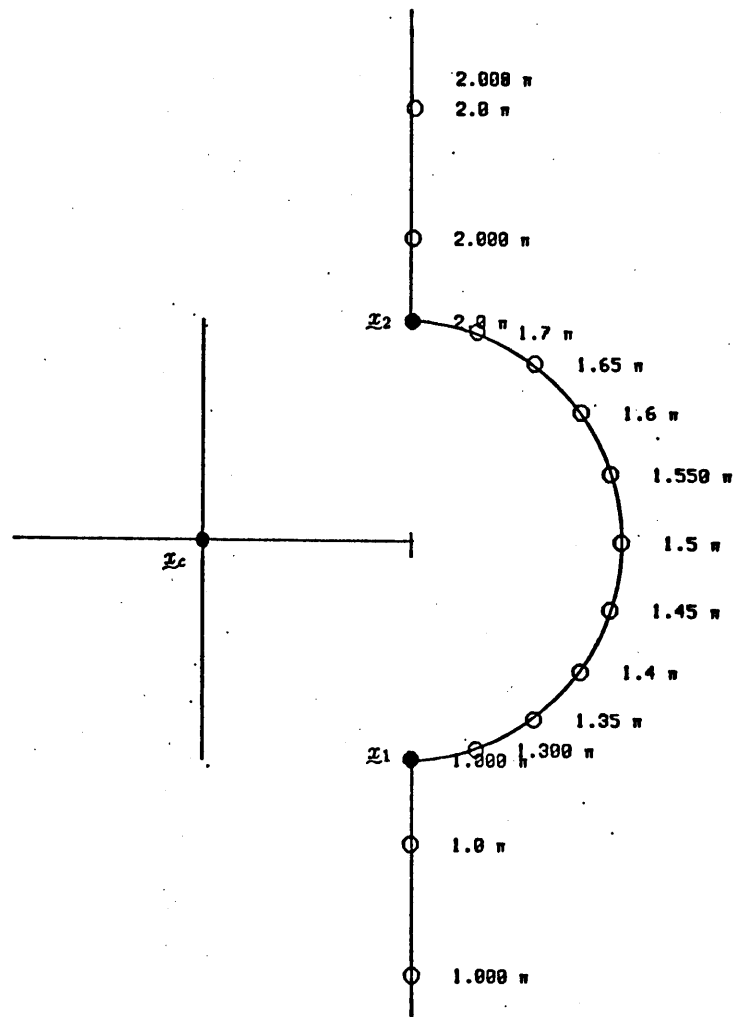
Figure 32. Rotation centers of pathological distribution.

not uniquely determined. In the case of sliding contact, the same phenomenon occurs. As before, the actual instantaneous rotation center cannot be determined without taking into account inertial forces.

There is one interesting difference between fixed contact and sliding contact: for fixed contact, the rotation mode is determined by the line of pushing, whose direction is determined by the pushing constraint alone. For sliding contact, the rotation mode is determined by the line of force, whose direction may depend on the orientation of the object, rather than on the orientation of the pushing constraint.
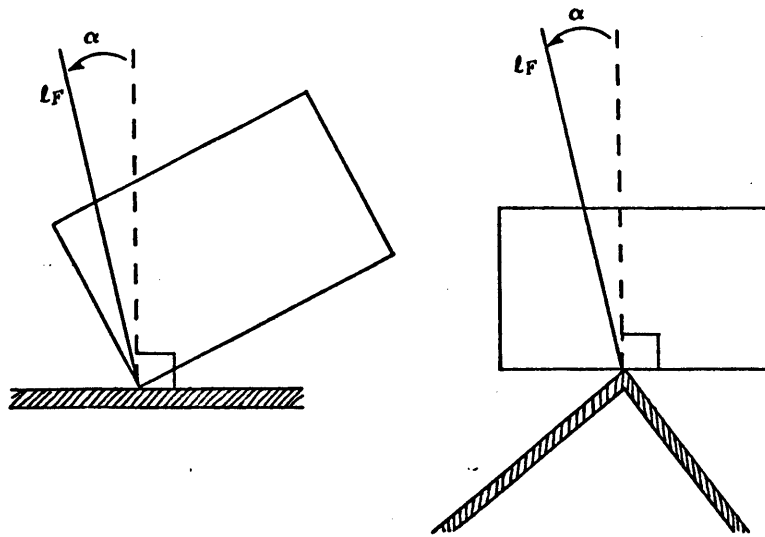
Figure 33. Line of force may depend on object orientation. ℓ_F is line of force.

Figure 33 shows both possibilities. In one case, we have contact between a vertex of the object and an edge of the pushing constraint, and the line of force is determined by the orientation of the pushing constraint. But in the other case, contact occurs between a vertex of the pushing constraint and an edge of the object, and the line of force is determined by the orientation of the object. When this occurs, a certain degree of control is lost; the rotation mode of the object cannot be controlled by varying the orientation of the pushing constraint.

2.3.2. Rotation Center

As in the case of fixed contact, we can calculate the location of the rotation center only when the support is known. The rotation center is found by numerically searching for the simultaneous root of the quasi-static equations 2.18 and 2.19. Figures 34 and 35 show plots of $Q_1(x_r)$ and $Q_2(x_r)$ for the case of a single point of support at $(1,0)^T$. Both of the surfaces have singularities at the single point of support, and both surfaces pass through the horizontal plane at this point. This has two important consequences: (1) roots tend to occur at areas of large pressure
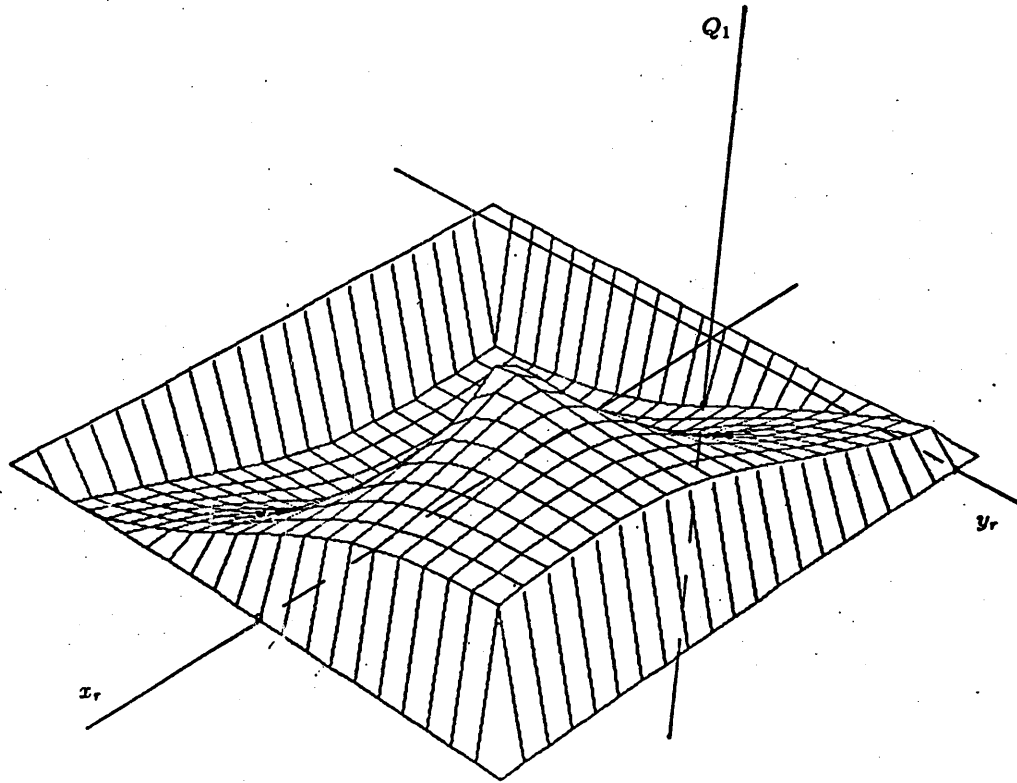
Figure 34. Example plot of $Q_1(x_r)$

(i.e. objects tend to rotate about points of support); and (2) numerical methods will have difficulty converging on the roots. The first point is interesting because it confirms and explains the tendency of objects to rotate about a point of support, and also because it suggests a strategy for making an object turn about a particular point.

The expected difficulty in applying numerical methods to the problem of finding the root did occur. Both a two-dimensional false-position approach [Acton 1970] and an accelerated Newton-Raphson approach [Brown 1967, Brown and Conte 1967] failed to converge reliably, even when the initial guesses were quite close to the actual root. Fortunately, another formulation of the search is possible, closely related to the physical interpretation of the quasi-static equations.

The basic idea is to reduce the two-dimensional sliding-contact case to the one-dimensional fixed-contact case. The reasoning we will use is similar to the
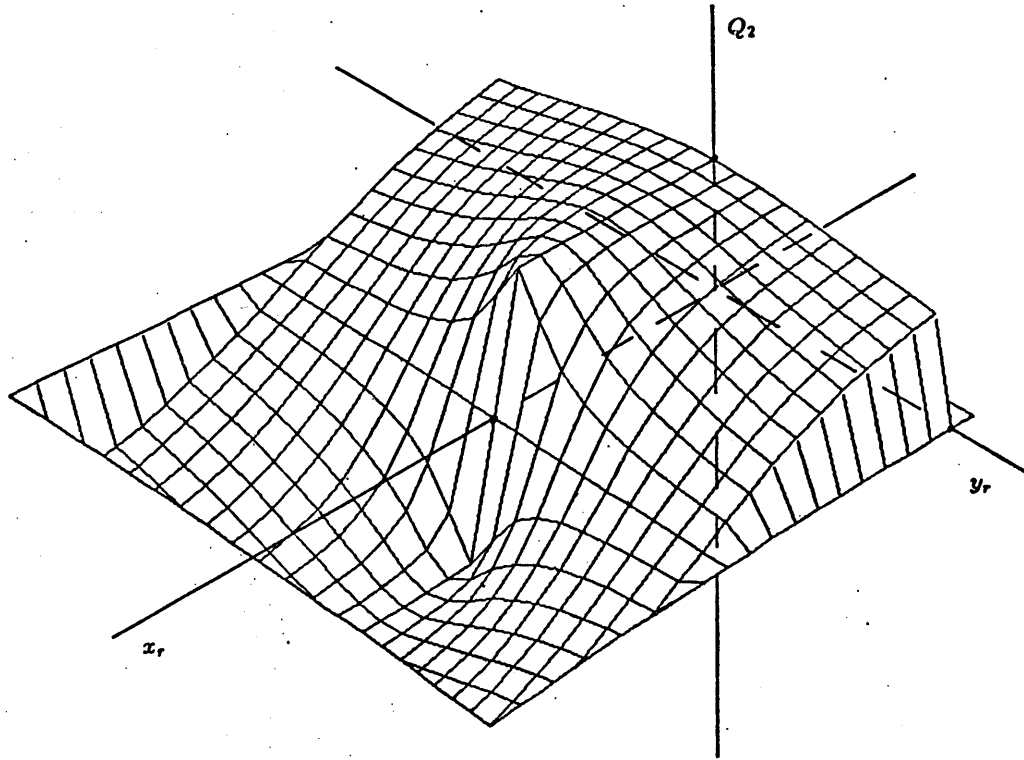
Figure 35. Example plot of $Q_2(x_r)$

proof of theorem 7. Assume that an object is being pushed with sliding contact. If we observe the line of motion of the contact point on the object, and then mimic this line of motion by pushing in the same direction with fixed contact, the object's motion must be the same. The value of this observation is that the numerical method of section 2.2.2 can be applied to find the rotation center given just the direction of motion of the contact point. For a fixed pressure distribution and object orientation, we can plot the locus of the rotation center as the line of motion varies, as in figure 36. Now, it is a simple matter to compute the total contact force, given a rotation center, so for each rotation center plotted in figure 36, we can note the angle of the line of force. Once these annotations are made, we can find the rotation center corresponding to a given direction of the line of force (henceforth the *angle of force*) simply by "looking it up" in the figure.

The method implemented is similar in approach. For a given direction of
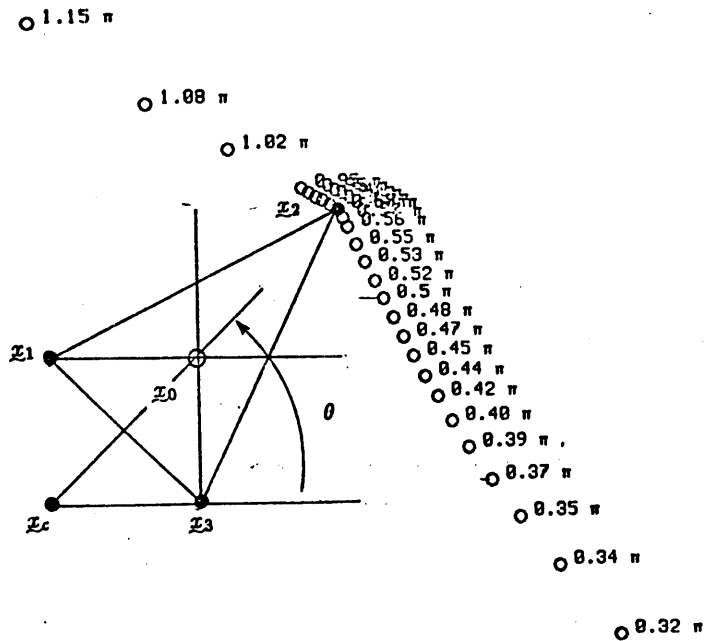
Figure 36. Plot of rotation centers vs. force angle

motion of the contact point the method of section 2.2.2 can readily calculate the rotation center, so the problem is reduced to finding the direction of motion corresponding to a given angle of force. This reduces our original two-dimensional problem to a one-dimensional problem. Finally, examination of the plot shows that the angle of force varies monotonically with the angle of motion (i.e. the numbers running up the plot only increase). Again the method of false-positions was applied. Convergence was quite reliable, usually occuring in about five seconds of Lisp Machine processor time, and in no case worse than a minute. (The precision required was .001 centimeters.)

2.4. Undetermined Contact Mode

So far, for each contact mode (left-sliding, right-sliding, and fixed), we have an inspection method of determining the rotation mode. However, it is rarely obvious what the contact mode is, making it impossible to determine whether to compare

76

the center of friction to the line of pushing, the left edge of the friction cone, or the right edge of the friction cone. The first goal of this section is to present a general inspection method for finding the rotation mode, which can be applied without foreknowledge of the contact mode. The second goal is to develop a numerical method for determining the exact location of the rotation center.

2.4.1. Rotation Mode

In the previous section, we made a slight change to theorem 4 which allowed its application in the case of sliding contact. We now note that theorem 9, which states that the center of friction and the center of rotation are on the same side of the line of force, applies to fixed contact as well as to sliding contact. The line of force is well-defined in any case: it is simply the line along which the contact force is applied. The only thing special about sliding-contact is that the line of force is easy to predict. Thus theorem 7 and theorem 9 can be applied simultaneously, regardless of the contact mode. We obtain:

Theorem 10. *With reference to the center of friction, the center of rotation, the line of force, and the line of motion: both centers lie to the left of both lines, or both centers lie to the right of both lines, or the two lines and the center of friction coincide and the center of rotation is on the line at infinity. Proof:* This is an immediate consequence of theorems 9 and 7. ∎

Corollary. *During fixed contact the line of force and the line of pushing lie on the same side of the center of friction.*

(This corollary was used in the proof of theorem 6.)

Theorem 11. *If the center of friction lies to the left of the friction cone, the object must rotate counter-clockwise. If the center of friction lies to the right of the friction cone, the object must rotate clockwise.*

Proof: If the center of friction lies to the left of the friction cone, then it lies to the left of the line of force. By theorem 10, the rotation center also lies to the left of the line of motion, which implies a counter-clockwise rotation. The other case is similar. ∎

77
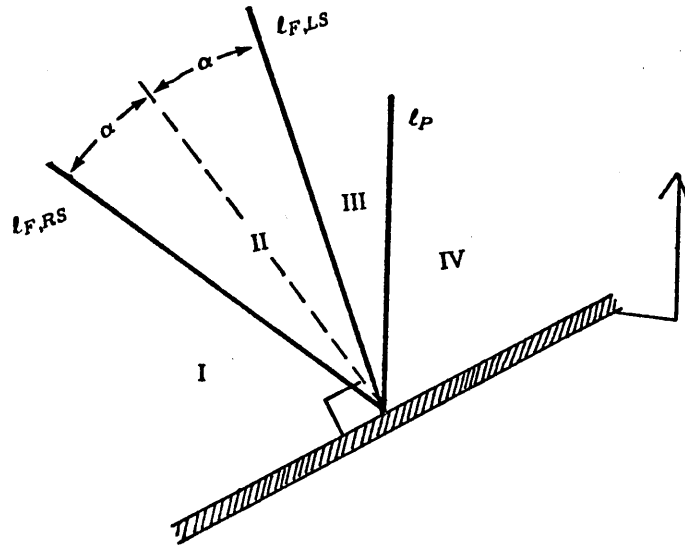
Figure 37. Zone Labeling $\ell_{F,RS}$ is the line of force for right-sliding contact. $\ell_{F,LS}$ is the line of force for left-sliding contact. ℓ_P is the line of pushing.

We are now ready to develop the method of determining the rotation mode for undetermined contact mode. For a given situation, we divide the plane into *zones*, as shown in figure 37. There are four zones, defined by the left and right edges of the friction cone, and the line of pushing. The zones are labeled in clockwise direction I, II, III, IV, without regard for where the line of pushing falls with respect to the friction cone.

Theorem 12. *Let the translations line be the boundary between zones II and III. If the center of friction falls to the left of the translations line clockwise rotation occurs. If the center of friction falls to the right of the translations line counter-clockwise rotation occurs. If the center of friction is on the translations line, translation occurs.*

Proof: The result is proven by cases, applying elementary kinematics and pushing theory to show that the predicted rotation mode is obtained for each zone.

First we consider the case of the line of pushing falling to the left of the friction cone (figure 38). If the center of friction falls in zone I, II, or IV, the predicted

rotation mode is obtained immediately by application of theorem 11. This leaves the case of the center of friction in the friction cone, i.e. inside zone III. The left edge of the friction cone is the line of force if right sliding occurs, and the right edge of the friction cone is the line of force if left sliding occurs, as indicated by the labels in the figure. By theorem 10, the line of motion must be on the same side of the center of friction as the line of force. Hence the line of motion for right sliding is constrained to lie to the left of the center of friction, which is indicated by the label "RS1". Likewise the left-sliding line of motion is constrained in the interval indicated by the label "LS1". The right-sliding line of motion is further constrained kinematically. If right-sliding is to occur, the right-sliding line of motion must lie to the right of the line of pushing, as indicated by the interval labeled "RS2". Likewise the left-sliding line of motion lies in the interval "LS2". At this point it is clear that left-sliding is altogether impossible—the intersection of the intervals "LS1" and "LS2" is empty. By theorem 4 fixed contact implies clockwise rotation. By theorem 9 right-sliding contact also implies clockwise rotation. This proves the result for the case of the the line of pushing to the left of the friction cone. The case of the line of pushing falling to the right of the friction cone is similar.

Figure 39 shows the case of the line of pushing falling inside the friction cone. Again, if the center of friction lies outside the friction cone, the result follows immediately by theorem 11, which takes care of zones I and IV. The figure illustrates the case of the center of friction in zone II. As before, the constraints on the lines of pushing for left-sliding and right-sliding are indicated in the figure. Right-sliding is impossible. Left-sliding is possible, but the line of motion must fall to the right of the center of friction, hence counter-clockwise rotation occurs, by theorem 9. If fixed contact occurs, counter-clockwise rotation occurs, by theorem 4. The proof for the center of friction in zone III is similar.

The results are summarized in table 1. In every case, the rotation mode is counter-clockwise for the center of friction in zones I and II, and clockwise for the center of friction in zones III and IV.

As we shall see, it is difficult to determine the contact mode, so the fact that this result is independent of the contact mode is critical.
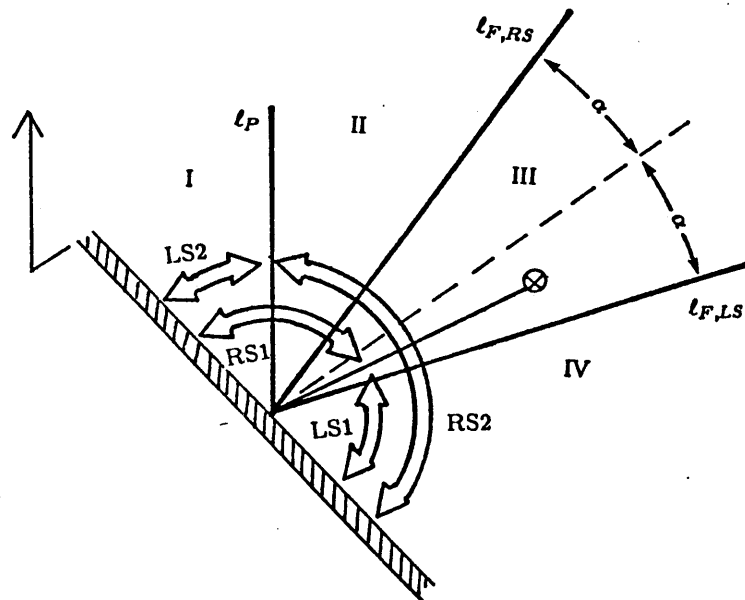
Figure 38. Line of pushing to the left of the friction cone.

2.4.2. Rotation Center

In this section we develop methods for determining the contact mode, which enables us to find the instantaneous rotation center in the general case. As in the previous section, this is accomplished by applying theorems 7 and 9.

The method requires a plot of the locus of the rotation center as the angle of force γ varies. Generation of these plots was described in section 2.3.2. The use of the plot is most easily demonstrated by example. Supposing that $\gamma = 0.4\pi$ (figure 40), the line of motion is orthogonal to the line from the contact point to $x_r(\gamma)$. If fixed contact occurs, then the normal to the pushing constraint must lie within $\tan^{-1}\mu$ of γ, and the line of pushing is the same as the line of motion. If left-sliding (right-sliding) occurs, then the right edge (left edge) of the friction cone is at an angle γ. The line of pushing must be to the right (left) of the line of motion. So for fixed contact, the line of pushing is determined and the pushing
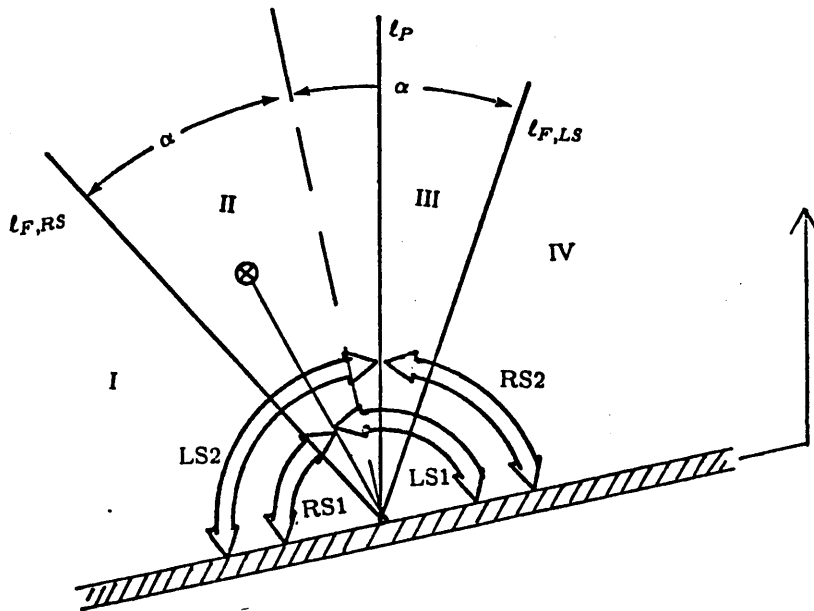
Figure 39. Line of pushing inside friction cone.

constraint orientation is constrained, but for left- or right- sliding contact, the pushing constraint orientation is determined and the line of pushing is constrained. For a given rotation center, the contact mode is not determined, which is readily verified by experiment. The constraints for each contact mode are illustrated in figure 40.

So it is easy to determine the set of possible pushing constraint orientations and lines of pushing for a given rotation center and contact mode. Of course, our purpose is the opposite, to determine the rotation center given the pushing constraint orientation and line of pushing. This is accomplished by assuming a particular contact mode and constructing the resulting rotation center. If this rotation center gives a line of motion consistent with the assumed contact mode, and a line of force consistent with the friction cone, then we have a solution. This is illustrated in figures 41 through 43. The pushing constraint and the line of pushing are shown in the figure as given, and the friction cone is also constructed. First we will assume fixed contact (figure 41.) The rotation center must be at the intersection

81
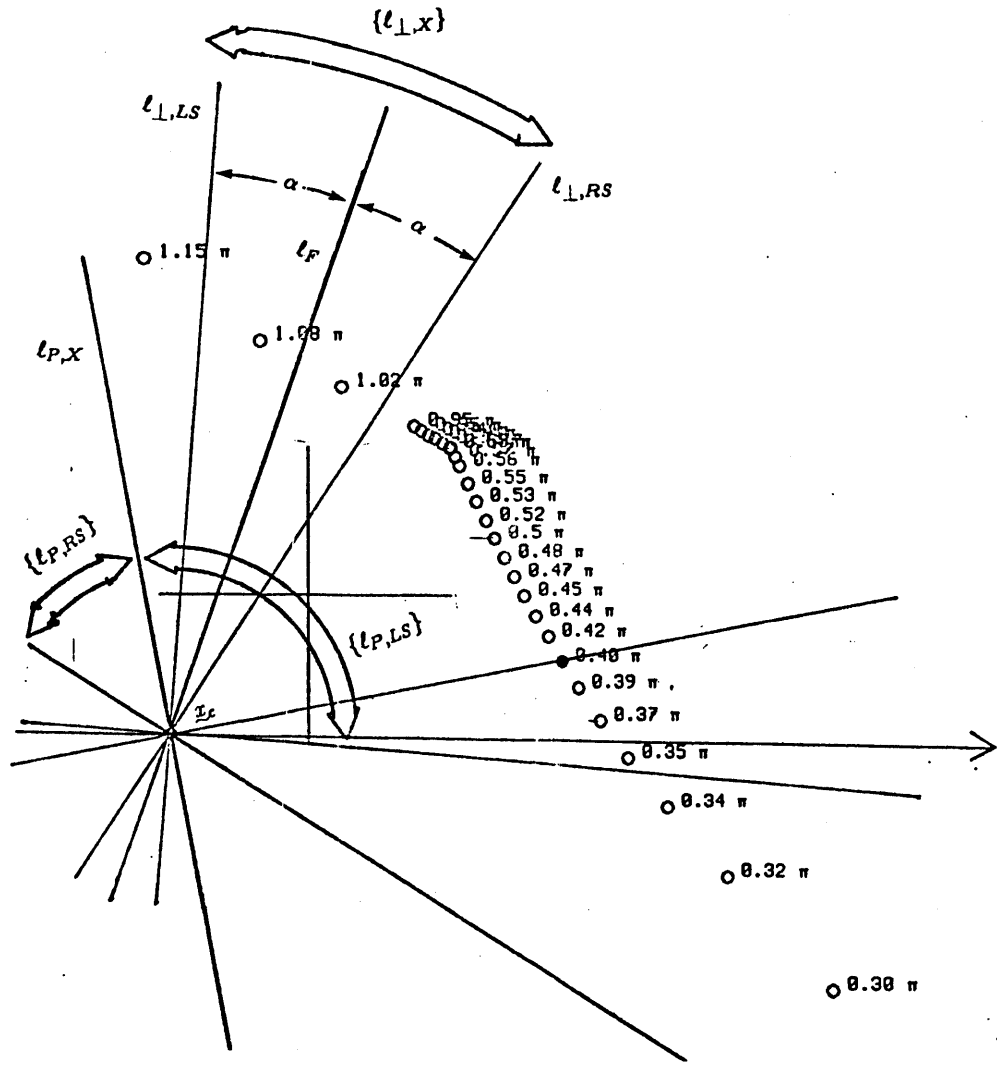
Figure 40. The three possible contact modes. $\gamma = 0.4\pi$. $\{\ell_{P,RS}\}$ and $\{\ell_{P,LS}\}$ are the sets of possible lines of pushing for right-sliding and left-sliding respectively. $\ell_{P,X}$ is the line of pushing for fixed contact. $\ell_{\perp,LS}$ and $\ell_{\perp,RS}$ are the constraint normals for left-sliding and right-sliding respectively. $\{\ell_{\perp,X}\}$ is the constraint normal for fixed contact. ℓ_F is the line of force.

of the normal to the line of pushing and the locus of rotation centers. From the locus we can read off the angle of force γ (.375π), which is outside the friction cone. Fixed contact is impossible.

Figure 42 is constructed assuming right-sliding contact. We construct the friction cone and obtain the angle of force $\gamma = .5\pi$. The corresponding rotation
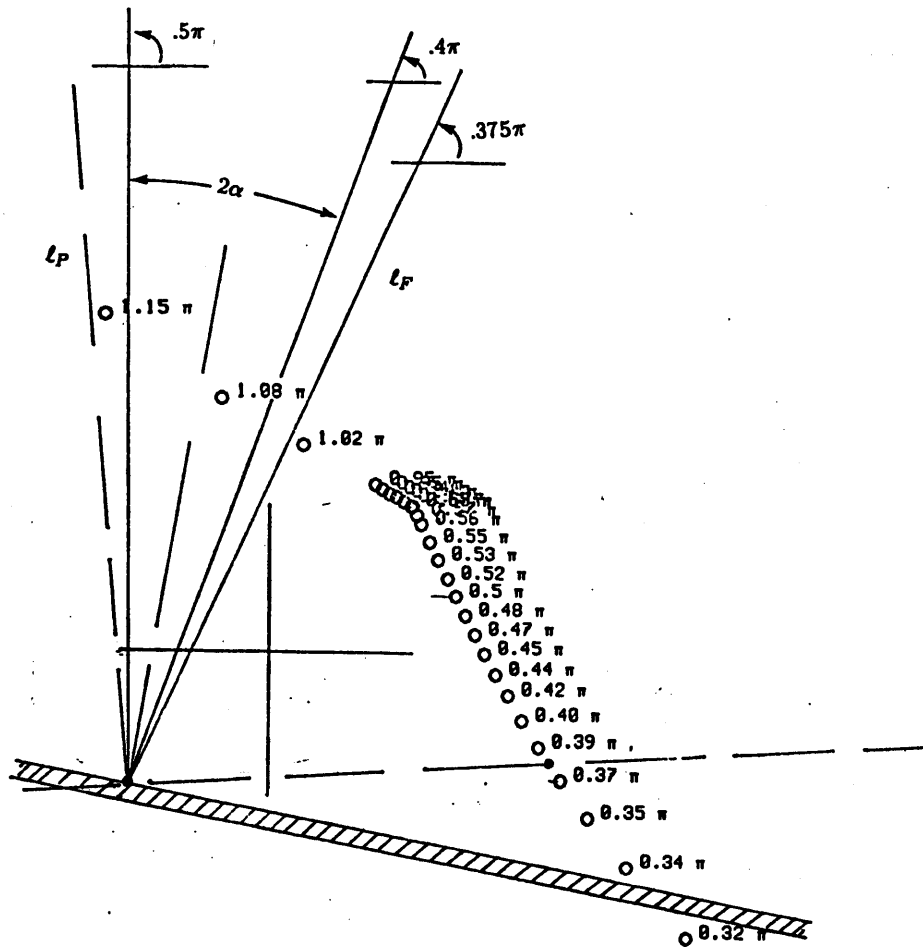
Figure 41. Finding the rotation center. Fixed contact impossible.

center is located, and a line drawn from the rotation center through the contact point. The normal to this line through the contact point is the line of motion of the contact point. The line of motion lies to the left of the line of pushing, inconsistent with the assumption of right-sliding contact.

Finally, we try left-sliding contact (figure 43.) The previous construction is repeated, except that this time the angle of force is $\gamma = .4\pi$. The line of motion constructed lies to the left of the line of pushing, as required for left-sliding.

It is clear that if this procedure finds a solution it is valid, and that if there is a
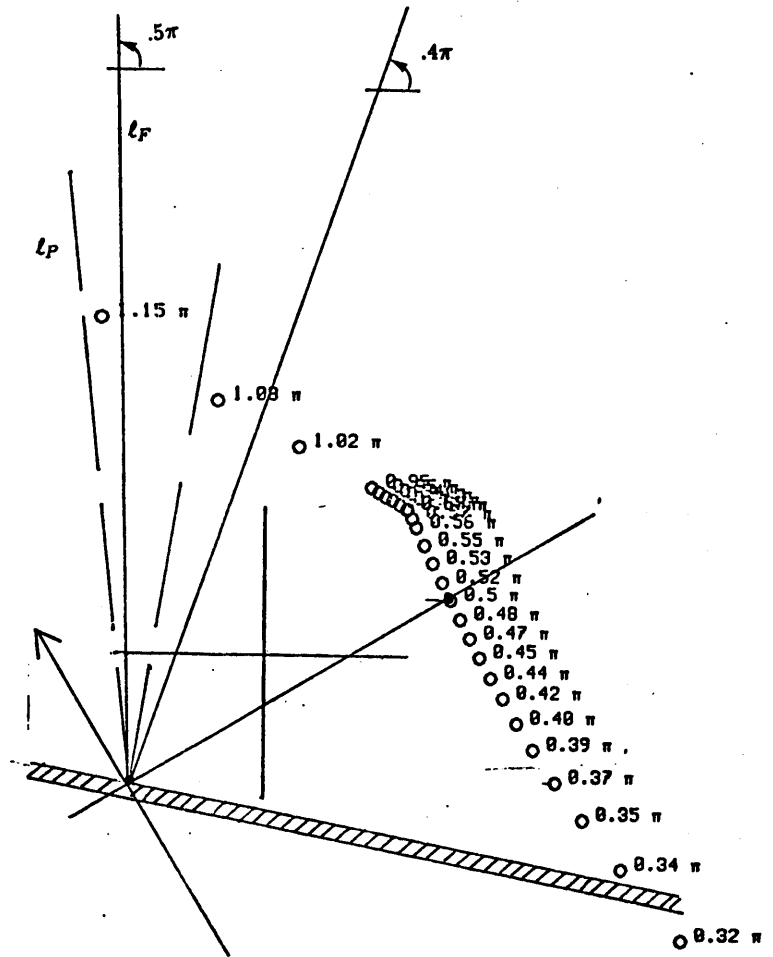
Figure 42. Finding the rotation center. Right-sliding impossible.

valid solution this procedure will find it, but it is not clear whether the procedure will always give a unique solution. This may seem paradoxical, because the existence of several solutions would suggest that classical mechanics is non-deterministic. However, we have already seen an example of this in section 2.3.1: if all the normal force is concentrated at two points, the rotation center may, in fact, be indeterminate. The root of this indeterminacy is the quasi-static assumption. Once inertial forces are considered the indeterminacy disappears.

There is one other interesting aspect of the locus of instantaneous rotation
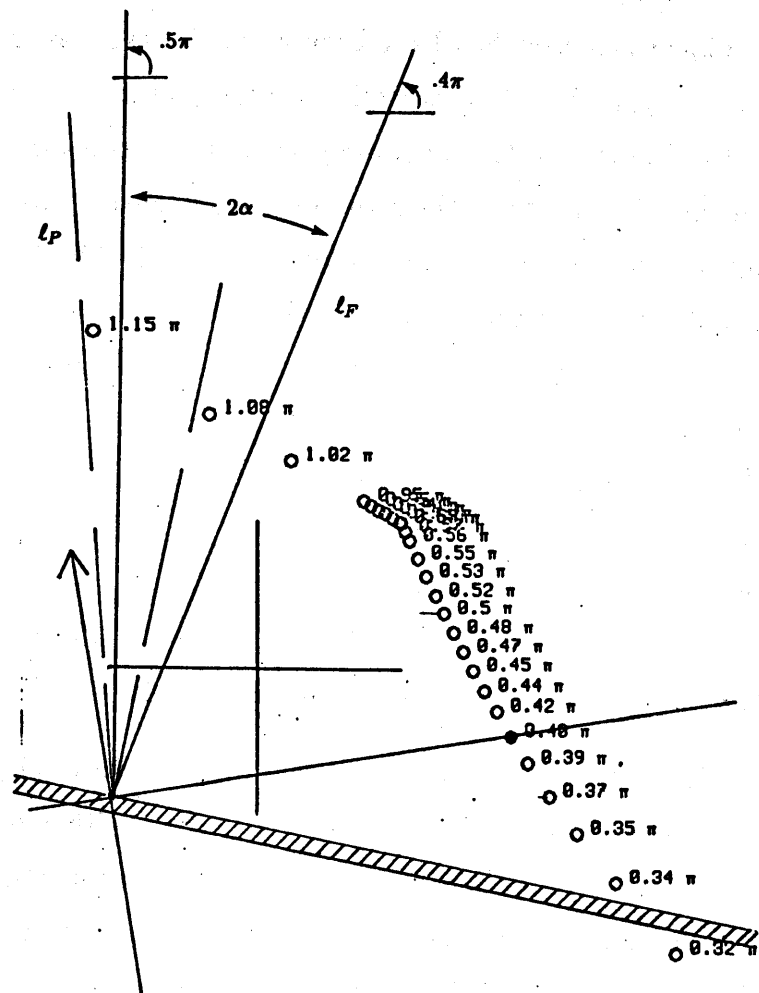
Figure 43. Finding the rotation center. Left-sliding gives solution.

centers. If the pressure distribution remains constant with respect to the object as the object moves, as it may for three-point support, and if the contact point is also constant, then the locus of rotation centers will translate and rotate with the object. In this case the locus of rotation centers is the moving centrode for every pushing motion that can be produced. This is halfway to a complete characterization of the motion of the object; a complete characterization also requires construction of the fixed centrode.

2.5. On Quasi-static Analysis

In the preceding sections a number of results concerning the nature of the motion of an object being pushed have been derived, based on the assumption that inertial forces are negligible. In this section this assumption is reviewed with an eye toward a careful characterization of those practical situations for which quasi-static analysis is meaningful. Perhaps the most important observation is that the quasi-static assumption, or some similar assumption, is inevitable if we wish to address the problem of determining the rotation mode given just a model of the object, the pushing constraint, and the line of pushing. In general, any rotation mode may occur if there is a large enough initial angular velocity. A particular moment will determine the angular acceleration, but will not preclude any particular angular velocity. Hence, the problem of greatest interest is undetermined, unless some additional assumption is made. The most reasonable interpretation of the problem is given by assuming quasi-static conditions; that is, we assume that the pushing motion is slow enough that inertial forces are negligible.

Quasi-static analysis is equivalent to the more traditional problem of sliding friction, which is to assume an object is motionless, but with some motion *impending*, and to find the characteristics of the impending motion. (Usually it is required to find the force or moment necessary to produce the motion, but occasionally it is required to find the direction of the impending motion or the instantaneous rotation center.) Impending motion problems involve no assumption on the inertial forces, because the object is motionless. It is only when we wish to address the actual motion of objects that an explicit assumption is necessary.

We shall refer to the solution of the full dynamic equations as the *dynamic solution*, and to the solution of the quasi-static equation as the *quasi-static solution*. By comparing the quasi-static solution with the phase-plane portraits of dynamic solutions, we shall find that for fixed applied forces, the quasi-static solution is valid when the product of the moment of inertia with the square of the pushing velocity is small. In most cases, the applied force is proportional to the mass of the object. When this is so, the quasi-static solution is valid if the product of the radius of inertia with the square of the pushing velocity is small.

We will consider the example of single point of support fixed-contact pushing of an object whose mass is also concentrated at a single point (figure 44). The pushing force is applied in the horizontal plane. Figure 45 shows phase-plane portraits of the dynamic solutions of this system for three different pushing velocities. The vertical axis is the normalized angular velocity $\dot{\theta}/v$, and the horizontal axis is the angle θ. In each case there is a stable equilibrium at $(-\pi/2, 0)$ and an unstable equilibrium at $(\pi/2, 0)$. If the pushing velocity is very small, the trajectories quickly converge to a single trajectory which is the quasi-static solution. As the pushing velocity is increased, inertial forces play a larger role until ultimately the frictional forces are irrelevant to the overall motion. The purpose of this section is to explain and quantify the convergence of the dynamic solutions to the quasi-static solution.

The dynamic solution of this system is the solution to the differential equation $I_c\ddot{\theta} = m_c(\dot{\theta}, \theta)$, where $m_c(\dot{\theta}, \theta)$ is the total moment of force about the vertical line through the contact point, and I_c is the total moment of inertia of the object about the same line. For the purposes of this section we will assume that the only applied forces are gravity and a contact force in the horizontal plane. Hence the total applied moment is given by equation 2.6 and we obtain

$$I_c\ddot{\theta} = m_f(\theta, \dot{\theta}/v)$$

where v is the pushing velocity. Here we are using a normalized angular velocity obtained by dividing by the pushing velocity. This will be useful for comparing the trajectories obtained with different pushing velocities. The quasi-static solution used in the preceding sections is the solution to

$$0 = m_f(\theta, \dot{\theta}/v).$$

At every point $(\theta, \dot{\theta})^T$ on the quasi-static trajectory, the moment of force is zero, so the angular acceleration of the dynamic solution has zero slope at that point. Conversely, if the dynamic solution has zero slope at a point, the moment is zero, so the point lies on the quasi-static trajectory. In phase-plane parlance, the quasi-static solution is the *zero-isocline* of the phase plane portrait [Stoker 1950].

Wherever the dynamic trajectory crosses the quasi-static trajectory in the phase plane, the dynamic trajectory has zero slope. The next problem is to ascertain
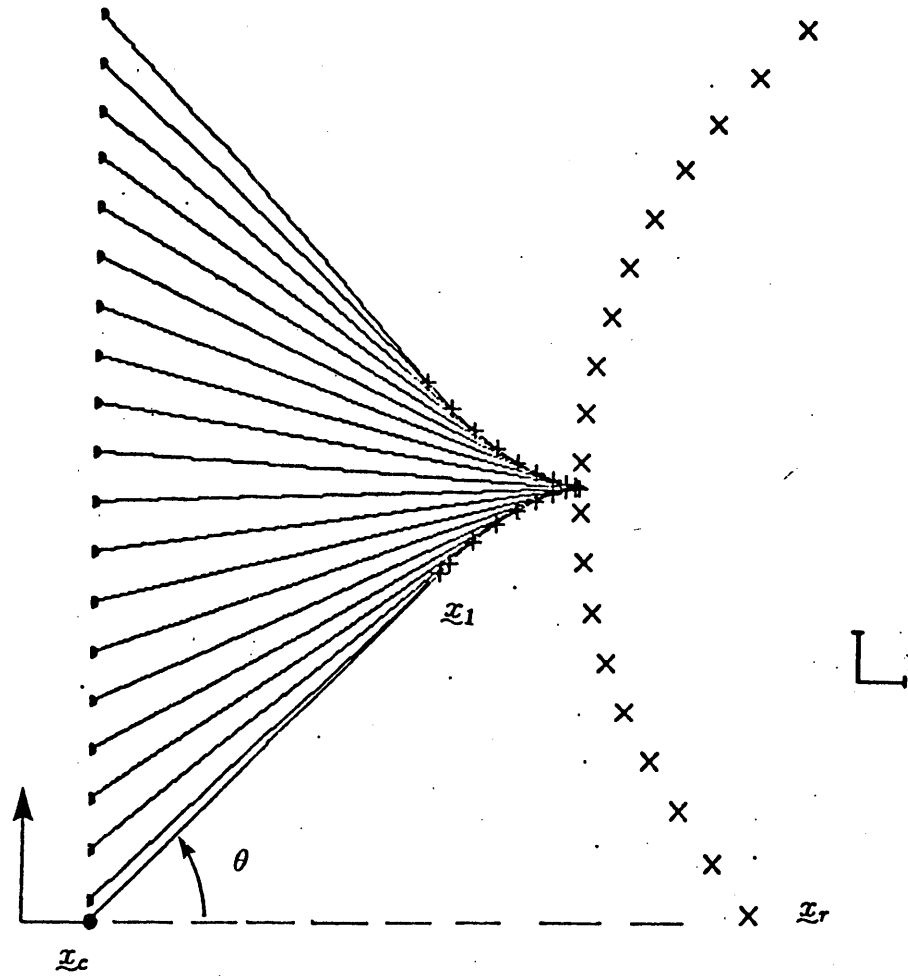
Figure 44. Pushing example for phase plane analysis. An object with a single point of support is being pushed from a distance of ten cm. • indicates the locus of the contact point, + gives the point of support, and × gives the rotation center.

the slope of the dynamic trajectory at other points in the phase plane. The slope in the phase plane is

$$\frac{d\dot{\theta}/v}{d\theta}.$$

An expression for the slope can be obtained by using the identity

$$\ddot{\theta} = v^2(\dot{\theta}/v)\frac{d\dot{\theta}/v}{d\theta}$$

in the dynamic equation

88
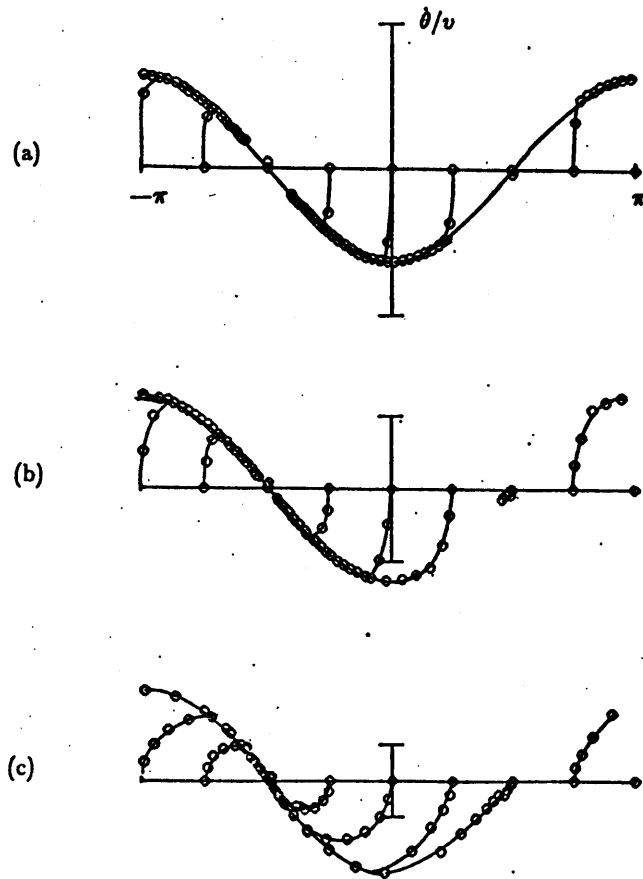
Figure 45. Phase plane plots. (a) v is 5 cm/sec. (b) 10 cm/sec. (c) 20 cm/sec.

$$I_c \ddot{\theta} = m_f(\theta, \dot{\theta}/v)$$

resulting in

$$\frac{d\dot{\theta}/v}{d\theta} = \frac{1}{v^2 I_c(\dot{\theta}/v)} m_f(\theta, \dot{\theta}/v).$$

We know that $m_f(\theta, \dot{\theta}/v)$ is monotonic decreasing in $\dot{\theta}/v$. Confining our attention to the region below the horizontal axis, we find that the slope is negative for points below the quasi-static trajectory, and positive for points above the quasi-static trajectory. As $v^2 I_c$ approaches zero, these slopes approach infinity. Given an object, the pressure distribution, and a range of normalized angular velocities $\dot{\theta}/v$

89

we can find a combination of maximum pushing velocity and angular inertia to produce an arbitrarily steep slope, causing the dynamic trajectory to approximate the quasi-static trajectory to whatever degree of precision is desired. It only remains to show that the particular combinations of pushing velocity and angular inertia are practical in manipulation. Figures 46 and 47 show phase-plane portraits of a small oak block and a hinge plate being pushed with fixed contact. The figures were obtained by simulation. The dynamic trajectories agree closely with the quasi-static trajectories, even at speeds approaching the maximum speed of our manipulator (about 30 cm/sec.)
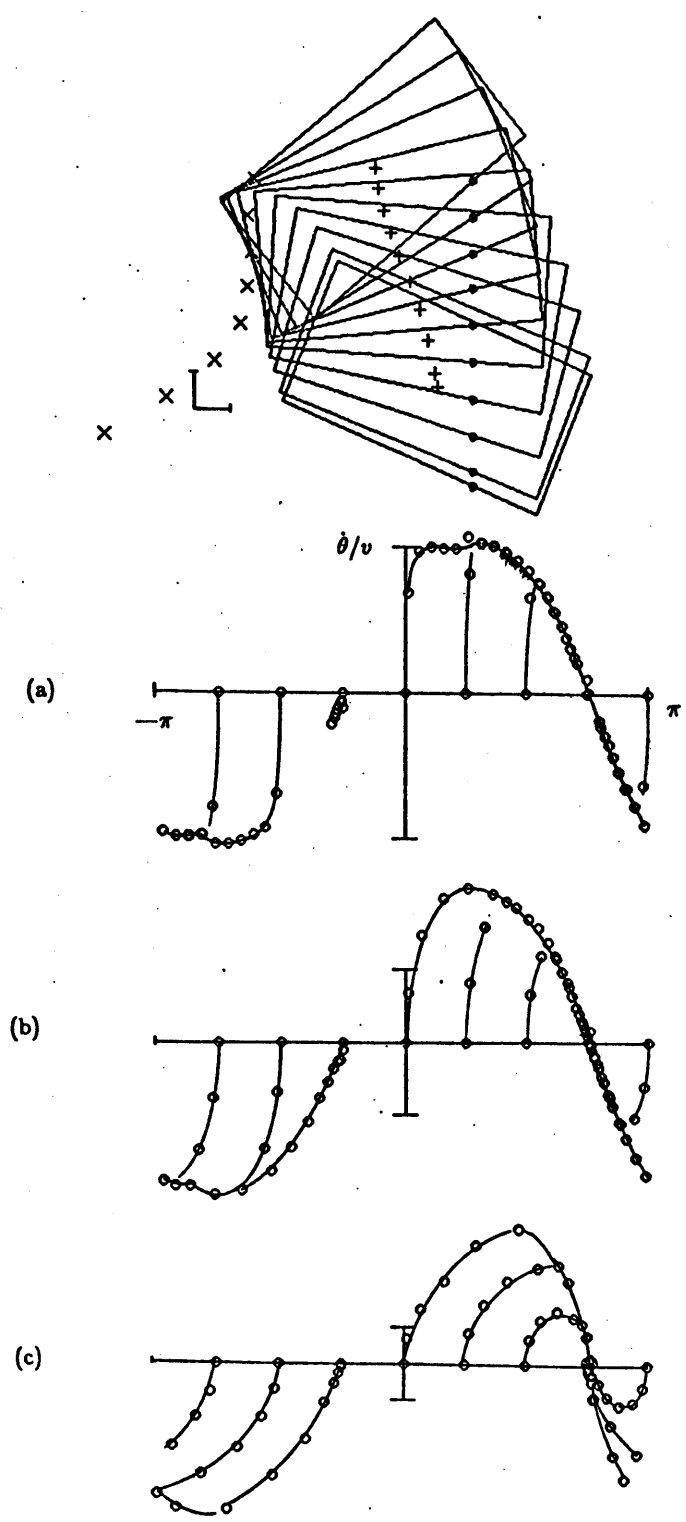
Figure 46. Phase plane portrait for oak block. (a) v is 5 cm/sec. (b) 10 cm/sec. (c) 20 cm/sec.
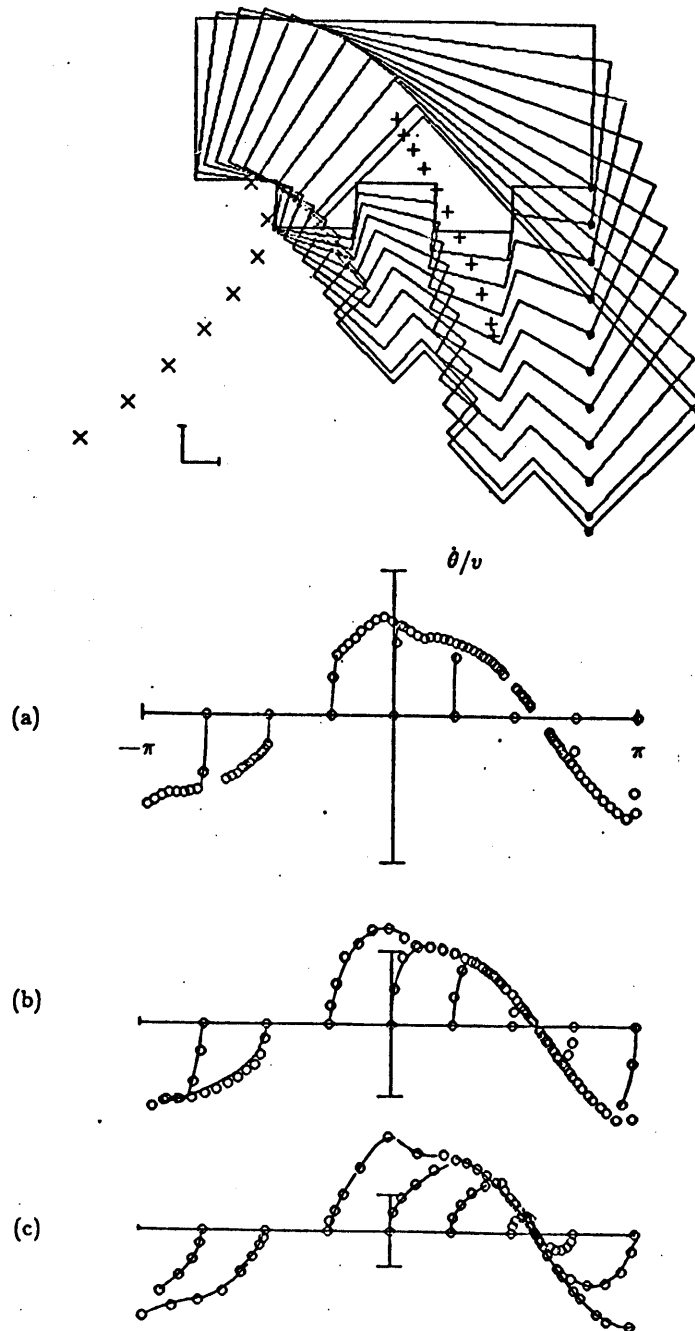
Figure 47. Phase plane portrait for hinge-plate. (a) v is 5 cm/sec. (b) 10 cm/sec. (c) 20 cm/sec.

Chapter 3

Application

The theory presented in chapter two represents a considerable increase over our previous level of understanding of manipulation without-prehension. Consequently, there are a large number of potential applications, some of which were outlined in section 1.1. The purpose of this chapter is to develop a few applications in detail and demonstrate implementations. There are two goals: to demonstrate that the theory developed in the previous chapter is relevant to real problems of manipulation; and to provide at least a cursory exploration of the issues standing between the present theory and implementation.

The first application is to the design of auxiliary machinery for eliminating uncertainty in the orientation and/or position of an object. It is assumed that the object's shape and center of mass are known. Methods are outlined which rotate the object to a desired orientation, without any sensory feedback. An implementation is demonstrated which feeds blocks to a robot manipulator. Implementation using the robot end-effector instead of a peripheral machine is discussed.

The second application is an automatic planner for grasping objects with a simple parallel-jaw gripper. When the range of possible initial orientations of the object is suitably restricted (e.g. to within $\pi/3$), and when the object shape is suitable, the program can plan a motion which will orient the object to a predictable orientation and acquire the object without sensory feedback.

The third application is the hinge-plate grasp verification re-visited. It is handled in greater detail, and the potential problems neglected in chapter one are addressed.

3.1. Automatic Orientation

In most robot manipulator applications, parts to be acquired by the manipulator must be reliably and accurately presented at a specified position and orientation. There is a resulting need for machines which can accept a part whose position and orientation is variable, and reliably move the part to the desired position and orientation. In general this is accomplished by special-purpose machines, which are designed for a specific part shape [*no author* 1969]. The main problem with this approach is that new machines have to be designed and fabricated for every new task. This compromises some of the advantages of robots—the robot may be reprogrammed for a new task quickly, but the supporting auxiliary machinery must go through a time-consuming and expensive development process. In this section we show a simple method for orienting a wide variety of parts which greatly simplifies the problem of designing the auxiliary orienting machine, or even allows the orienting to be performed by the robot, eliminating the auxiliary machine altogether. The method employs a fence which causes the object to attain a known orientation just by pushing in a straight line. The motion and orientation of the fence are determined by the shape of the object and the location of its center of friction. The approach may be implemented by a simple rod fixed across a conveyor belt, or by adding a simple auxiliary fence to the robot. The latter alternative is used here.

Figure 48 shows a box being pushed by a straight fence. In the configuration shown in the figure, the box's orientation is stable. If we consider a perturbation raising the right vertex from the fence, we will have contact between the left vertex and the fence. The center of friction is in zone IV, so the object will rotate back in a clockwise direction by theorem 12. Likewise, a small clockwise rotation puts the center of friction in zone I, giving a small corrective counter-clockwise rotation. This is the beginning of an automatic orientation method, since if the box is "near" the desired orientation, it will converge to it. Of course, local convergence is not
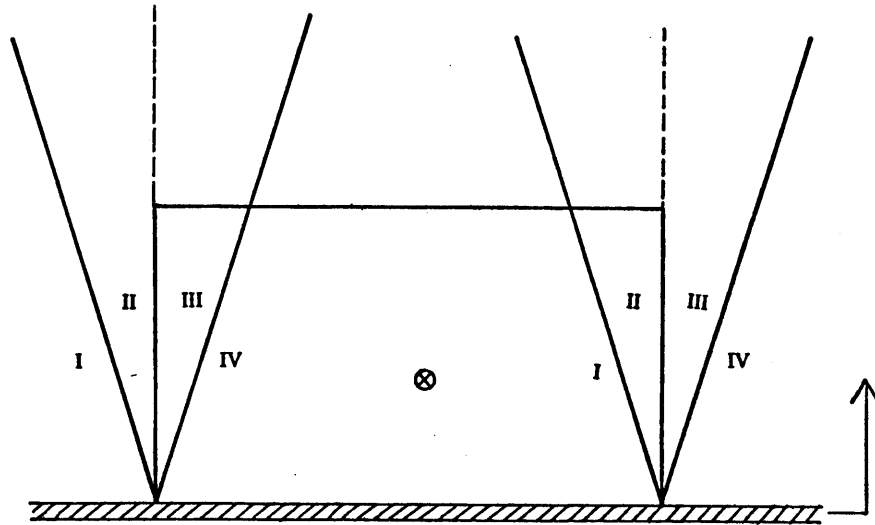
Figure 48. A box being pushed by a straight fence

usually enough; we would like the object to attain the desired orientation for any initial orientation falling within a specified range.

Figure 49 illustrates a simple method for finding all of the stable orientations of the box of figure 48, and identifying the regions of convergence. First we orient the figure so that the translations line is vertical. We roll the box, without sliding, through a complete revolution along the pushing constraint, marking the path of the center of friction. Every orientation of the object is mapped into a point on the curve described. For a given point on the curve, the contact point for the corresponding orientation must lie on the line orthogonal to the curve. Hence this orthogonal line passes through the contact point and the center of friction. If the tangent to the path has positive slope, the center of friction lies in zone I or II, and counter-clockwise rotation occurs. If it has negative slope, clockwise rotation must occur. Equilibria occur where the slope of the tangent is zero, i.e. where the curve is horizontal. Stable equilibria correspond to local minima in the curve, and unstable equilibria correspond to local maxima of the curve. In this respect the curve behaves like a potential curve, but the analogy breaks down—there is no conservative force field.

This construction simplifies design of automatic orientation machines. We

95

rotate the entire figure to an angle minimizing the number of local minima attainable from the range of possible initial orientations of the object. Then it is necessary to arrange for the translations line to lie on the vertical of the rotated figure.

The process is best illustrated by example. We wish to attain a repeatable orientation and position for a rectangular block. This will be accomplished with two fences—one fence is used to orient the block, and a second fence is used to position it. We plan the first motion by calculating the path of the center of friction as the block is rolled along the first fence (figure 49). In this orientation, there are four stable orientations of the block. The goal is to rotate the figure until line ℓ_1 has a negative slope and ℓ_2 has a positive slope, eliminating two of the stable orientations. The rotated construction is drawn in figure 50. It is now necessary to arrange for the translations line to be vertical. Unfortunately, if we examine the friction cone for the fence (which is aluminum) and the block (which is unfinished maple), it is impossible to get a translations line closer to the vertical than the left edge of the friction cone. Aluminum is too slippery for this application, so the fence was covered with a bicycle inner tube. The new friction cone admits the desired translations line, which is achieved by driving the fence parallel to the vertical. This motion will successfully orient the block to one of two orientations.

The second stage is to repeatably locate the block, without un-orienting the block (changing the orientation might be okay, as long as the new orientation is predictable). At the initiation of the second stage, the block's orientation is determined, and the block's location has a single degree of uncertainty—that is, it may be anywhere on a line segment tangent to the first fence. To reduce the remaining uncertainty the second fence is swept along this locus of possible block locations. The direction of motion and orientation of the second fence are chosen so that the block's orientation is stable during the second stage.

This motion sequence was programmed and tested on the M.I.T. Purbrick arm [Purbrick 1982]. Figure 51 is a photograph of the arm equipped with the two fences. This arm is particularly appropriate for this demonstration, because the first two motions of the arm are supplied by an x–y table. The fences are actually fixed, and the motion is obtained by moving the x–y table beneath them. Figure 52 shows
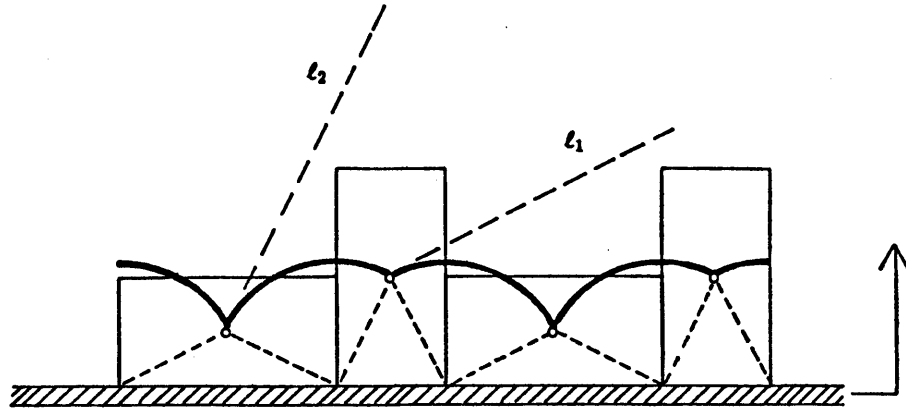
Figure 49. Locus of Center of Friction

the path of the x–y table. Segment 1 is the first stage of the motion, which orients the block. Segment 2 backs the block off of the first fence, to prevent any motion during the second stage. Segment 3 is the second stage, pushing the block to the desired location. Segment 4 moves the block beneath the gripper.

The motion sequence was tested by having the arm drop the block pseudo-randomly in the general vicinity of the first fence. After the orienting and positioning motions, the arm attempts to grasp the block and repeat the sequence. A record of the initial test is given in figure 53. The initial position and orientation is noted for each trial (the circle indicates the center of the bottom face of the block, and the line segment is parallel to the longer edge). Successes are indicated by filled-in circles, failures by open circles. The arm succeeded in 17 out of 20 trials. In each of the failures, the block was properly oriented, but just beyond the reach of the second fence during the second stage. The primary difficulty in programming this test was to stay within the limits of joint travel of the x–y table.

A second test was performed, with the configuration of the block constrained
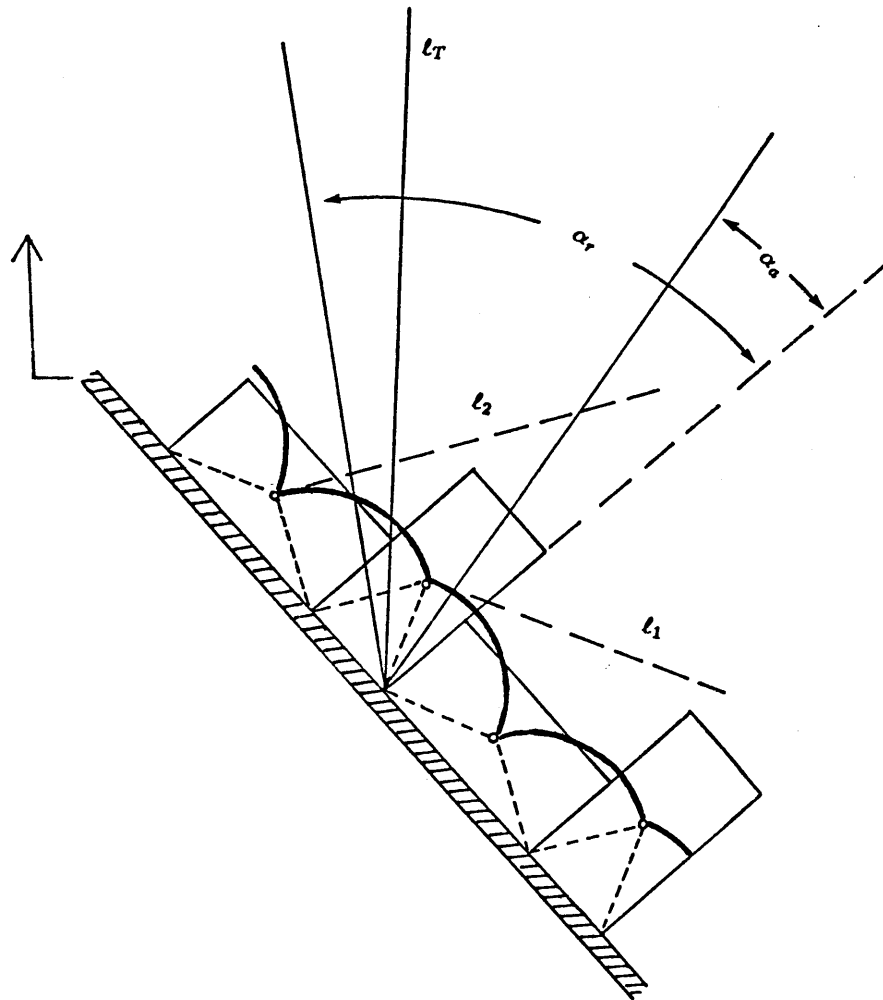
Figure 50. Planning the Orientation Stage α_a is the friction angle for oak on aluminum; α_r is the friction angle for oak on rubber. ℓ_T is the desired translations line.

so that the block lay completely inside the square shown in figure 53. In this case, the block was successfully oriented and positioned in each of 25 consecutive trials.

To execute the first and second stage required a total of seven seconds. Probably the most interesting aspect of the test was that the entire experiment, including design and installation of the fences, manufacture of blocks, program planning,
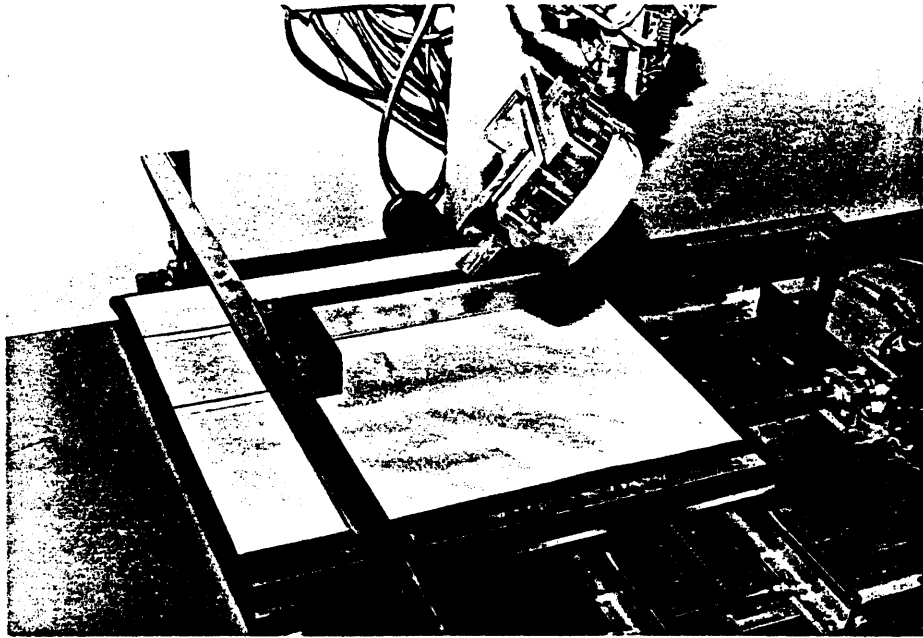
Figure 51. The Purbrick Arm

coding, some debugging of the control system, and the final testing, required less than 24 man-hours. The cost of materials for the fences was less than three dollars.

Single Stage Orienting and Positioning

A minor variation in stage one of the procedure described above allows an object's position and orientation to be completely determined by a single uniform motion. This is analogous to the hinge grasping maneuver described in chapter 1. The main idea is to arrange for the object to slide down the fence to a projecting stop after the orientation phase. An example of planning this operation is given in figure 54. We have arranged that the center of friction falls between the line of pushing and the friction cone. For the case shown, we can deduce that right-sliding must occur. By the corollary to theorem 10, if fixed contact occurs the line of force must lie on the same side of the center of friction as the line of pushing. This would imply a line of force outside the friction cone, which is impossible, so fixed contact
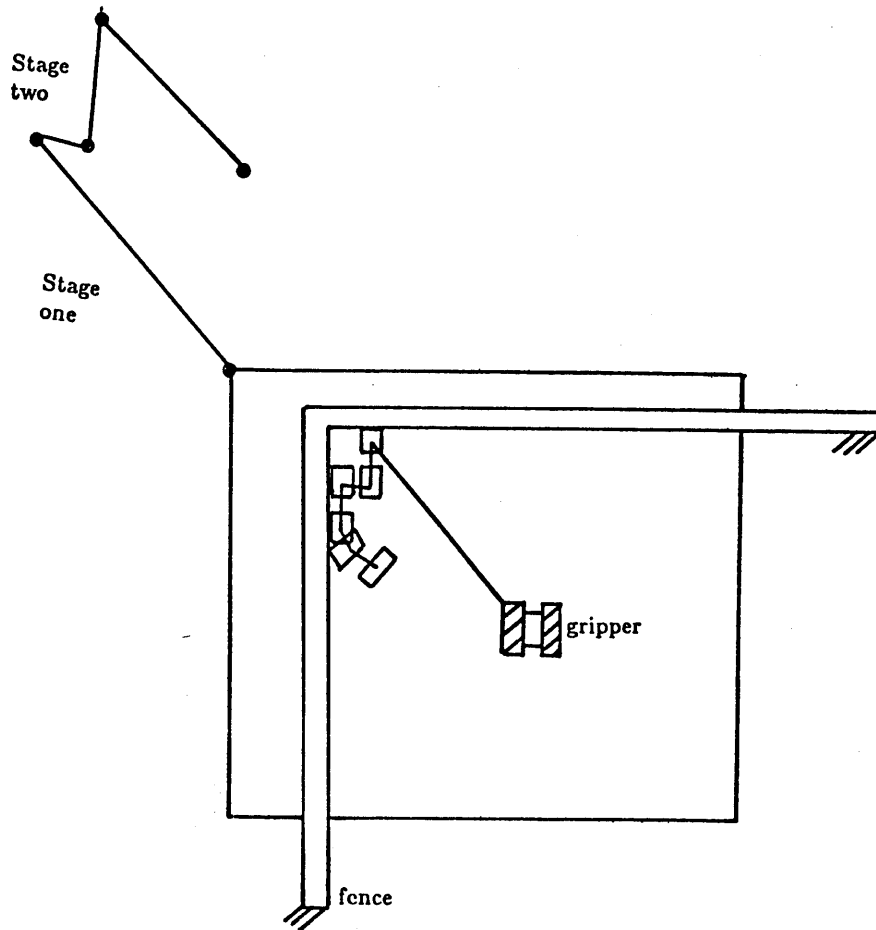
Figure 52. Orienting and Positioning the Block

does not occur. Left-sliding cannot occur, because it would require a line of motion on the opposite side of the center of friction from the friction cone, which violates theorem 10. By elimination, right-sliding contact must occur.

This method requires that the center of friction be outside the friction cone, which gives an upper bound on the coefficient of friction. As noted above, to orient an object often imposes a lower bound on the coefficient of friction. These two requirements may conflict. As a general rule, single stage orienting and positioning is difficult if the initial orientation of the object is completely unknown. The
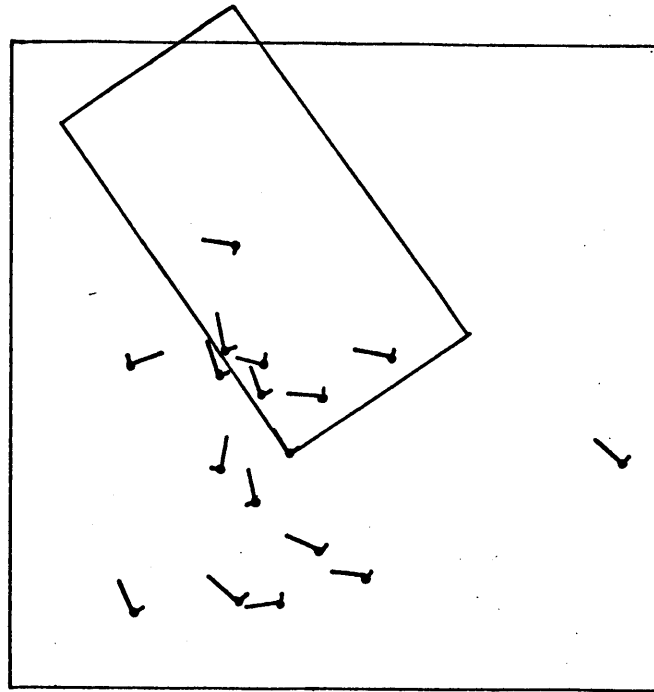
Figure 53. Test of block positioning and orienting. The three open circles indicate failures of stage two. The rectangle is drawn to indicate the size of the block. The large square was used to constraint the configuration of the block for the second run.

procedure is more suitable when bounds on initial orientation exist.

Gripper Design

The idea of using a fence to locate objects is immediately applicable to the design of grippers. By implementing the fence with one or both fingers, we extend the capabilities of the robot. Its dependence on the array of surrounding special-purpose equipment is reduced, with an accompanying increase in flexibility, and reductions in money, space, development time, and execution time. Figure 8 shows three different grippers which can orient, position, and grasp a block with a single,
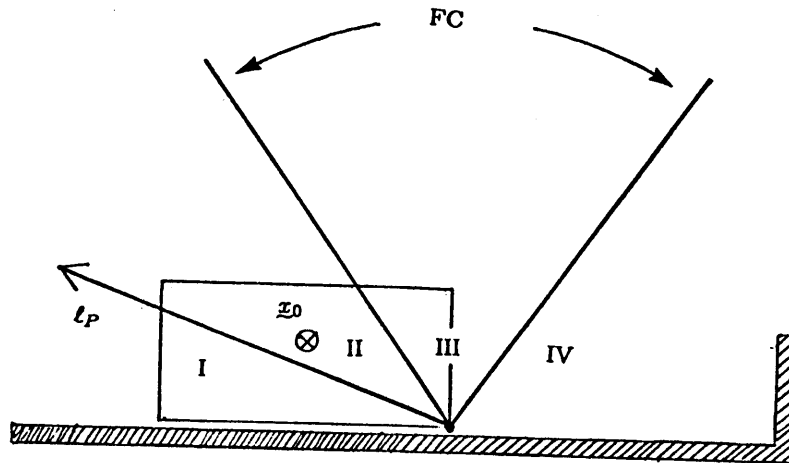
Figure 54. Single stage orienting and positioning. FC indicates the friction cone. ℓ_P is the line of pushing.

uniform, open-loop motion. The first of these works in a fashion similar to the hinge grasp example. The second works using the single stage orienting and positioning maneuver described above. The object is assumed to be constrained in position and orientation to the extent that it will hit the finger and converge to the correct orientation, at which point it slides until it strikes the projecting stop on the finger. The third gripper in figure 8 is similar in use to the second, but it has the great advantage of generality. It is not constructed especially for a given object; it accommodates different shapes by reconfiguring the fingers.

3.2. Automatic Planning of Grasping

In this section, a method is developed for planning a grasp maneuver, given the shape of the object and the range of possible initial orientations. The planned grasp motion maximizes a stability margin to minimize the sensitivity of the operation to errors in orientation or coefficient of friction. The method was implemented on the Lisp Machine [Weinreb and Moon 1981], and planned grasp operations which were successfully executed by the Purbrick Arm.

For each edge of the object, the procedure calculates the best finger orientation and line of pushing, and computes a stability margin. The edge giving the best stability margin is selected for the final grasping motion. It is then necessary to

102

determine the length of travel necessary to orient the object, so that the closing of the second finger is timely but not premature. The hard part is planning the finger orientation and motion for a given edge, so the solution of that task is presented in detail. The input is:

1. OBJECT, which is obtained by projecting the real object onto the support plane and taking the convex hull. Its representation in the machine includes a list of vertices, a list of edges, a location, and an orientation.

2. ORIENTATION-INTERVAL, an interval of angles which represent the set of possible initial object orientations.

Examples of calculating the finger orientation, the finger velocity, and the stability margin for each edge are shown in figures 56 and 57. The steps in this body are:

1. FEASIBLE-FINGER-NORMALS is computed. This represents the finger orientations which are included in the set of possible initial orientations of the edge and are guaranteed to hit this edge first. If this set is empty, go to the next edge.

2. NOMINAL-GOOD-INTERVAL is computed. This is the set of translations lines which guarantee local convergence assuming that the object is at its nominal orientation (zero).

3. GOOD-INTERVAL is computed. This is the set of translations lines which give convergence for any object orientation in ORIENTATION-INTERVAL. This set is the set of angles α such that if ORIENTATION-INTERVAL is rotated by α it is contained in NOMINAL-GOOD-INTERVAL. If GOOD-INTERVAL is empty, go to the next edge.

From this point, the goal is to find a motion giving a translations line as near the middle of GOOD-INTERVAL as possible. For a translations line inside GOOD-INTERVAL, the stability margin MARGIN is defined to be the distance to the nearest boundary of GOOD-INTERVAL. If the translations line is outside GOOD-INTERVAL, MARGIN is negative. Maximizing MARGIN gives a translations line as insensitive to error as possible.

103

The next step is to see whether the friction cone can be placed so that the optimal translations line is inside the friction cone. If it can, this maximizes MARGIN.

4. Compute the mean of GOOD-INTERVAL—BEST-ANGLE—and try to put the translations line on BEST-ANGLE. If this is possible then a friction cone placed at BEST-ANGLE must have a non-empty intersection with FEASIBLE-FINGER-NORMALS. This intersection is computed and saved as BEST-FEASIBLE-INTERVAL. If it is non-empty the FINGER-NORMAL, FINGER-VEL, and MARGIN are computed and saved for comparison with other edges.

If the friction cone cannot be placed to contain BEST-ANGLE, the next best thing is to get any angle of GOOD-INTERVAL inside the friction cone.

5. Compute GROWN-GOOD-INTERVAL. This is the set of all angles expressible as the sum of an angle in the interval $[-\alpha, \alpha]$ and an angle in the interval GOOD-INTERVAL. This is intersected with FEASIBLE-FINGER-NORMALS to obtain OK-FEASIBLE-INTERVAL. If OK-FEASIBLE-INTERVAL is non-empty, the boundary nearer BEST-ANGLE maximizes MARGIN for this edge. FINGER-NORMAL, FINGER-VEL, and MARGIN are computed and saved for comparison with other edges.

This procedure is executed for each edge. The combination of edge, FINGER-NORMAL, and FINGER-VEL which maximizes MARGIN is the motion chosen for execution by the manipulator.

The procedure was coded and run on the M.I.T. Lisp Machine [Weinreb and Moon 1981]. Appendix I contains a listing of the code. Grasping motions were planned for two objects: the part of a bicycle derailleur used to clamp it to the bicycle; and an oddly-shaped nut with a spring attached, used in a steel frame modular construction system (figure 55.) The convex-hull of the projections of the objects was determined by hand and entered into the computer. Figures 56 and 57 show the constructions outlined above for each of the two objects. In the case of the spring-nut, it is noteworthy that the longest edge is not chosen, because the center of gravity is much closer to a different edge.
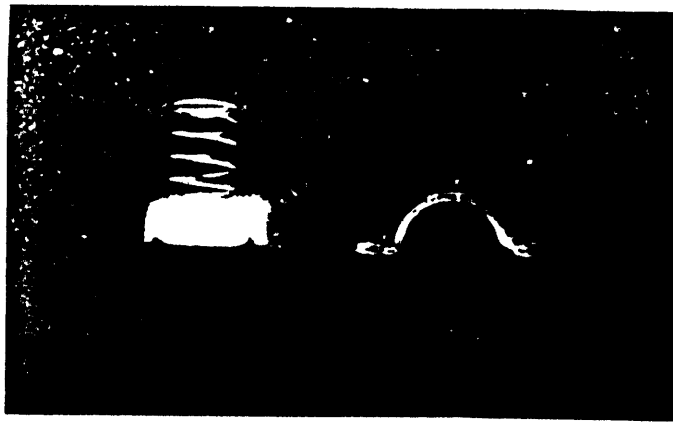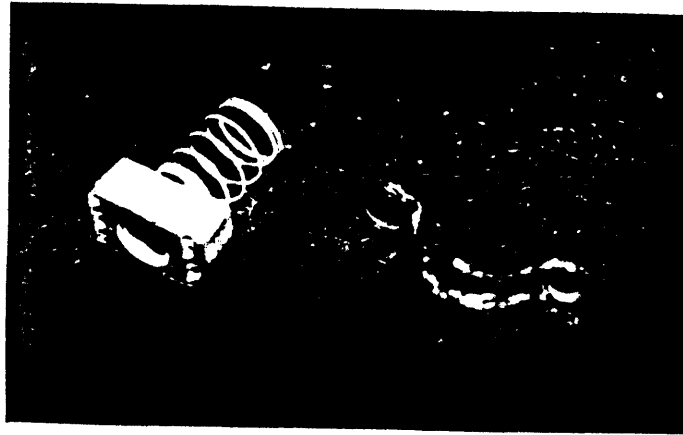
Figure 55. Parts for testing PLAN-GRASP.

3.3. Verification of Grasping

The previous section demonstrated automatic planning of grasping operations which eliminate uncertainty in the initial orientation of an object. In this section we demonstrate verification of grasping maneuvers which eliminate uncertainty in initial orientation and position. We have already seen a verification of one such grasping operation: the hinge-plate grasp described in chapter one. The basic steps in that proof showed that with one-finger contact the hinge must rotate to two-finger contact; that with two-finger contact the orientation is stable; and that with two-finger contact, one finger against its hinge-sleeve, the orientation is still stable. The difficulty remaining is to derive conditions on the initial finger separation and the finger-closing velocity such that two finger contact occurs before the fingers close too much. The approach taken here is to consider the set of all possible rotation

EDGE-INDEX:	1	2	3	4	5	6	7	10	11
FEASIBLE-FINGER-NORMALS:									
NOMINAL-GOOD-INTERVAL:									
GOOD-INTERVAL:									
GROWN-GOOD-INTERVAL:									
OK-FEASIBLE-INTERVAL:									
BEST-ANGLE:									
BEST-FEASIBLE-INTERVAL:									
FINGER-NORMAL:									
FINGER-VEL:									
MARGIN:	-1.0	-1.0	-1.0	0.19	-1.0	0.93	-1.0	-1.0	0.29
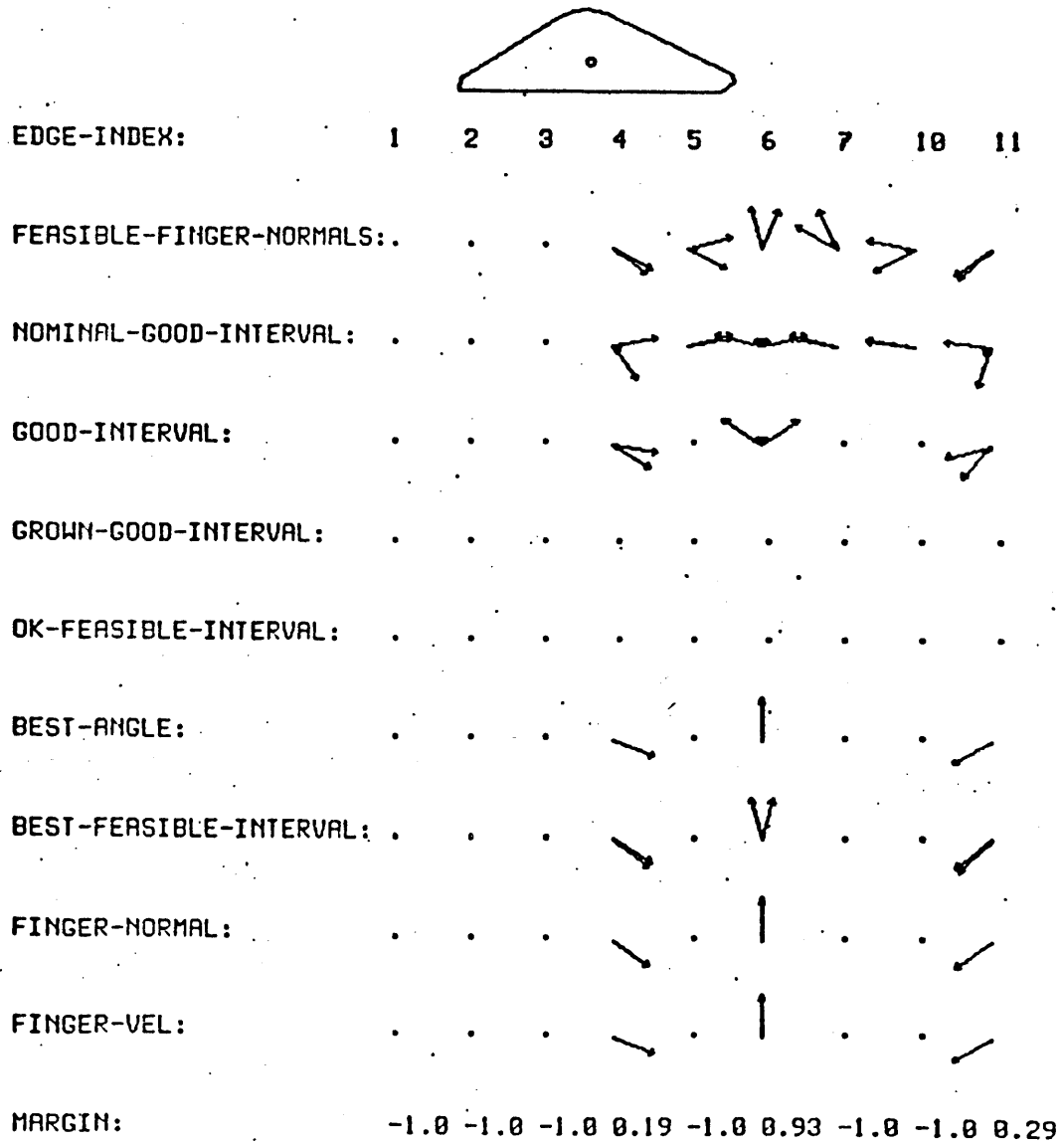
Figure 56. PLAN-GRASP running on the bicycle part.

Figure 57. PLAN-GRASP running on the spring-nut.

centers with one-finger contact, and use this set to find an upper bound on the finger closing velocity.

Figure 58 is a plot of the possible rotation centers for the contact point at the very corner of the hinge. Since we have contact between a point of the finger and an edge of the hinge-plate, the pushing constraint normal is determined by the hinge-plate, and the friction cone rotates with the hinge-plate. The possible lines of force must lie in the friction cone, and generate the set of rotation centers indicated by the thicker curve. If we now slide the contact point along the edge of the hinge-plate toward the hinge-sleeve, the thicker curve sweeps out a set of possible rotation centers. Figure 59 shows this set, and also the set of rotation centers which may be obtained by fixed-contact pushing when the finger is in contact with the hinge-sleeve. The greatest distance from the rotation centers to the contact points is r_{max}, which will be used to obtain an upper bound on the finger-closing speed.

To prevent the fingers from closing too soon, we will obtain an upper bound on the amount of time required for orientation of the hinge. The angular velocity of the object depends on the rotation center, the object orientation, and the finger velocity. Figure 60 shows the construction used. $\hat{u}$ is the unit vector orthogonal to the hinge-plate edge. $\underline{v}_f$ is the finger velocity, and $\underline{v}_c$ is the velocity of the contact point. The finger velocity has a component $\dot{h}$ representing the motion of the hand and a component $\dot{l}$ representing the closing of the fingers. The orientaton of the object is θ. The range of possible initial orientations of the object is $[\theta_0, \theta_1]$, with $\Delta\theta = \theta_1 - \theta_0$. The total amount of finger-closing required for grasping the hinge-sleeves is Δl. The distance to the rotation center is r.

To determine the angular velocity we will divide the velocity of the contact point $\underline{v}_c$ by the distance to the rotation center r. To determine the velocity of the contact point requires both the rotation center and the pushing constraint. Because of the pushing constraint, the projections of the finger velocity and the contact velocity onto the constraint normal $\hat{u}$ must be equal:

$$\underline{v}_f \cdot \hat{u} = \underline{v}_c \cdot \hat{u}$$

Carrying out the dot product:
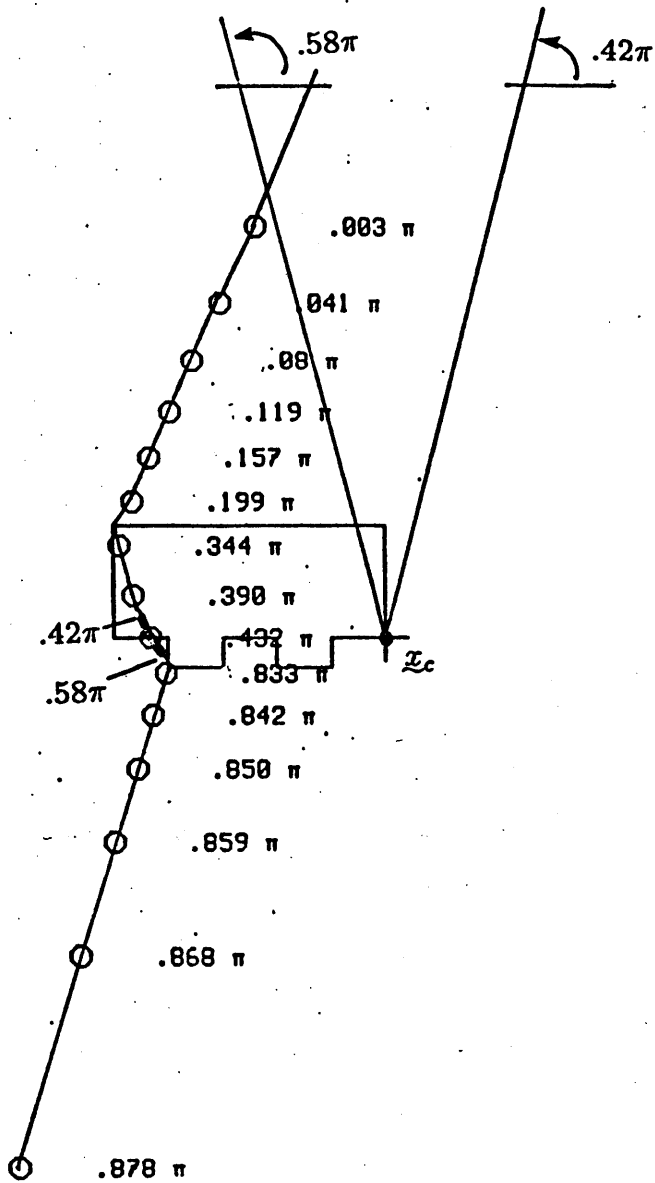
Figure 58. Rotation center locus for hinge-plate. The part of the locus delimited by force angles .42π and .58π is feasible.

$$h \cos \theta + l \sin \theta = |\underline{v}_c| \cos b$$

Substituting $r\dot{\theta}$ for $|\underline{v}_c|$ and solving for θ:

$$\dot{\theta} = \frac{h \cos \theta + l \sin \theta}{r \cos b}$$
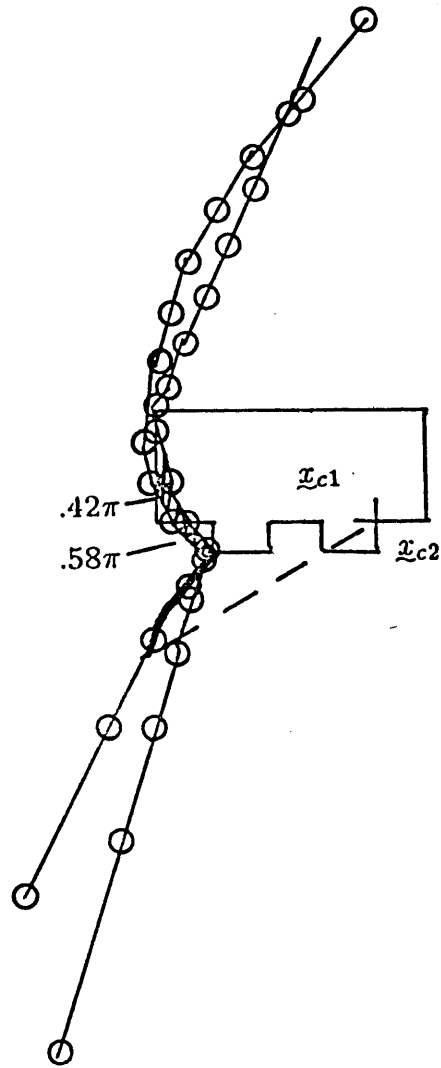
Figure 59. Possible rotation centers for hinge-plate.

Now the idea is to prevent the fingers from closing before the orientation is complete. We want an upper bound on the angular velocity, for which we will use $\Delta\theta/\dot{\theta}^*$, where $\dot{\theta}^*$ is a lower bound for the velocity. For plausible values of l, h and the minimum initial orientation θ_0, a lower bound for the velocity is given by
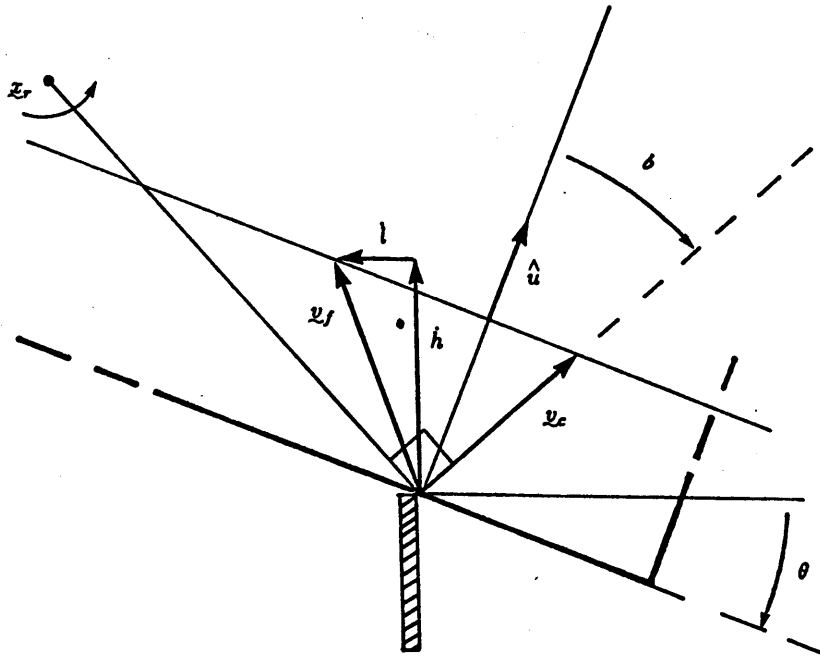
Figure 60. Finding upper bound on orientation time.

$$\dot{\theta}^* = \frac{\dot{h}\cos\theta_0 + \dot{l}\sin\theta_0}{r_{max}\cos b}$$

Now the finger-closing time must not be less than the maximum time to orient the object:

$$\frac{\Delta l}{\dot{l}} \geq \frac{\Delta\theta}{\dot{\theta}^*}$$

Substituting for $\dot{\theta}^*$ and solving for $\dot{l}$ we obtain:

$$\dot{l} \leq \frac{\Delta l\dot{h}\cos\theta_0}{\Delta\theta r_{max}\cos b - \Delta l\sin\theta_0}$$

which can be used to verify the last detail of the hinge grasping example.

Chapter 4

Concluding Remarks and Suggestions for Future Work

The goal of this section is to discuss some of the primary ideas appearing in this thesis as they relate to future robotics research.

Mechanics of Manipulation

The general focus of this work is on the mechanics of the manipulator–object pair. I believe that this is a fertile area for research which will prove important to the development of better manipulator control and planning systems. The mechanics of quasi-static planar pushing includes only one of several possible modes of manipulation of an object. Other common modes need to be identified and studied. A particularly important mode of manipulation is the collision of the manipulator with an object. These collisions are inevitable, and an important aspect of many robot manipulator applications. Non-planar motion is obviously very important. Likewise the motion of objects with multiple pushing constraints requires more attention.

Applications to Robotic Manipulation

The applications developed in this thesis need further elaboration. More experience in the use of manipulation without prehension is necessary. The method developed for automatic planning of grasping maneuvers is too restrictive, and needs to be integrated with previous work addressing aspects of grasping other than uncertainty, such as stability and path planning. The applications to design of grippers and other auxiliary machinery need to be developed further. Simulations based on the theory of pushing should be developed.

There are also a number of specific problems in the results of chapter two which require further attention. First of all, it was generally assumed that the pressure was bounded, i.e. that any normal force was applied over finite area. Although this assumption is defensible on physical grounds, it is useful to include the mathematical idealization of applying a non-zero normal force at a point, or on a line. Indeed, we have frequently done so throughout the thesis. It would also be desirable to extend the results of theorems 4 and 9, which were restricted to force distributions with support other than the x–axis in the former case, and to situations giving a non-zero determinant D in the latter case. Although these cases may not give uniquely determined rotation centers, I believe that the only failure occurs when the theorems predict translation and rotation occurs. This is not terribly awkward, because in most applications the translation would have been unstable anyway. None of the applications demonstrated in the thesis used theorem 4 or theorem 9 to guarantee translation, except indirectly when they were used to show that an orientation was stable.

Although it was proven that pushing at a point not in the horizontal plane does not hinder determination of the mode of rotation, it was not proven that the moment as a function of the rotation center is monotonic, nor was it shown under what circumstances this function is single-valued. Both of these questions must be addressed, and numerical methods need to be developed for this case.

Table 1

zone	contact mode	line of pushing w.r.t. friction cone		
		left	in	right
I	left·	ccw	ccw	ccw
	right	ccw	ccw	ccw
	fixed	ccw	ccw	ccw
II	left	ccw	ccw	ccw
	right	ccw	×	×
	fixed	ccw	ccw	ccw
III	left	×	×	ccw
	right	ccw	ccw	ccw
	fixed	ccw	ccw	ccw
IV	left	ccw	ccw	ccw
	right	ccw	ccw	ccw
	fixed	ccw	ccw	ccw

```
;;;;;;;;;;;;;;;;;;;;;;;;;;;;;;;;;;;;;;;;;;;;;;;;;;;;;;;;;;;;;;;;;;;
;;;
;;;                   definitions of data structures
;;;
;;;;;;;;;;;;;;;;;;;;;;;;;;;;;;;;;;;;;;;;;;;;;;;;;;;;;;;;;;;;;;;;;;;

;;;
;;; (DEFSTRUCT (<type> <options>)
;;;   <slot spec 1>
;;;   .
;;;   .
;;;   .
;;;   <slot spec n> )
;;; where <slot spec k> is either <slot name> or (<slot name>
;;; <nominal value>) defines a constructor macro MAKE-<type>, and
;;; accessor macros <type>-<slot-name> For example, the first DEFSTRUCT
;;; creates the macros MAKE-VECTOR, VECTOR-X, and VECTOR-Y.
;;;

(defstruct (vector (:type :named-array)
                    :conc-name)
  (x 0.0)
  (y 0.0))

(defstruct (point (:include vector)
                  :conc-name))

(defstruct (object (:type :named-array)
                    ":conc-name)
  (angle 0)
  (position (make-point))
  (list-of-vertices nil)
  (list-of-edges nil)
  (mass))

(defstruct (vertex (:type :named-array)
                   (:include vector)
                   :conc-name)
  object
  index
  cof-angle)

(defstruct (edge (:type :named-array)
                 :conc-name)
  object
  index
  v1
  v2
  normal-angle)

(defstruct (finger (:type :named-array)
                   :conc-name)
  (normal-angle 0)
  (length 5.0)                            ; nominal face width is 5 cm
  (center (make-point)))
```

```
;;; angles are represented as fixed-point 24-bit numbers, in units of (2
;;; * pi)/2**24.  arithmetic is done modulo 2**24., i.e. modulo 2*pi An
;;; interval is represented by its lowest and highest angles, defined
;;; counter-clockwise.  The intervals are closed at the low end, open at
;;; the high end.

(defstruct (angle-interval (:type :named-array)
                                   :conc-name)
  (low 0)
  (high 0))




;;;;;;;;;;;;;;;;;;;;;;;;;;;;;;;;;;;;;;;;;;;;;;;;;;;;;;;;;;;;;;;;;;;;;;;;
;;;
;;;                     Operations
;;;
;;;;;;;;;;;;;;;;;;;;;;;;;;;;;;;;;;;;;;;;;;;;;;;;;;;;;;;;;;;;;;;;;;;;;;;;

;;; vector arithmetic

(defun vector-plus (v1 v2 &optional (v3 (make-vector)))
  (setf (vector-x v3) (+ (vector-x v1) (vector-x v2)))
  (setf (vector-y v3) (+ (vector-y v1) (vector-y v2)))
  v3)

(defun vector-diff (v1 v2 &optional (v3 (make-vector)))
  (setf (vector-x v3) (- (vector-x v1) (vector-x v2)))
  (setf (vector-y v3) (- (vector-y v1) (vector-y v2)))
  v3)

(defun scalar-product (s v &optional (dest (make-vector)))
  (setf (vector-x dest) (* s (vector-x v)))
  (setf (vector-y dest) (* s (vector-y v)))
  dest)

(defun vector-length (v)
  (sqrt (float (+ (^ (vector-x v) 2)
                  (^ (vector-y v) 2)))))

(defun angle-of-vector (vector)
  (radians-to-angle (atan (vector-y vector)
                          (vector-x vector))))

;;; other vector operations

(defun unit-vector (angle)
  (make-vector x (cos (angle-to-radians angle))
               y (sin (angle-to-radians angle))))

(defun rotate-vector (v angle
                      &aux (c (cos (angle-to-radians angle)))
                           (s (sin (angle-to-radians angle))))
  (make-vector x (- (* c (vector-x v)) (* s (vector-y v)))
               y (+ (* s (vector-x v)) (* c (vector-y v)))))
```

116

```
;;; angle arithmetic

(defun angle-plus (a1 a2)
  (%24-bit-plus a1 a2))

(defun angle-diff (a1 a2)
  (%24-bit-difference a1 a2))

(defun angle-to-radians (a1)
  (// (* (si:24-bit-unsigned a1) 2 pi) (^ 2 24.)))

(defun radians-to-angle (r)
  (si:make-24-bit-unsigned
    (fix (* (// r 2 pi) (^ 2 24.)))))



;;; other angle operations

(defun angle-between (a b c)
  (< (si:24-bit-unsigned (angle-diff a b))
     (si:24-bit-unsigned (angle-diff c b))))

(defun interval-includes-angle-p (interval angle)
  (angle-between
    angle
    (angle-interval-low interval)
    (angle-interval-high interval)))

(defun rotate-interval (int angle
                          &optional (dest (make-angle-interval)))
  (setf (angle-interval-low dest)
        (angle-plus (angle-interval-low int) angle))
  (setf (angle-interval-high dest)
        (angle-plus (angle-interval-high int) angle))
  dest)

;;; this returns length of an interval in RADIANS.  If the low and the
;;; high of an interval are the same, this indicates the whole circle,
;;; which comes out to zero in angle units.  Of course, it is impossible
;;; to represent an empty interval with our encoding, so no information
;;; would be lost using angle units.

(defun angle-interval-length (interval)
  (let ((angle-length
          (angle-diff (angle-interval-high interval)
                      (angle-interval-low interval))))
    (if (zerop angle-length)
        (* 2 pi)
        (angle-to-radians angle-length))))

(defun copy (int1 int2)
  (setf (angle-interval-low int2)(angle-interval-low int1))
  (setf (angle-interval-high int2)(angle-interval-high int1))
  int2)

;;; returns mean of an angle-interval

(defun angle-interval-mean (int)
  (angle-plus (angle-interval-low int)
              (// (angle-diff (angle-interval-high int)
                              (angle-interval-low int))
                  2)))
```

```
;;; interval of angles which can be represented as sum of an angle from
;;; int1 and an angle from int2

(defun co-intervals (int1 int2 &optional (dest (make-angle-interval)))
  (setf (angle-interval-low dest) (angle-plus (angle-interval-low int1)
                                              (angle-interval-low int2)))
  (setf (angle-interval-high dest) (angle-plus (angle-interval-high int1)
                                               (angle-interval-high int2)))
  dest)


;;; computes an interval d s.t. (co-intervals int-inside d) ==> int-outside.
;;;  empty d indicated by nil.

(defun ci-intervals (int-outside int-inside
                     &optional (dest-interval (make-angle-interval)))
  (cond ((< (angle-interval-length int-inside)
            (angle-interval-length int-outside))
         (setf (angle-interval-low dest-interval)
               (angle-diff (angle-interval-low int-outside)
                           (angle-interval-low int-inside)))
         (setf (angle-interval-high dest-interval)
               (angle-diff (angle-interval-high int-outside)
                           (angle-interval-high int-inside)))
         dest-interval)
        (t nil)))

(defun interval-includes-angle-bit (interval angle)
  (if (interval-includes-angle-p interval angle)
      1
      0))

;;; computes simple intersection of two intervals, i.e. doesn't know how
;;; to describe union of two intervals, so returns nil instead.  switches
;;; on 4-bit number indicating inclusion of vertex of one interval in the
;;; other interval.

(defun simple-intersect (int1 int2 &optional (int3 (make-angle-interval)))
  (if (or (null int1) (null int2))
      nil
      (selectq (+ (interval-includes-angle-bit int1 (angle-interval-low int2))
                  (* 2 (interval-includes-angle-bit
                        int1
                        (angle-interval-high int2)))
                  (* 4 (interval-includes-angle-bit
                        int2
                        (angle-interval-low int1)))
                  (* 8 (interval-includes-angle-bit
                        int2
                        (angle-interval-high int1))))
        (0 nil)                                    ; empty intersection
        (15. nil)                                  ; not simple intersection
        (3 (copy int2 int3))
        (12. (copy int1 int3))
        (6 (setf (angle-interval-low int3) (angle-interval-low int1))
           (setf (angle-interval-high int3) (angle-interval-high int2))
           int3)
        (9. (setf (angle-interval-low int3) (angle-interval-low int2))
            (setf (angle-interval-high int3) (angle-interval-high int1))
            int3)
        (otherwise (ferror nil "Impossible set of inclusions")))))
```

```
;;; operations on objects

;;; returns preceding edge in list of edges of object

(defun preceding-edge (object edge-index
                        &aux (list-of-edges (object-list-of-edges object))
                             (length (length list-of-edges)))
  (nth (remainder (+ edge-index length -1)
                  length)
       list-of-edges))

(defun succeeding-edge (object edge-index
                        &aux (list-of-edges (object-list-of-edges object))
                             (length (length list-of-edges)))
  (nth (remainder (1+ edge-index)
                  length)
       list-of-edges))




;;;;;;;;;;;;;;;;;;;;;;;;;;;;;;;;;;;;;;;;;;;;;;;;;;;;;;;;;;;;;;;;;;;;;;;
;;;
;;;                     constants
;;;
;;;;;;;;;;;;;;;;;;;;;;;;;;;;;;;;;;;;;;;;;;;;;;;;;;;;;;;;;;;;;;;;;;;;;;;

(defconst zero-vector (make-vector))

(defconst angle-pi (radians-to-angle pi))
(defconst angle-half-pi (// angle-pi 2))

(defconst coefficient-of-friction 0.25)          ; Leonardo's value
(defconst friction-angle (radians-to-angle coefficient-of-friction))

;;; define acceptable margin

(defvar margin-threshold 0.0)
```

```
;;;;;;;;;;;;;;;;;;;;;;;;;;;;;;;;;;;;;;;;;;;;;;;;;;;;;;;;;;;;;;;;;;;;;;;;;;;
;;;
;;;                    PLAN-GRASP
;;;
;;;;;;;;;;;;;;;;;;;;;;;;;;;;;;;;;;;;;;;;;;;;;;;;;;;;;;;;;;;;;;;;;;;;;;;;;;;;

;;; for each edge i
;;;    calculate feasible finger angle and finger vel
;;;    maximizing stability margin
;;;
;;; select edge with largest stability margin
;;;
;;; if margin < stability-threshold, report failure
;;;
;;; guess necessary length of travel
;;;
;;; return edge index, finger angle, finger vel, travel, and trace.


(defun plan-grasp (object orientation-interval
                   &aux (record (make-plan-grasp-record
                                   object object
                                   orientation-interval orientation-interval)))

  (do ((edge-index 0 (1+ edge-index))
       edge
       best-edge-index                          ; best edge so far
       (best-margin -1)                         ; ditto for margin
       (best-finger-normal nil)                 ; ditto for finger normal
       (best-finger-vel nil)                    ; ditto for finger vel

       ;; range of angles between preceding edge normal and succeeding edge
       ;; normal

       (edge-contact-interval nil nil)

       ;; interval of finger normal angles such that initial contact will occur
       ;; with v1 or v2 before another vertex, for any object orientation in
       ;; orientation-interval

       (feasible-finger-normals nil nil)

       ;; if object were in orientation 0 with 0 variation, this would be
       ;; good-interval

       (nominal-good-interval nil nil)

       ;; angles of lines which, when drawn from v1 will pass to the left of the
       ;; c.o.f., and when drawn from v2 will pass to the right of the c.o.f.,
       ;; for any object orientation in orientation-interval.

       (good-interval nil nil)

       ;; the interval of angles which are the sum of an angle in good-interval
       ;; and an angle in the friction cone

       (grown-good-interval nil nil)

       ;; intersection of grown-good-interval with feasible-finger-normals

       (ok-feasible-interval nil nil)

       (best-angle nil nil)                     ; mean of good-interval
```

120

```
        ;; intersection of friction cone constructed
        ;; about best-angle with
        ;; feasible-finger-normals

        (best-feasible-interval nil nil)

        (finger-normal nil nil)             ; best finger normal for edge
        (finger-vel nil nil)                ; best finger vel for edge
        (margin -1.0 -1.0)                  ; stability margin for edge
        )


        ;; loop through all edges

        ((= edge-index (length (object-list-of-edges object)))

         (if (> best-margin margin-threshold)    ; if good enough,
                                                 ; return parms

             (list best-edge-index best-finger-normal
                   best-finger-vel
                   (plan-grasp-travel
                     best-edge-index best-finger-normal
                     best-finger-vel object orientation-interval)
                   record )

           "no feasible grasp" record))         ; else report failure

    ;; get edge, and angles of preceding and succeeding edges

    (setf edge (nth edge-index (object-list-of-edges object)))
    (setq edge-contact-interval
          (make-angle-interval
            low (edge-normal-angle (preceding-edge object edge-index))
            high (edge-normal-angle (succeeding-edge object edge-index))))

    ;; check for convexity

    (if (not (interval-includes-angle-p
               edge-contact-interval
               (edge-normal-angle edge)))
        (ferror nil "object not convex"))

    ;; compute feasible-finger-normals

    (setq feasible-finger-normals
          (simple-intersect
            (ci-intervals edge-contact-interval orientation-interval)
            (rotate-interval orientation-interval
                             (edge-normal-angle edge))))


    ;; proceed only if feasible-finger-normals is non-empty

    (if (not (null feasible-finger-normals))
        (progn

          ;; compute good-interval

          (setq nominal-good-interval
                (make-angle-interval low (vertex-cof-angle (edge-v1 edge))
                                     high (vertex-cof-angle (edge-v2 edge))))
          (setq good-interval (ci-intervals nominal-good-interval
                                            orientation-interval))
```

121

```
;; proceed only if good-interval is non-empty

(if (not (null good-interval))

     ;; The object of this code is to choose the finger-vel and finger
     ;; normal so that the middle of the vel, the left, and the right
     ;; edges of the friction cone (i.e. the translations line) is in
     ;; good-interval.

     ;; first, compute best-angle, grow by [-atan(mu), atan(mu)), and
     ;; intersect with feasible-angles.  If non-empty, choose
     ;; finger-normal in result and vel = best-angle.  Margin is half
     ;; of (length good-interval)

     (progn
       (setq best-angle
             (angle-interval-mean good-interval)

             best-feasible-interval
             (simple-intersect
               feasible-finger-normals
               (rotate-interval (make-angle-interval
                                   low (angle-diff 0 friction-angle)
                                   high friction-angle)
                                 best-angle)
               ))
       (if (not (null best-feasible-interval))
           (if (interval-includes-angle-p best-feasible-interval
                                          best-angle)
               (setq finger-normal best-angle
                     finger-vel best-angle
                     margin (// (angle-interval-length good-interval)
                                2))
               (if (angle-between
                     (angle-interval-low best-feasible-interval)
                     best-angle
                     (angle-interval-high best-feasible-interval))
                   (setq finger-normal
                         (angle-interval-low best-feasible-interval)
                         finger-vel
                         best-angle
                         margin
                         (// (angle-interval-length good-interval) 2))
                   (setq finger-normal
                         (angle-interval-high best-feasible-interval)
                         finger-vel
                         best-angle
                         margin
                         (// (angle-interval-length good-interval) 2))
                   ))
```

```
;; next, grow good-interval by [0, atan(mu)), and intersect
;; with feasible-finger-normals.  If non-empty, finger-normal
;; is low angle of result of intersection, and margin is diff
;; between high of grown-good-interval and finger-normal, vel
;; = best-angle.

(progn
  (setq grown-good-interval
        (co-intervals
          good-interval
          (make-angle-interval
            low 0
            high friction-angle))
      ok-feasible-interval
        (simple-intersect
          feasible-finger-normals
          grown-good-interval))
  (if ok-feasible-interval
      (setq finger-normal
            (angle-interval-low ok-feasible-interval)
            finger-vel
            best-angle
            margin
            (angle-to-radians
              (angle-diff
                (angle-interval-high grown-good-interval)
                (angle-interval-low ok-feasible-interval))))))

;; next, grow good-interval by [-atan(mu), 0), and
;; intersect with feasible-finger-normals.  If non-empty,
;; finger-normal is high angle of result of intersection,
;; and margin is diff between finger-normal and low of
;; grown good-interval.  vel = best-angle.

(progn
  (setq grown-good-interval
        (co-intervals
          good-interval
          (make-angle-interval
            low (angle-diff 0 friction-angle)
            high friction-angle))

      ok-feasible-interval
        (simple-intersect
          feasible-finger-normals
          grown-good-interval))

  (if ok-feasible-interval
      (setq finger-normal
            (angle-interval-low ok-feasible-interval)
            finger-vel
            best-angle
            margin
            (angle-to-radians
              (angle-diff
                (angle-interval-high grown-good-interval)
                (angle-interval-low
                  ok-feasible-interval))))
      (setq finger-normal nil
            finger-vel nil
            margin -1))))))
```

```
                        ;; If there is an ok or good feasible finger-normal, and if
                        ;; margin is greater than best-margin, save finger-normal,
                        ;; finger-vel, margin, and edge-index.

                        (if (> margin best-margin)
                            (setq best-margin margin
                                  best-finger-normal finger-normal
                                  best-finger-vel finger-vel
                                  best-edge-index edge-index)))
                   )))
      ))


;;; given an object and a pushing motion, estimate time for orientation to
;;; converge

(defun plan-grasp-travel (edge-index finger-normal
                          finger-vel object orientation-interval
                          &aux (edge (nth edge-index
                                          (object-list-of-edges object)))
                               (v1 (edge-v1 edge))
                               (v2 (edge-v2 edge))
                               (max-xr 0.0)
                          )

  ;; for each of v1, v2, guess the three vertices, other than contact point,
  ;; giving maximum distance to center of rotation, assuming fixed contact.
  ;; Maximum xr's occur at extremes of orientation-interval, so compute for each
  ;; vertex and save larger.  Multiply by total angular excursion to obtain
  ;; upper bound on total pushing distance required for orientation to be
  ;; complete.

  (mapc #'(lambda (v)
            (let* ((supports (max-moment-supports v object))
                   (xr (center-of-rotation object supports v finger-vel)))
              (if (> xr max-xr)
                  (setq max-xr xr))))
        (list v1 v2))

  (* (angle-interval-length orientation-interval)
     max-xr))
```

124

References

no author 1969

American Machinist Special Report No. 632, "Orienting Parts for Assembly," *American Machinist,* July 28, 1969.

Acton 1970

Acton, F. S., *Numerical Methods that Work,* Harper & Row, 1970.

Albus and Evans 1976

Albus, J. S., and Evans, J. M., "Robot Systems," *Scientific American,* February, 1976.

Ambler et. al. 1975

Ambler, A. P., Barrow, H. G., Brown, C. M., Burstall, R. M., and Popplestone, R. J., "A Versatile System for Computer-Controlled Assembly," *Artificial Intelligence,* vol. 6, 1975.

Ambler and Popplestone 1975

Ambler, A. P., and Popplestone, R. J., "Inferring the Positions of Bodies from Specified Spatial Relationships," *Artificial Intelligence,* vol. 6, 1975.

Amontons 1699

Amontons, G., "De la résistance causée dans les machines," Mémoires de l'Académie Royale des Science, 1699, pp. 206-227.

Bejczy 1974

Bejczy, A. K., "Robot Arm Dynamics and Control," Jet Propulsion Laboratory Technical Memo 33-669, February, 1974.

Bolles and Paul 1973

Bolles, R., and Paul, R., "The Use of Sensory Feedback in a Programmable Assembly System," Stanford Artificial Intelligence Laboratory Memo AIM-220, October, 1973.

Bowden and Tabor 1950

Bowden, F.P. and Tabor, D., *Friction and Lubrication of Solids*, Clarendon Press, Oxford, 1950.

Brown 1967

Brown, K. M., "Algorithm 316; Solution of Simultaneous Non-Linear Equations," *Communications of the ACM*, vol. 10, no. 11, November, 1967.

Brown and Conte 1967

Brown, K. M., and Conte, S. D., "The Solution of Simultaneous Nonlinear Equations," *Proceedings, ACM National Meeting*, 1967.

Coulomb 1781

Coulomb, C. A., "Théorie des machines simples en ayant égard au frottement de leurs parties et à la roideur des cordages ...," Mémoires de Mathématique et de Physique présentés à l'Académie Royale des Sciences, par divers savans, Paris, 1781.

Craig and Raibert 1979

Craig, J. J., and Raibert, M. H., "A Systematic Method of Hybrid Position/Force Control of a Manipulator," *IEEE Compsac '79*, November 7, 1979.

Darringer and Blasgen 1975

Darringer, J. A., and Blasgen, M. W., "MAPLE: A High Level Language for Research in Mechanical Assembly," IBM Research Report RC-5606, September, 1975.

Den Hartog 1956

Den Hartog, J. P., *Mechanical Vibrations*, McGraw Hill, New York, 1956.

Drake 1977

Drake, S. H., "Using Compliance in Lieu of Sensory Feedback for Automatic Assembly," Ph.D. Thesis, MIT Department of Mechanical Engineering, September, 1977.

Ernst 1961

Ernst, H. A., "MH-1, A Computer-Operated Mechanical Hand," Sc.D. Thesis, MIT, December, 1961.

Fahlman 1973

Fahlman, S. E., "A Planning System for Robot Construction Tasks," MIT Artificial Intelligence Laboratory Technical Report 283, May, 1973.

Finkel et. al. 1974

Finkel, R., Taylor, R., Bolles, R., and Feldman, J., "AL, A Programming System for Automation," Stanford Artificial Intelligence Laboratory Memo AIM-243, November, 1974.

Gillmor 1971

Gillmor, C. S., *Coulomb and the Evolution of Physics and Engineering in Eighteenth-Century France,* Princeton University Press, Princeton, New Jersey, 1971.

Goto et. al. 1974

Goto, T., Inoyama, T., and Takeyasu, K., "Precise Insert Operation by Tactile Controlled Robot," *2nd Conference on Industrial Robot Technology,* March, 1974.

Goto et. al. 1980

Goto, T., Takeyasu, K., and Inoyama, T., "Control Algorithm for Precision Insert Operation Robots," *IEEE Transactions on Systems, Man, and Cybernetics,* vol. SMC-10, no. 1, January, 1980.

Groome 1972

Groome, R. C., "Force Feedback Steering of a Teleoperator System," M. S. Thesis, MIT Department of Aeronautics and Astronautics, August 14, 1972.

Grossman and Taylor 1978

Grossman, D. D., and Taylor, R. H., "Interactive Generation of Object Models with a Manipulator," *IEEE Transactions on Systems, Man, and Cybernetics*, vol. SMC-8, no. 9, September, 1978.

Grunbaum 1967

Grunbaum, *Convex Polytopes*, Interscience Publishers, John Wiley, 1967.

Hanafusa and Asada 1977a

Hanafusa, H., and Asada H., "A Robotic Hand with Elastic Fingers and its Application to Assembly Process," IFAC Symp. on Information and Control Problems in Manufacturing Technology, Tokyo, 1977.

Hanafusa and Asada 1977b

Hanafusa, H., and Asada H., "Stable Prehension by a Robot Hand with Elastic Fingers," Proc. 7th International Symposium on Industrial Robots, October, 1977.

Hilbert and Cohn-Vossen 1952

Hilbert, D., and Cohn-Vossen, S., *Geometry and the Imagination*, Chelsea, New York, 1952.

Hollerbach 1980

Hollerbach, J. M., "A Recursive Lagrangian Formulation of Manipulator Dynamics," *IEEE Trans. Systems, Man, Cybernetics*, vol. SMC-11, no. 11, November, 1980.

Horn and Raibert 1978

Horn, B. K. P., and Raibert, M. H., "Configuration Space Control," *The Industrial Robot*, pp. 69-73, June, 1978.

Inoue 1971

Inoue, H., "Computer Controlled Bilateral Manipulator," *Bulletin of the JSME*, vol. 14, no. 69, 1971.

Inoue 1974

Inoue, H., "Force Feedback in Precise Assembly Tasks," MIT Artificial Intelligence Laboratory Memo no. 308, August 1974.

Jellett 1872

Jellett, J. H., *A Treatise on the Theory of Friction*, MacMillan, London, 1872.

Kahn and Roth 1971

Kahn, M. E., and Roth, B., "The Near-Minimum-Time Control of Open-Loop Articulated Kinematic Chains," ASME *Journal of Dynamic Systems, Measurement, and Control*, September, 1971.

Khatib 1980

Khatib, O., "Commande dynamique dans l'espace opérationnel des robots manipulateurs en présence d'obstacles," Thèse de Docteur-Ingénieur, Ecole Nationale Supérieure de l'Aéronautique et de l'Espace, Toulouse, France, December, 1980.

Kolmogorov and Fomin 1970

Kolmogorov, A. N., and Fomin, S. V., *Introductory Real Analysis*, Prentice-Hall, 1970 (republished by Dover, 1975.)

Leonardo da Vinci 14??

Leonardo da Vinci, manuscript, Codice Atlantico, Biblioteca Ambrosiana, Milano.

Lieberman and Wesley 1975

Lieberman, L. I., Wesley, M. A., "AUTOPASS: A Very High Level Programming Language for Mechanical Assembler Systems," IBM Research Report RC-5599, August, 1975.

Lozano-Perez 1976

Lozano-Perez, T., "The Design of a Mechanical Assembly System," MIT Artificial Intelligence Laboratory Technical Report 397, 1976.

Lozano-Perez 1980

Lozano-Perez, T., "Spatial Planning with Polyhedral Models," PhD Thesis, MIT Department of Computer Science and Electrical Engineering, June, 1980.

Lozano-Perez 1981

Lozano-Perez, T., "Automatic Planning of Manipulator Transfer Movements," *IEEE transactions on Systems, Man, and Cybernetics*, vol. SMC-11, no. 10, October, 1981.

Lozano-Perez 1982

Lozano-Perez, T., talk presented at "High Level Programming Systems for Robotics" workshop, MIT, January 21-22, 1982.

Lozano-Perez and Wesley 1979

Lozano-Perez, T., and Wesley, M. A., "An Algorithm for Planning Collision-Free Paths Among Polyhedral Obstacles," *Communications of the ACM*, vol. 22, no. 10, October, 1979.

Luh et. al. 1980a

Luh, J., Walker, M., and Paul, R., "On-line Computational Scheme for Mechanical Manipulators," *Transactions of the ASME; Journal of Dynamic Systems, Measurement, and Control*, vol. 102, June, 1980.

Luh et. al. 1980b

Luh, J., Walker, M., and Paul, R., "Resolved-Acceleration Control of Mechanical Manipulators," *IEEE Transactions on Automatic Control*, vol. AC-25, no. 3, June, 1980.

Luh et. al. 1983

Luh, J. Y. S., Fisher, W. D., and Paul, R. P. C., "Joint Torque Control by a Direct Feedback for Industrial Robots," *IEEE Transactions on Automatic Control*, January, 1983.

MacMillan 1936

MacMillan W.D., *Dynamics of Rigid Bodies*, Dover, New York, 1936.

Mason 1981

Mason, M. T., "Compliance and Force Control for Computer Controlled Manipulators," *IEEE Transactions on Systems, Man, and Cybernetics*, Vol SMC-11, no. 6, June 1981.

Meyer 1981

Meyer, Jeanine, "An Emulation System for Programmable Sensory Robots," *IBM Journal of Research and Development*, vol. 25, no. 6, November, 1981.

Minchin 1884

Minchin, G.M., *A Treatise on Statics*, Clarendon Press, Oxford, 1884.

Moseley 1839

Moseley, H., *Illustrations of Mechanics*, London, 1839.

Nevins and Whitney 1974

Nevins, J. L., and Whitney, D. E., "The Force Vector Assembler Concept," *First IFToMM Symposium on Theory and Practice of Robots and Manipulators*, 1974.

Okada 1979a

Okada, T., "Computer Control of Multijointed Finger System," *Proceedings of the Sixth International Joint Converence on Artificial Intelligence*, August, 1979.

Okada 1979b

Okada, T., "Object-Handling System for Manual Industry," *IEEE Transactions on Systems, Man, and Cybernetics*, vol. SMC-9, no. 2, February, 1979.

Paul 1972

Paul, R., "Modelling, Trajectory Calculation and Servoing of a Computer Controlled Arm," Stanford Artificial Intelligence Laboratory Memo AIM-177, November 1972.

Paul 1979

Paul, R., "Manipulator Cartesian Path Control," *IEEE Transactions on Systems, Man, and Cybernetics*, vol. SMC-9, no. 11, November, 1979.

Paul 1981

Paul, R. P., *Robot Manipulators: Mathematics, Programming, and Control,*
MIT Press, 1981.

Paul and Shimano 1976

Paul, R., and Shimano, B., "Compliance and Control," *Proceedings, 1976
Joint Automatic Control Conference,* 1976.

Paul et. al. 1981

Paul, R. P., Shimano, B., and Mayer, G. E., "Kinematic Control Equations
for Simple Manipulators," *IEEE Transactions on Systems, Man, and
Cybernetics,* vol. SMC-11, no. 6, June, 1981.

Paul et. al. 1981

Paul, R. P., Shimano, B., and Mayer, G. E., "Differential Kinematic Control
Equations for Simple Manipulators," *IEEE Transactions on Systems, Man,
and Cybernetics,* vol. SMC-11, no. 6, June, 1981.

Pieper 1968

Pieper, D. L., "The Kinematics of Manipulators Under Computer Control,"
Stanford Artificial Intelligence Memo No. 72, October, 1968.

Pingle et. al. 1974

Pingle, K., Paul, R., Bolles, R., "Programmable Assembly, Three Short
Examples," Film, Stanford Artificial Intelligence Laboratory, October 1974.

Popplestone 1979

Popplestone, R. J., "Specifying Manipulation in Terms of Spatial Relationships,"
Dept. of Artificial Intelligence, U. of Edinburgh, No. 117, June, 1979.

Popplestone et. al. 1978

Popplestone, R. J., Ambler, A. P., and Bellos, I. M., "RAPT: A Language for
Describing Assemblies," *The Industrial Robot,* September, 1978.

Popplestone et. al. 1980

Popplestone, R. J., Ambler, A. P., and Bellos, I. M., "An Interpreter for a Language for Describing Assemblies," *Artificial Intelligence*, Vol. 14, pp. 79-107, 1980.

Prescott 1923

Prescott, J., *Mechanics of Particles and Rigid Bodies*, Longmans, Green, and Co., London, 1923.

Purbrick 1982

Purbrick, J. A., "A Cartesian Manipulator System," MIT Artificial Intelligence Laboratory, Working Paper 232, in preparation, 1982.

Raibert 1977

Raibert, M. H., "Analytical Equations vs. Table Look-up for Manipulation: a Unifying Concept," *Proc. IEEE Conf. on Decision and Control*, New Orleans, pp. 576-579, December, 1977.

Raibert 1978

Raibert, M. H., "A Model for Sensorimotor Control and Learning," *Biol. Cyber.*, vol. 29, pp. 29-36, 1978.

Raibert and Craig 1981

Raibert, M. H., and Craig, J. J., "Hybrid Position/Force Control of Manipulators," *Journal of Dynamic systems, Measurement, and Control*, vol. 102, June, 1981.

Rektorys 1969

Survey of Applicable Mathematics, Iliffe, London, 1969.

Reuleaux 1876

Reuleaux, F., *The Kinematics of Machinery*, Macmillan, 1876. (Republished by Dover, 1963.)

Salisbury 1980

Salisbury, J. K., "Active Stiffness control of a Manipulator in Cartesian Coordinates," *19th IEEE Conference on Decision and Control*, December, 1980.

Salisbury and Craig 1981

Salisbury, J. K., and Craig, J. J., "Articulated Hands: Force Control and Kinematic Issues," *Proceedings, 1981 Joint Automatic Control Conference*, June, 1981.

Shimano 1978

Shimano, B. E., "The Kinematic Design and Force Control of Computer Controlled Manipulators," Ph.D. thesis, Stanford University Computer Science Department, Stanford Artificial Intelligence Laboratory AIM 313, March, 1978.

Silver 1973

Silver, D., "The Little Robot System," MIT Artificial Intelligence Laboratory Memo No. 273, January, 1973.

Simunovic 1975

Simunovic, S. N., "Force Information in Assembly Processes," *Proceedings 5th International Symposium on Industrial Robots*, September 22-24, 1975.

Soroka 1980

Soroka, B. I., "Debugging Robot Programs with a Simulator," *CADCAM-8 Conference*, November, 1980.

Stoker 1950

Stoker, J. J., *Nonlinear Vibrations in Mechanical and Electrical Systems*, Wiley, New York, 1950.

Summers and Grossman 1981

Summers, P. D., and Grossman, D. D., "XPROBE: An Experimental System for Programming Robots by Example," IBM Research Report RC-9082, October 16, 1981.

Takase et. al. 1974

Takase, K., Inoue, H., Sato, K., and Hagiwara, S., "The Design of an Articulated Manipulator with Torque Control Ability," *Proceedings, 4th International Symposium on Industrial Robots*, 19-21 November, 1974.

Takeyasu et. al. 1976

Takeyasu, K., Goto, T., and Inoyama, T., "Precision Insertion Control Robot and Its Application," *Transactions of the ASME; Journal of Engineering for Industry*, November, 1976.

Taylor 1976

Taylor, R. H., "A Synthesis of Manipulator Control Programs from Task-Level Specifications," Stanford Artificial Intelligence Memo 282, July, 1976.

Taylor 1979

Taylor, R. H., "Planning and Execution of Straight-line Manipulator Trajectories," *IBM Journal of Research and Development*, vol. 23, no. 4, July, 1979.

Truesdell 1968

Truesdell, C., *Essays in the History of Mechanics*, Springer-Verlag, New York, 1968.

Udupa 1977

Udupa, S., "Collision Detection and Avoidance in Computer Controlled Manipulators," PhD Thesis, Dept. Elec. Engrg., Cal Tech, 1977.

Uicker et. al. 1964

Uicker, J. J., Denavit, J., and Hartenberg, R. S., "An Iterative Method for the Displacement Analysis of Spatial Mechanisms," *Transactions of the ASME; Journal of Applied Mechanics*, June, 1964.

Watson 1976

Watson, P. C., "A Multidimensional System Analysis of the Assembly Process as Performed By a Manipulator," P-364, Charles Stark Draper Laboratory, Inc., August, 1976.

Watson and Drake 1975

Watson, P. C., and Drake, S. H., "Pedestal and Wrist Force Sensors for Automatic Assembly," *Proceedings 5th International Symposium on Industrial Robots*, September 22-24, 1975.

Weinreb and Moon 1981

Weinreb, D., and Moon, D., *Lisp Machine Manual*, MIT Artificial Intelligence Laboratory, July, 1981.

Whitney 1969

Whitney, D. E., "Resolved Motion Rate Control of Manipulators and Human Prostheses," *IEEE Transactions on Man-Machine Systems*, vol. MMS-10, no. 2, June, 1969.

Whitney 1972

Whitney, D. E., "The Mathematics of Coordinated Control of Prosthetic Arms and Manipulators," *Transactions of the ASME; Journal of Dynamic Systems, Measurement, and Control*, December, 1972.

Whitney 1977

Whitney, D. E., "Force Feedback Control of Manipulator Fine Motions," ASME *Journal of Dynamic Systems, Measurement, and Control*, June, 1977.

Will and Grossman 1975

Will, P. M., and Grossman, D. D., "An Experimental System for Computer Controlled Mechanical Assembly," *IEEE Transactions on Computers*, vol. c-24, no. 9, September, 1975.

Young 1978

Young, K. D., "Controller Design for a Manipulator Using Theory of Variable Structure Systems," *IEEE Transactions on Systems, Man, and Cybernetics*, vol. SMC-8, no. 2, February, 1978.